AN ENERGY METHOD FOR

EARTHQUAKE RESISTANT DESIGN OF RC STRUCTURES

by

Surat Terapathana

A Dissertation Presented to the
FACULTY OF THE USC GRADUATE SCHOOL
UNIVERSITY OF SOUTHERN CALIFORNIA
In Partial Fulfillment of the
Requirements for the Degree
DOCTOR OF PHILOSOPHY
(CIVIL ENGINEERING)

May 2012

Acknowledgments

I am pleased to express my gratitude to my principal advisor, Professor James C. Anderson, who reviewed and provided me several valuable ideas toward this document. As well, I would like to be grateful for those who participated as my Qualifying and Dissertation committee: Prof. L. Carter Wellford, Prof. Vincent W. Lee, Prof. Hung L. Wong, and Prof. Chunming Wang. They all affect the accomplishment of this document

Table of Contents

List of Tables

List of Figures

Abstract

In order to effectively design reinforced concrete moment frames to withstand earthquake ground motions, it is necessary to accurately predict the seismic demands on the building system including the effects of duration together with the usual constraints defined by building codes. In this study, the use of plastic design procedures and an energy balance equation are described. The energy balance equation becomes an additional constraint in which the energy input (energy demand) to the structure by the earthquake will be balanced by energy absorbed by the structure and by energy dissipated from the structure. Hysteretic energy is selected and employed as energy demand since it relates directly to the inelastic deformation demands of a structure subjected to earthquake ground motion.

Within this thesis, the design procedure for reinforced concrete frames that includes energy demand is presented. Reinforced concrete moment frames for low-rise and mid-rise buildings are selected and designed as case studies. Nonlinear dynamic time history analyses are conducted for two sets of earthquake records, representative of far field records and near fault records, in order to estimate the hysteretic energy demand over the height of the building. Plastic design and minimum cost concepts are developed as an objective function which is minimized subject to the constraints by using linear programming. Finally, the designed frames are evaluated and verified according to present building code and FEMA 356 requirements. This procedure is repeated until the energy demand by the ground motion is less than the energy capacity of the structure.

Chapter 1

Introduction

1.1 Statement of Problem

To maintain structural behavior in the elastic range for major earthquakes is safe but not economical. Allowing the structural members to enter the inelastic range at a certain points is acceptable among international consensus. As a result, an earthquake-resistant structural design was developed assuming inelastic behavior would occur. The general philosophy of this methodology was proposed by S. Zagajeski and V. Bertero (1977): a) to prevent non-structural damage in minor earthquake ground shaking which may occur frequently during the service life of the structure; b) to prevent structural damage and minimize nonstructural damage in occasional moderate earthquake ground shakings; and c) to avoid collapse or serious damage in rare major earthquake ground shakings. Several researchers and practicing engineers are currently promoting the new seismic design based on this methodology. Most of them emphasize the displacement-based design concept. Their goal is to control the structure within the maximum lateral displacement demand. Moreover, current code design such as the 1997 Uniform Building Code (UBC), which emphasizes the force-based design procedure, also realizes the importance of this methodology. They introduce modification factors to reduce seismic force and overstrength demands to the design level related to the ductility characteristic of each building type. The larger value of the modification factor implies

the higher ductility capacity. However, demands in the displacement-based design concept and force-based design concept are restricted to the peak responses of structure subjected to the earthquake. Lacking in consideration is the earthquake sequence and time-history responses in design.

The design of an earthquake-resistant structure is not only a function of the peak response demand but also a function of the time history response demand. Cumulative nonlinear response such as plastic energy is an effective quantity to represent time history response. It gives a good indication of how the structure has performed nonlinearly during the earthquake ground motions. Especially, in Reinforced Concrete (RC) structures this energy may indicate damages of structural members such as cracking and plastic deformation due to yielding of the reinforcing steel. The ability to absorb and dissipate this energy in structures is a main concern according to the earthquake-resistant structural design methodology. Energy-Based Design (EBD) concept seems to be suitable choice to select under this circumstance.

The purpose of this thesis is to introduce the basic concepts that are necessary for energy-based design and to derive the suitable energy-based design procedures with their associated assumptions for the design of reinforced concrete frames. The application of these concepts is used to revise the design of three-story and nine-story RC moment frames subject to design earthquake records. In this paper, two sets of records, SAC LA10/50 records and SAC Near Fault records, are considered. The SAC LA 10/50 records represent 20 far field modified ground records whose probabilities of exceedence are 10% in 50 years for Los Angeles region. The SAC Near Fault records are the set of

20 ground motions corresponding to near-source motion on firm ground, which can be developed in UBC Seismic Zone 4. Hysteretic energy demands, which are primarily used for design, are derived by performing nonlinear time history analyses of these two frames subject to these records. Subsequently, the performance of these designed reinforced concrete frames under an ensemble of strong motion records will be analyzed and discussed. Damage indices, which provide a measure of the sustained damage of the structural frame after responding to the earthquake, is also discussed. The advantage of this index is that it considers both the damage cause by peak deformation and by hysteretic energy dissipation due to repeated cyclic loading.

Moreover, the comparison such as nonlinear responses and cost between energy-based design concept and 1997 UBC-based design concept to reinforced concrete moment frames is included and discussed.

To accomplish the above goals, there are six related chapters to be considered and included. The brief descriptions for each chapter are demonstrated as the following:

Chapter 2: Energy responses of structural frames subjected to earthquake ground motions are the main focus for this thesis. In this chapter, energy characteristic and definitions of energy terms will be described based on Single Degree of Freedom System (SDOF) and Multi-Degree of Freedom System (MDOF). Two main energy methodologies, relative and absolute energies concepts are represented along with how they are consequently derived.

Chapter 3: Basic plastic design methodology related to frame structures will be explained. Suitable collapse mechanisms for moment frame such as beam mechanism

and side sway mechanisms will be selected and derived along with their failure load. Transformation of each collapse mechanism to an energy equation, which is employed as a constraint in design process is also included.

Chapter 4: Application of optimization methodology to RC frame design based on the energy-based concept will be explained within this chapter. Selected constraint equations, necessary for optimization process, will be derived along with corresponding collapse mechanisms and practical and code considerations. The significant nonlinear responses required by 1997 UBC such as story drift are mentioned and considered within this chapter. The entire process is described by a given flow chart as illustrated in Fig. 4.1 of Chapter 4. To enhance more understanding to the procedure, a simple example of a RC two-story, one bay frame will be examined and designed based on energy-based concept.

Chapter 5: To clarify the energy-based concept, the RC three-story and nine-story concrete moment frames will be selected and revised. The original building is designed based on special moment resisting frame concept by 1997 UBC. Results of the nonlinear responses such as plastic rotations, damage indices, drift index, and hysteretic energy demands are presented in this chapter.

Chapter 6: Conclusions related to energy-based design concept will be presented based on comparison of the results of the RC three-story and nine-story building EBD relative to the original sizes by1997 UBC–based design. The recommendation for further study also is included in this chapter.

1.2 Literature and Historical Background

In the late fifties, an energy-based design concept was initially introduced by G.W. Housner (1956) at the First World Conference on Earthquake Engineering on the 50th anniversary of the 1906 San Francisco earthquake. He inferred the proportional energy that a structure should absorb plastically during earthquake. In an elastic SDOF system, the maximum absorbed energy (E_a) is directly related equal to the recoverable strain energy, $E_a = (mA)S_D/2 = mV^2/2$ where m is the mass, S_D is the spectral displacement, and V is the pseudo-velocity. In an inelastic system the absorbed energy is becomes the summation of recoverable strain energy (E_s) and irrecoverable hysteretic energy (E_h). Based on Housner's idea, several researchers suggested the use of an energy balance equation to improve the estimation of the maximum input energy.

In 1960 and 1961, J.A. Blume introduced the Reserve Energy Technique to account for inelastic action with the capacity of structure to dissipate energy. The technique had empirical relationships and approximations in order to reduce the complexity of inelasticity and energy problems. G.V. Berg and S.S. Thomaides (1960) presented the spectral study of the energy relations for a single degree of freedom, elasto-plastic system subjected to strong ground motions. In 1965, P.C. Jennings studied and developed the general hysteretic law and the calculation of the statistics of the response of simple yielding structures to an ensemble of artificial earthquake ground motions. S.C. Goal and G.V. Berg (1968) presented the influence of the important ground motion parameters and characteristics subject to the inelastic response parameters for buildings

of 10, 25, and 40 stories in height. The estimated amount and distribution of energy dissipation along the height was shown.

In 1975, B. Kato and H. Akiyama studied the energy theory to estimate the earthquake damage of structures. Using this theory, the total input energy is defined as the total energy, demand, by the earthquake while the corresponding resistance of the building is the energy absorption capacity of the structure. R.Y. Soni, J. Krishna, and B. Chandra (1977) studied the seismic behavior of engineering structures through the mechanics of energy absorption controlled by the force-deflection relation. They introduced two parameters, Energy Coefficient and Sway Ratio, to relate the seismic energy demand with the associated ductility for elasto-plastic systems.

Kato and Akiyama (1982) designed a steel structure based on the energy concept. It followed the concept that a structure can safely resist a severe earthquake ground motion if its energy absorption capacity is greater than the energy input by earthquake. In 1984, Zahrah and Hall focused on seismic energy absorption in a Single-Degree-of-Freedom (SDOF) systems. Later, in 1985, Akiyama followed Housner's concept to extend his study on energy-based design in detailed formulations for one-story frame through multi-story frame. Tembulkar and Nau (1987) studied seismic energy dissipation capacity and inelastic structural modeling.

Many researchers attempted to develop methodology to estimate the hysteretic energy demand to accompany the design approach. In 1988, Uang and Bertero analyzed the physical meaning of two energy equations, absolute energy and relative energy of structural systems. They constructed inelastic input energy spectra for SDOF systems

and estimated inelastic input energy for a Multi-Degree-of-Freedom (MDOF) systems based on the SDOF systems. In 1989, P. Fajfar, T. Vedic, and M. Fischinger studied on SDOF energy demand for structures subjected to a group of standard Californian accelerograms, severe ground motion records obtained during the 1985 Mexico City earthquake and three different groups of strong motion records recorded in Southern Europe. The demand is expressed in terms of damage model and period of structure. In 1995, A. Nurtug and H. Sucuoglu established procedure to develop seismic energy for linear SDOF system. Ground motion is represented by its pseudo-velocity spectra and effective duration while SDOF is defined by natural period of vibration and viscous damping ratio. F. Mollaioli and L. Decanini (1998) and G. Manfredi (2001) developed the procedures for the determination of input energy spectra.

F. Mollaioli and L. Decanini (2001) provided a deeper focus on energy demand. They studied the influences of earthquake characteristics and earthquake resisting structures to inelastic energy demand. Two parameters have been introduced, the response modification factor and the ratio of the area where enclosed by inelastic input energy spectrum to the subjected elastic value. Ductility of structural members, soil type, source-to-site distance and magnitude are among the considered factors. Procedures to build inelastic design earthquake input energy spectra are summarized and presented.

To obtain energy demands for structure, there are many procedures developed by different researchers subjected to the specific response characteristic of a given system but few published papers demonstrate how energy demand relates to the structural design procedure. Leelataviwat et al (1999), Leelataviwat et al (2002) and R. Estes (2003)

developed design procedures for steel structures based on the energy concept. Up to now, design procedures for reinforced concrete structures have not been presented.

Chapter 2

Concepts of Energy Methods in Seismic Design

Allowing the proposal by G.W. Housner (1956), energy-based design method has gained more extensive study by many researchers. His concept emphasizes on studying of energy terms in the structure during earthquake ground motion. Basically, after transferring total input energy to the structure, some will remain and form the motion of structure, called kinetic energy. Some go for deformation of structural members, known as strain energy while the rest of energy will need to be dissipated through damping and inelastic deformation. Based on this knowledge, he categorized energy terms into elastic energy and plastic energy (they will be discussed in later section). He inferred that the safe design could be obtained if the sum of elastic energy and plastic energy which is considered as energy supply is greater than or equal to the total input energy which considered as energy demand.

To understand more on the energy response of a structure, a Single-Degree-of -Freedom (SDOF) system, shown in Fig. 2.1, is a fundamental model needed for initial investigation. The well-known basic equation of a lumped-mass SDOF system subjected to a ground motion excitation is illustrated in Eq. 2.1:

$$m\ddot{v}_t + c\dot{v} + f_s = 0 \qquad (2.1)$$

Where m is mass; c is viscous damping; f_s is restoring force, v_t and v are total and relative displacement, respectively.

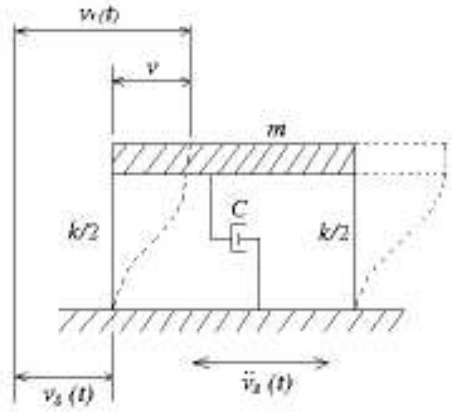

Fig. 2.1: SDOF system subjected to an earthquake ground motion

Uang and Bertero (1988) derived two consistent definitions of energy method; absolute energy and relative energy. Referring to Fig. 2.1, an absolute energy equation can be derived by replacing v with $v_t - v_g$ and integrating the whole respects to displacement. Result in Eq. 2.1 becomes:

$$\frac{m(\dot{v}_t)^2}{2} + \int c\dot{v}dv + \int f_s dv = \int m\ddot{v}_t dv_g \qquad (2.2)$$

The term on the right-hand side indicates the total input energy exerted by earthquake, may be called (E_i). The first term on the left side represents energy resulted

by motion of mass, known as an absolute kinetic energy (E_k). The damping energy (E_d) and absorbed energy (E_a) are represented in second and third terms on the right hand side, respectively. However, E_a can be divided into recoverable energy, called a strain energy (E_s) and irrecoverable hysteretic energy, called hysteretic energy dissipation (E_h). Then the Eq. 2.2 can be demonstrated in revised balance energy form as the following:

$$E_i = E_k + E_d + E_s + E_h \tag{2.3}$$

Alternatively, summation of kinetic energy (E_k) and strain energy (E_s) are known as elastic energy (E_e) and hysteretic energy (E_h) with damping energy (E_d) are called plastic energy (E_p).

However, if replacing $v_t = v + v_g$ into Eq. 2.1 instead and integrating the whole respects to displacement, the structural system can be modified and illustrated as in Fig 2.2. The derived energy equations enable to pronounce as the relative energy equation as Eq. 2.4 and its equilibrium equation will be summarized form which is illustrated as in Eq. 2.5:

$$\frac{m\left(\dot{v}\right)^2}{2} + \int c\dot{v}dv + \int f_s dv = -\int m\ddot{v}_g dv \tag{2.4}$$

$$E_i' = E_k' + E_d + E_s + E_h \tag{2.5}$$

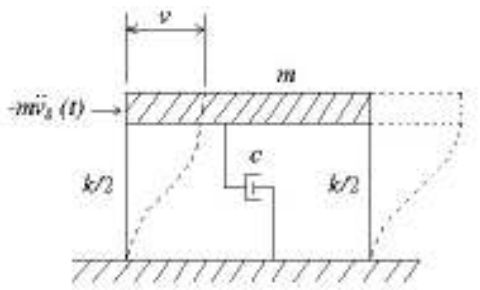

Fig. 2.2: Equivalent fixed-base system

It clearly differs on the input energy term between Eqs. 2.2 and 2.4. Obviously, the relative energy equation physically depends on the static equivalent lateral force, $\int m\ddot{v}_g dv$, while the absolute energy equation relies on $\int (m\ddot{v}_t)\, dv_g$ term. Uang and Bertero (1988) investigated the physical meaning of each term in these two energy balance equations. They found that at some specific ductility ratio the input energy demands calculated by these equations are significantly different. Especially, underestimating the maximum input energy may occur using relative energy for long period structures. Therefore, they have inferred that the absolute energy equation is more meaningful.

Plots of sample SDOF system can be illustrated; relative energy and absolute energy in Figs. 2.3 and 2.4, respectively, noting that D.E. = damping energy; H.E. = hysteretic energy; K.E. is kinetic energy; and S.E. = strain energy. The mass of system is 70.2 kips mass, 3 % critical damping, elastro-plastic material with stiffness of 140 kip/in along with 3% strain hardening and yielding strength of 15 kip. It is subjected to the

1940 Imperial Earthquake - El Centro. The SDOF program, NONLIN, has been used to perform the nonlinear dynamic time history analysis. The program is obtained from the Federal Emergency Management Agency (FEMA) and is available free at their website.

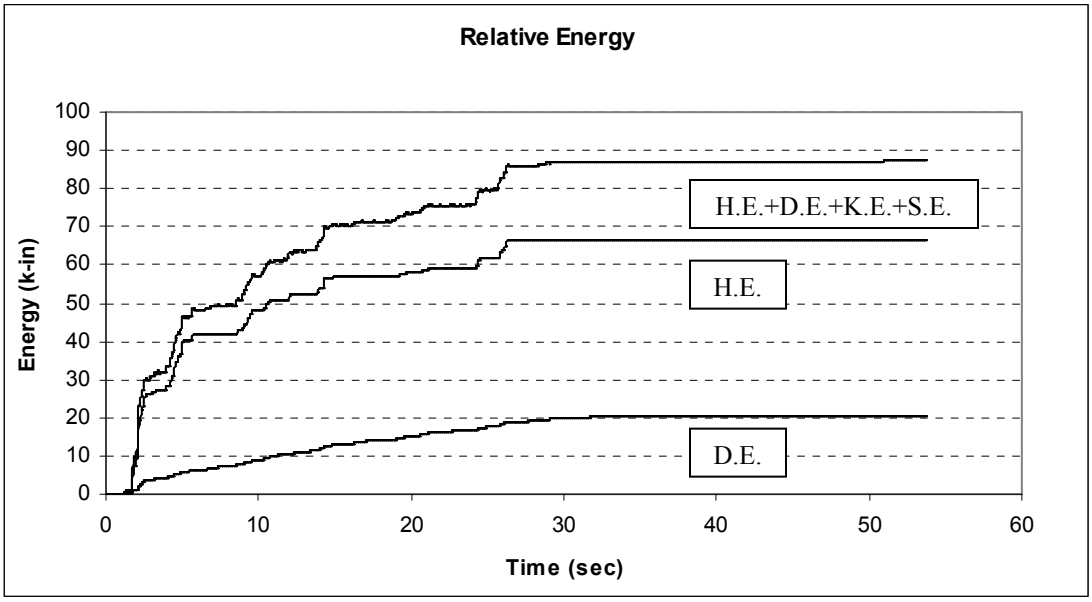

Fig. 2.3: The relative energy plot for SDOF system.

So far, an absolute energy equation for Multi-Degree-of-Freedom (MDOF) system can directly derive based on the described SDOF system as the following:

$$\frac{1}{2}\dot{V}_t^T M \dot{V}_t + \int \dot{V}^T C dV + \int F_s^T dV = \int \left(\sum_{i=1}^{N} M_i \ddot{V}_{ti} \right) dv_g \qquad (2.6)$$

Where M , C , and V are the diagonal mass matrix, viscous damping matrix, and relative

displacement matrix, respectively; m_i is the lumped mass subjected to i^{th} floor, $\ddot{v}$ is the absolute acceleration at the i^{th} floor.

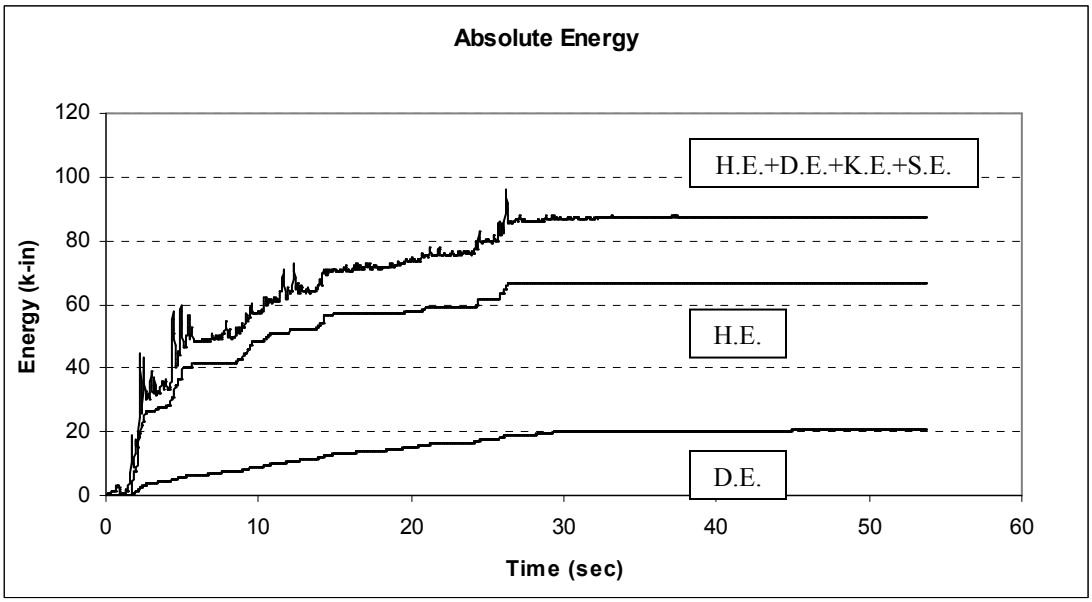

Fig. 2.4: The absolute energy plot for SDOF system.

However, it clearly shows that the total energy input transmitted to the structure can be dissipated by two ways, damping energy and hysteretic energy. Only the amount of the dissipated energy due to the inelastic deformation is considered to damage the structure subjected to seismic action. Related to these criteria, structure collapse can be alternately explained as a lack of ability to dissipate hysteretic energy through inelastic deformation. Afterward, hysteretic energy is used as design parameter in energy design among many researchers, Akiyama (1985), Leelataviwat et al (1999), and R. Estes

(2003). In RC structures, hysteretic energy also seems to be a suitable parameter due to representing cumulative nonlinear responses such as cracking and plastic hinging of the ductile members.

Many researchers have optionally employed this hysteretic energy to be part of a measure for component, story, and overall damage levels as seen in Park and Ang (1984), Kunnath et al. (1992). It indicates the capabilities of structural members to withstand and dissipate this energy during an earthquake.

To determine the design energy input, many researchers have developed their own procedures, Housner (1956), Zahrah and Hall (1984), Akiyama (1985), Uang and Bertero (1988), Fajfar, Vidic and Fischinger (1989), Mollaioli and Decanni (1998), and Manfredi (2001). However, in this thesis it will be obtained by inelastic dynamic time history analysis program named as IDARC version 4.0 which licensed from the State University of New York at Buffalo.

Chapter 3

Collapse Mechanism and Energy Consideration in Structural Frame

Although most structural design is currently based on elastic analysis, it is inadequate in providing information such as the collapse loads and the modes of collapse at present, growing demands in limit-state design allow many researchers to concentrate on an inelastic analysis method like plastic design. The advantage of plastic analysis is the ability to determine the collapse load equation of a structure by accounting for each possible collapse mechanism after the resisting capacities of its members have been determined. The plastic design concept has an important role in the energy-based design concept. It transforms the significant collapse mechanisms of the structural frame into constraint equations for optimized design purposes.

The main objective of this chapter is to introduce the fundamental concepts for plastic design methodology: how the collapse mechanism and its related collapse loads can be derived subject to the structural frame: how these collapse mechanisms relate to a multi-story frame: how each the collapse mechanisms become the energy terms. The simplified energy equations corresponding to the plastic design concept are derived and included at the end. All of these will subsequently form a solid foundation for the energy-based design concept in the later chapter.

3.1 The Collapse Load in Plastic Design

A simply supported beam with the mid-span concentrated load as shown in Fig. 3.1 is selected as a fundamental model to demonstrate how the plastic design concept analyzes a collapse load of the system. The corresponding force and deformation relationship of this beam section is defined and illustrated in Fig. 3.2. It may be commonly known as elastic-perfectly plastic relationship. The elastic deformation and corresponding bending moment increases at mid-span during slowly increasing of load P from point O to point A. After the maximum moment capacity of the section is reached at point A, the elastic deformation will shift to plastic deformation. This time, rotation (θ) continuously increases without increase in the bending moment (M). The bending moment at point A is called as plastic moment (M_P) while its related section behavior is referred to as a plastic hinge as shown in Fig. 3.3. Note, the plastic hinge location can be graphically demonstrated as dot in Fig. 3.3 which is an assumption of the method. In actuality the plastic hinge is spread over a finite length.

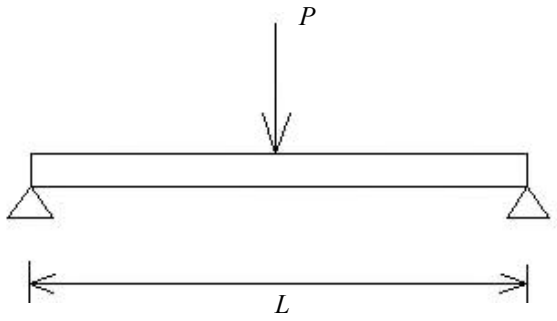

Fig. 3.1: Simple support beam with load at mid-span

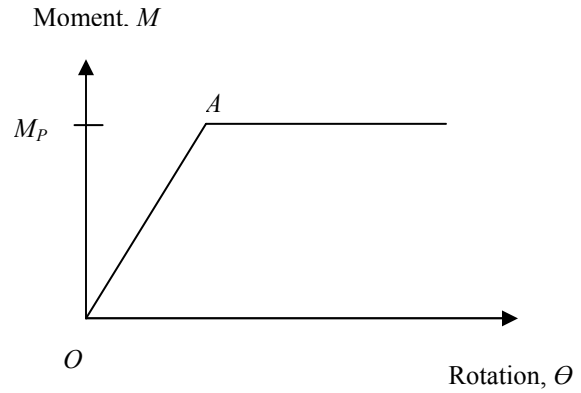

Fig. 3.2: Elastic-perfectly plastic relationship

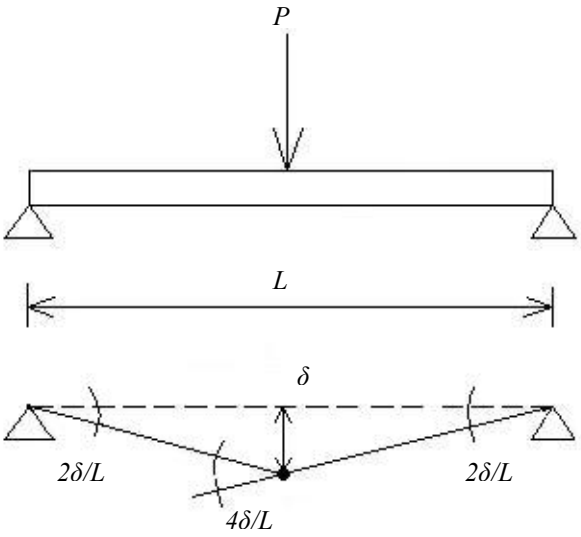

Fig. 3.3: Deformation after yielding has been reached

As illustrated in Fig. 3.3, based on the value of the collapse load of the simple beam can be developed as the following page by equating external work to internal strain energy represented by rotation if the plastic hinge.

$$P\delta = M_P(4\delta / L) \tag{3.1}$$

Afterward, the collapse load can be directly obtained as the following:

$$P = \frac{4M_P}{L} \tag{3.2}$$

However, Heyman (1971) stated that the above relation would be correct under the assumption that the elastic deflection of the beam is small compared with the subsequent plastic deflections. With a larger system like a structural frame, more load consideration may be taken into account compared to beam and column. Several collapse loads appear. As shown in Fig.3.4a, a simple frame is acted on by two independent loads, gravity load (P) and lateral load (V). They induce up to three possible collapse mechanisms; one is for gravity load, another is for lateral load, and the other is for combined gravity and lateral loads. The gravity load causes a beam mechanism while lateral load develops a sway mechanism to the frame. Both are considered independently as shown in Figs. 3.4b and 3.4c, respectively. The combined mechanism developed by these two independent mechanisms can be accounted for as illustrated in Fig. 3.4d.

Referring to the methods for simple supported beam mentioned earlier, the collapse loads corresponding to single bay frame can be similarly and directly developed as the following page:

- Independent mechanism

Beam mechanism:

$$P = \frac{8M_P}{L} \tag{3.3}$$

Sway mechanism:

$$V = \frac{4M_P}{H} \tag{3.4}$$

- Combined mechanism

$$P\delta_P + V\delta_H = 6M_P\theta \tag{3.5}$$

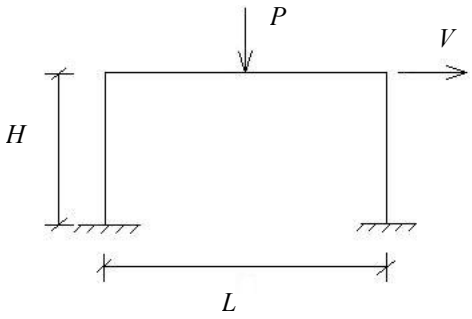

Fig. 3.4a

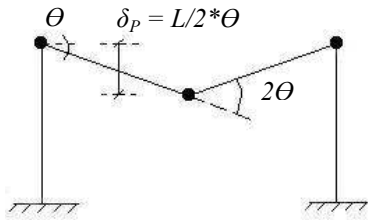

Fig. 3.4b

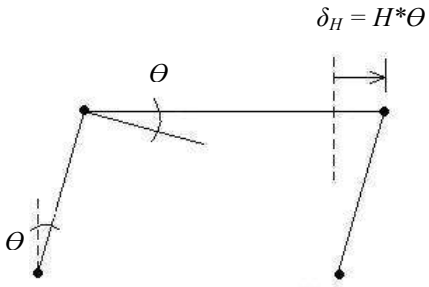

Fig. 3.4c

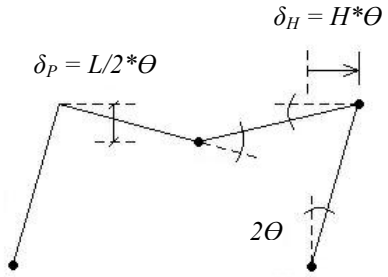

Fig. 3.4d

Fig. 3.4: Possible failure mechanisms for one story frame

Alternatively, the above collapse loads can be explained in graphically demonstrated as in Fig. 3.5. A point lying inside the boundary represents a combination of load without collapse state. The point lying on the boundary represents a state of collapse for the frame while a point outside the boundary means over loading.

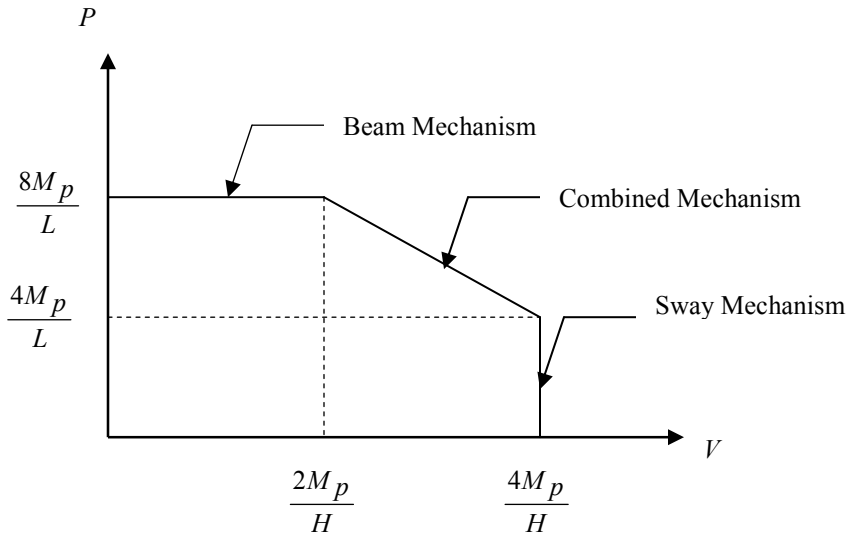

Fig. 3.5: Collapse load envelope related to one story frame

3.2 Energy Consideration in Structural Frame

Referring to plastic design methodology, the external work can be obtained as the product of the external load and its corresponding displacement (δ). The internal work is the sum of the plastic moment capacities times their plastic rotations. Assuming the geometrical shape of structural elements in collapse mechanisms does not change during loading, it results in the equality between an internal work and an external work. Within

this thesis, design input energy is introduced and equated to the internal or external work along with suitable acceptance criteria to obtain the required plastic moment capacity of the members.

For example, the sway mechanism in Fig. 3.4 c, the external work can be directly obtained as the product of the lateral load (V) and the related displacement ($H\theta$). The internal work is the summation of four existing locations of plastic hinge moment (M_P) multiplied by their related rotations (θ).

Up to this point, the stability of the structure can be explained alternatively depending on its ability to dissipate the design input energy through deformations in structural elements such as beams and columns without collapse of structure.

3.3 Collapse Mechanisms and Energy Consideration of Multistory Frame

Consider the four-story moment frame in Fig. 3.6a; it is acted on by several lateral and gravity loads. There are four possible collapse mechanisms, beam mechanism, two side-sway mechanisms and combined mechanism, to select and consider. In the case that lateral force is small compared to gravity load, the structural collapse due to beam mechanism as shown in Fig. 3.6b will control. Otherwise, if only lateral load which causes the frame side-sway controls, there are two collapse mechanisms; strong beam-weak column and strong column-weak beam as demonstrated as in Figs. 3.6c and 3.6d, respectively. However, to account for a combination of side sways and beam mechanisms, the combined mechanism, as shown in Fig. 3.6e has to be included.

Referring to the plastic design concept; the bending moment that causes a plastic hinge to form in structural elements is defined as plastic moment (M_p). From a design point of view, in a reinforced concrete structure, it is convenient to set the ultimate moment capacity of the reinforced concrete section equal to the plastic moment at the hinge location. Its benefits will become suitable in optimization design in the later chapters.

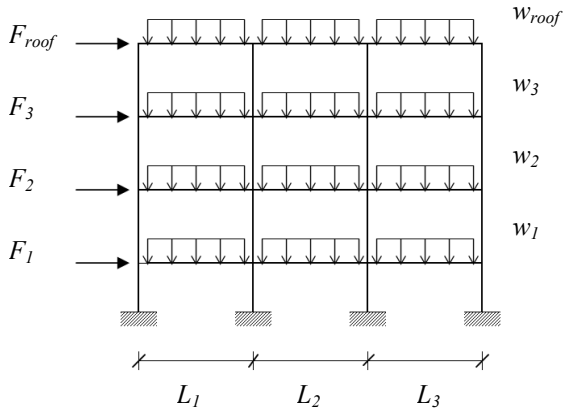

Fig 3.6a: Four story building acted by external force

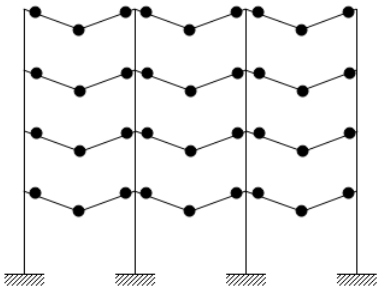

Fig 3.6b: Beam mechanism

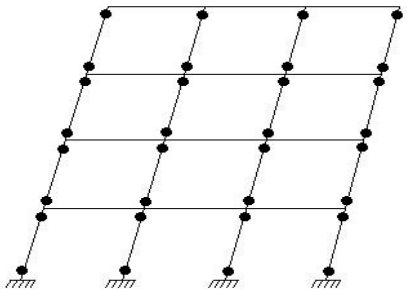

Fig 3.6c: Strong beam-weak column mechanism

Fig. 3.6: Collapse mechanisms related to four-story building

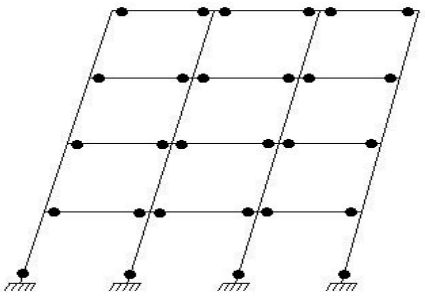

Fig 3.6d: Strong column-weak beam mechanism

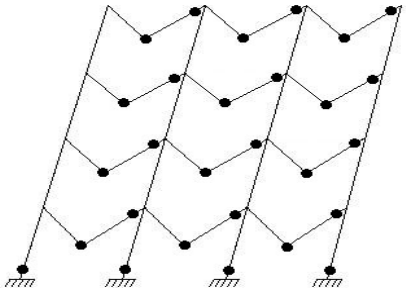

Fig 3.6e: Combined mechanism

Fig. 3.6: Continued

Consideration of a large multistory frame, allows many possible collapse mechanisms and many constraint equations, whose solutions are overly cumbersome to achieve. A safe method was proposed after Ridha and Wright (1967). One story at a time is considered beginning with the uppermost story. In each story, the gravity loads, the lateral loads for the upper stories, and the column axial loads and moments from the upper story are considered. The safe design at each story occurs if all external work, which includes effects from the story itself and upper stories above, are equal to the internal work.

The defined plastic moment at each hinge location is shown in Fig. 3.7: subscript (BE = section at beam end, BM = section at beam middle, CE = exterior column, CI = interior column, CEA = exterior column (above), CIA = interior column (above); super subscript (TOP = top steel bars, BOT = bottom steel bars) and N means number of bay.

Following the above concept for a typical building frame, assuming all bays keep the same span as L and beam size remains constant at a particular story level, the

collapse mechanisms for each story level will be as shown in Figs. 3.8 through 3.10. The derived internal work and external work can be obtained as in Eqs. 3.8 through 3.19. The left hand side of each equation represents internal work while external work is on the right hand side.

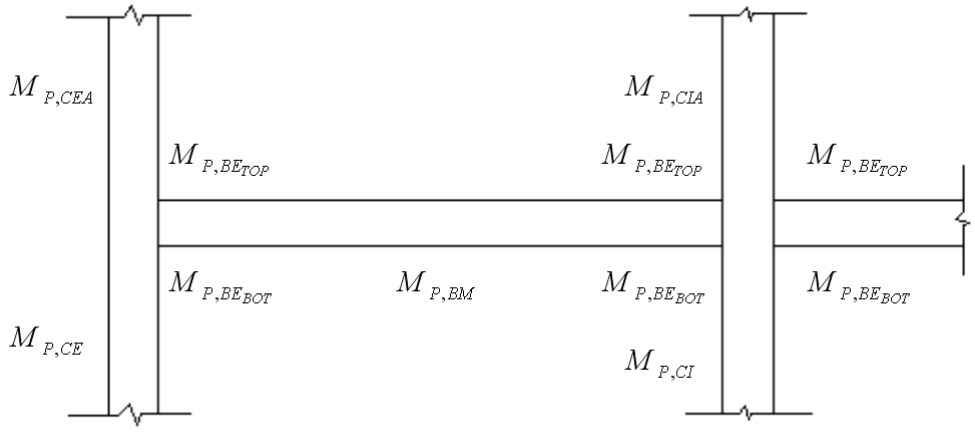

Fig. 3.7: Defined bending moment locations

- Roof level

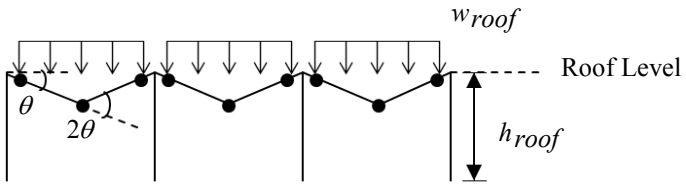

Fig 3.8a

Fig. 3.8: Collapse mechanisms at roof level

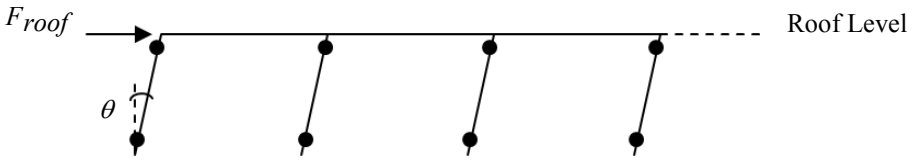

Fig 3.8b

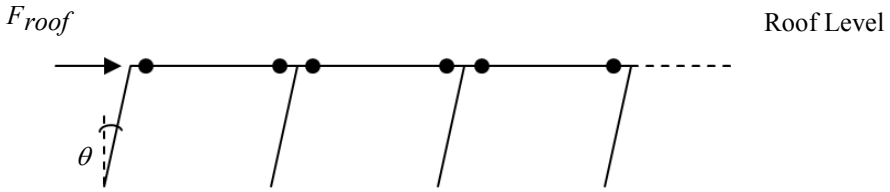

Fig 3.8c

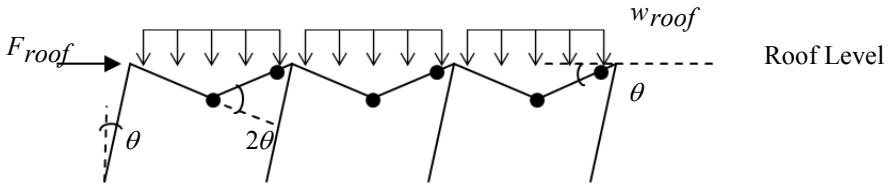

Fig 3.8d

Fig. 3.8: Continued

1. Beam Mechanism (refer to Fig. 3.8a)

$$N(2M_{P,BE_{TOP}} * \theta + M_{P,BM} * 2\theta) = N\left(w_{roof} * \theta * \frac{L^2}{4}\right) \qquad (3.6)$$

2. Strong Beam-Weak Column Mechanism (refer to Fig. 3.8b)

$$(N-1)M_{P,CI} * 2\theta + 2 * M_{P,CE} * 2\theta = F_{roof} * h_{roof} * \theta \qquad (3.7)$$

3. Strong Column-Weak Beam Mechanism (refer to Fig. 3.8c)

$$(N-1)M_{P,CI} * \theta + 2M_{P,CE} * \theta + N(M_{P,BE_{TOP}} * \theta + M_{P,BE_{BOT}} * \theta) = F_{roof} * h_{roof} * \theta \tag{3.8}$$

4. Combined Mechanism (refer to Fig. 3.8d)

$$(N-1)M_{P,CI} * \theta + 2M_{P,CE} * \theta + N(2M_{P,BE_{TOP}} * \theta + M_{P,BM} * 2\theta) = N\left(w_{roof} * \theta * \frac{L^2}{4}\right) + F_{roof} * h_{roof} * \theta \tag{3.9}$$

- Inter-story level

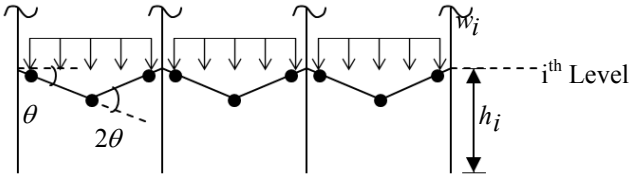

Fig 3.9a

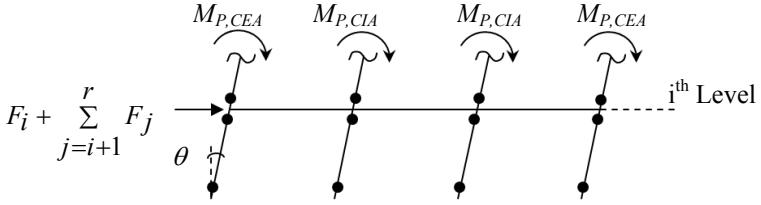

Fig 3.9b

Fig. 3.9: Collapse mechanisms at inter-story level

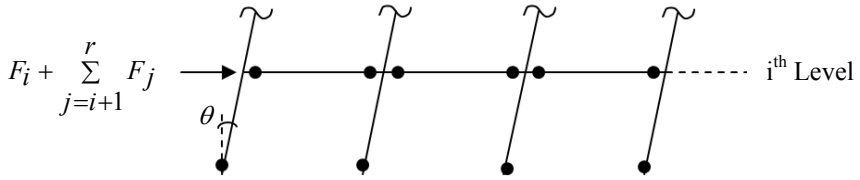

Fig 3.9c

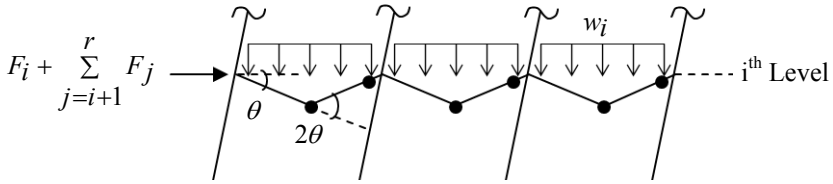

Fig 3.9d

Fig. 3.9: Continued

1. Beam Mechanism (refer to Fig. 3.9a)

$$N(2M_{P,BE_{TOP}} * \theta + M_{P,BM} * 2\theta) = N\left(w_i * \theta * \frac{L^2}{4}\right) \tag{3.10}$$

2. Strong Beam-Weak Column Mechanism (refer to Fig. 3.9b)

$$(N-1)(2M_{P,CI} * \theta) + 2M_{P,CE} * 2\theta - (N-1)M_{P,CIA} * \theta - 2M_{P,CEA} * \theta = \left(F_i + \sum_{j=i+1}^{r} F_j\right) * h_i * \theta \tag{3.11}$$

3. Strong Column-Weak Beam Mechanism (refer to Fig. 3.9c)

$$(N-1)M_{P,CI} * \theta + 2M_{P,CE} * \theta + N(M_{P,BE_{TOP}} * \theta + M_{P,BE_{BOT}} * \theta) = \left(F_i + \sum_{j=i+1}^{r} F_j\right) * h_i * \theta \quad (3.12)$$

$r = total\ story\ level$

4. Combined Mechanism (refer to Fig. 3.9d)

$$(N-1)M_{P,CI} * \theta + 2M_{P,CE} * \theta + N(M_{P,BM} * 2\theta + 2M_{P,BE_{TOP}} * \theta) = N\left(w_i * \theta * \frac{L^2}{4}\right) + \left(F_i + \sum_{j=i+1}^{r} F_j\right) * h_i * \theta \quad (3.13)$$

Where $r = total\ story\ level$

- Ground level

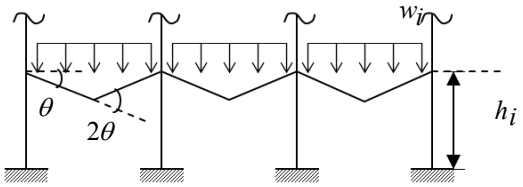

Fig. 3.10a

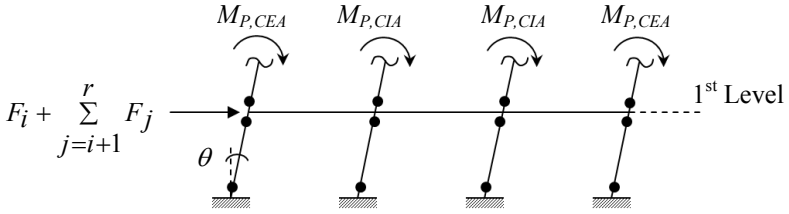

Fig. 3.10b

Fig. 3.10: Collapse mechanisms at ground level

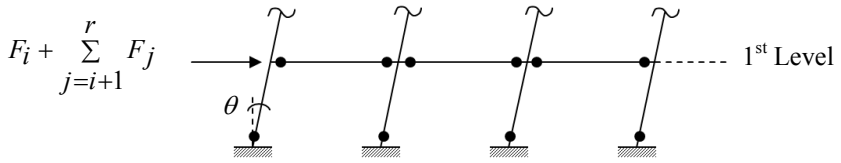

Fig. 3.10c

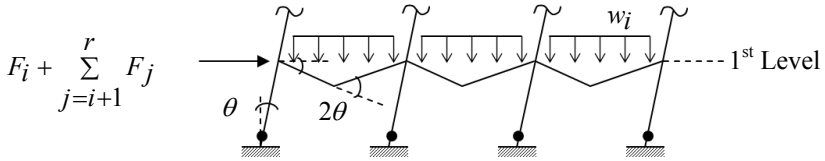

Fig. 3.10d

Fig. 3.10: Continued

1 Beam Mechanism (refer to Figure 3.10a)

$$N(2M_{P,BE_{TOP}} * \theta + M_{P,BM} * 2\theta) = N\left(w_1 * \theta * \frac{L^2}{4}\right) \tag{3.14}$$

2. Strong Beam-Weak Column Mechanism (refer to Fig. 3.10b)

$$(N-1)(2M_{P,CI} * \theta) + 2M_{P,CE} * 2\theta - (N-1)M_{P,CIA} * \theta - 2M_{P,CEA} * \theta = \left(F_1 + \sum_{j=2}^{r} F_j\right) * h_1 * \theta \tag{3.15}$$

3. Strong Column-Weak Beam Mechanism (refer to Fig. 3.10c)

$$N(M_{P,BE_{TOP}} * \theta + M_{P,BE_{BOT}} * \theta) + 2(M_{P,CE} * \theta) + (N-1)M_{P,CI} * \theta = \left(F_i + \sum_{j=i+1}^{r} F_j\right) * h_i * \theta \quad (3.16)$$

4. Combined Mechanism (refer to Fig. 3.10d)

$$N(M_{P,BM} * 2\theta + 2M_{P,BE_{TOP}} * \theta) + 2(M_{P,CE}) * \theta + (N-1)M_{P,CI} * \theta = N\left(w_i * \theta * \frac{L^2}{4}\right) + \left(F_1 + \sum_{j=2}^{r} F_j\right) * h_1 * \theta \quad (3.17)$$

Where $r = total\ story\ level$

Obviously, the sway mechanisms demonstrate as in Eqs. 3.7 through 3.9, 3.11 through 3.13, and 3.15 through 3.17, which their external works by lateral loads of story above are accounted. However, as seen in Figs. 3.9b and 3.10b, plastic hinges are located on above columns also, the internal work resulted by upper columns require to include as in Eqs. 3.11 and 3.15.

For energy-based design, Housner (1956) inferred that the external work could suitably be replaced by the design energy demand as discussed in chapter 2. As a result, the Eqs. 3.6 through 3.17 represent collapse mechanisms can be replaced their external works by the design energy demands. Then, the structural design can be performed afterward. The details to clarify how these revised equations can be obtained and applied to reinforced concrete frame design based on energy-based concept will be presented in later chapters.

Chapter 4

Optimal Design of Reinforced Concrete Frame

The design procedure for RC frames based on energy-based concept, the procedure can be summarized as shown in Fig. 4.1. However, two important procedures are required to accomplish this: I) analyze the minimum required bending moments for each structural element (section 4.1); II) the optimized design of beam or column elements corresponding to the results from part I (section 4.2). Within part I, suitable equations from the collapse mechanisms developed in chapter 3 and practical and code consideration for RC structures mentioned later in this chapter, will be transformed into constraint equations that relate to structural elements for optimal design considering energy demand and code requirements. A suitable objective equation that attempts to minimize the cost relative to these constraint equations will be considered. Finally, required minimum bending moments for each beam and column are the results. In part II, the results from part I will be carefully considered for each member element before the determination of optimal design for beam and column sizes and related reinforcement are selected.

The purpose of this chapter is to clarify the above procedure in details. It will show how to select and obtain the energy demand which is suitable for the RC structure: how to derive the appropriate constraint equations subject to the collapse mechanism, inclusion of practical and code considerations, and energy demands. Moreover, to

enhance more understanding of this basic concept, the design of simple two-story one bay RC frame will be presented within this chapter.

4.1 Minimize the Required Bending Moments for Each Structural Member

To obtain the required bending moments, the objective equation, the energy constraint equations subjected to collapse mechanisms from chapter 3 and practical and code consideration need be satisfied. The objective equation is to minimize cost of structural element. In this thesis, cost is represented as a function of bending moments and their related locations. To obtain the optimized solutions, the simplex method is used to perform. However, the simplex method concepts are explained in details as shown in Appendix section B.

4.1.1 Constraint Equations

- Energy constraints

As mentioned earlier, a suitable set of collapse mechanism equations as shown in Chapter 3 (Eqs. 3.6 through 3.17) will be selected and considered. Seismic energy demand will replace the right hand side of each collapse mechanism equation as external energy. These revised equations are then transformed into energy constraint equations. Referring to Fig. 3.6b in Chapter 3, if only the beam mechanism controls the system, then the energy demand is directly obtained by a product of gravity loads and their corresponding displacements. In the rest of the mechanisms shown in Figs. 3.6c through

3.6e, the side-sway of the frame due to the lateral seismic loads plays an important role in the system behavior. This will clearly be shown in later section.

Related works by A. Teran (2001), indicated that plastic energy seems to be an appropriate design parameter that matches with the earthquake-resistant design purpose. Its benefits include consideration of the cumulative plastic deformation demands that account for both earthquake magnitude and duration. Then plastic deformation energy will be suitably considered as energy demand. However, as discussed earlier in Chapter 2, the input energy from the earthquake can be dissipated through two mechanisms; hysteretic energy and damping energy. Hysteretic energy is more meaningful in energy-based design because it can represent how much the structure needs to deform through inelastic deformation related to damage. It can appropriately explain the damage of the structure as used in researchers such Park and Ang (1984), Kunnath et al. (1992). The ability to dissipate the hysteretic energy is directly dependent on member size and reinforcement. Therefore, it is reasonable to consider the hysteretic energy as energy demand within this thesis.

Obviously, related to the constraint equations, the energy demand plays a very important role in this energy-based design. It determines how much energy capacity the beams and columns need to be designed to effectively dissipate the corresponding energy demands for a specific type of structure. Larger required energy dissipation requires more energy capacity of the corresponding member. However, to obtain the reliable energy demand, selecting a suitable design earthquake ground motion is very important.

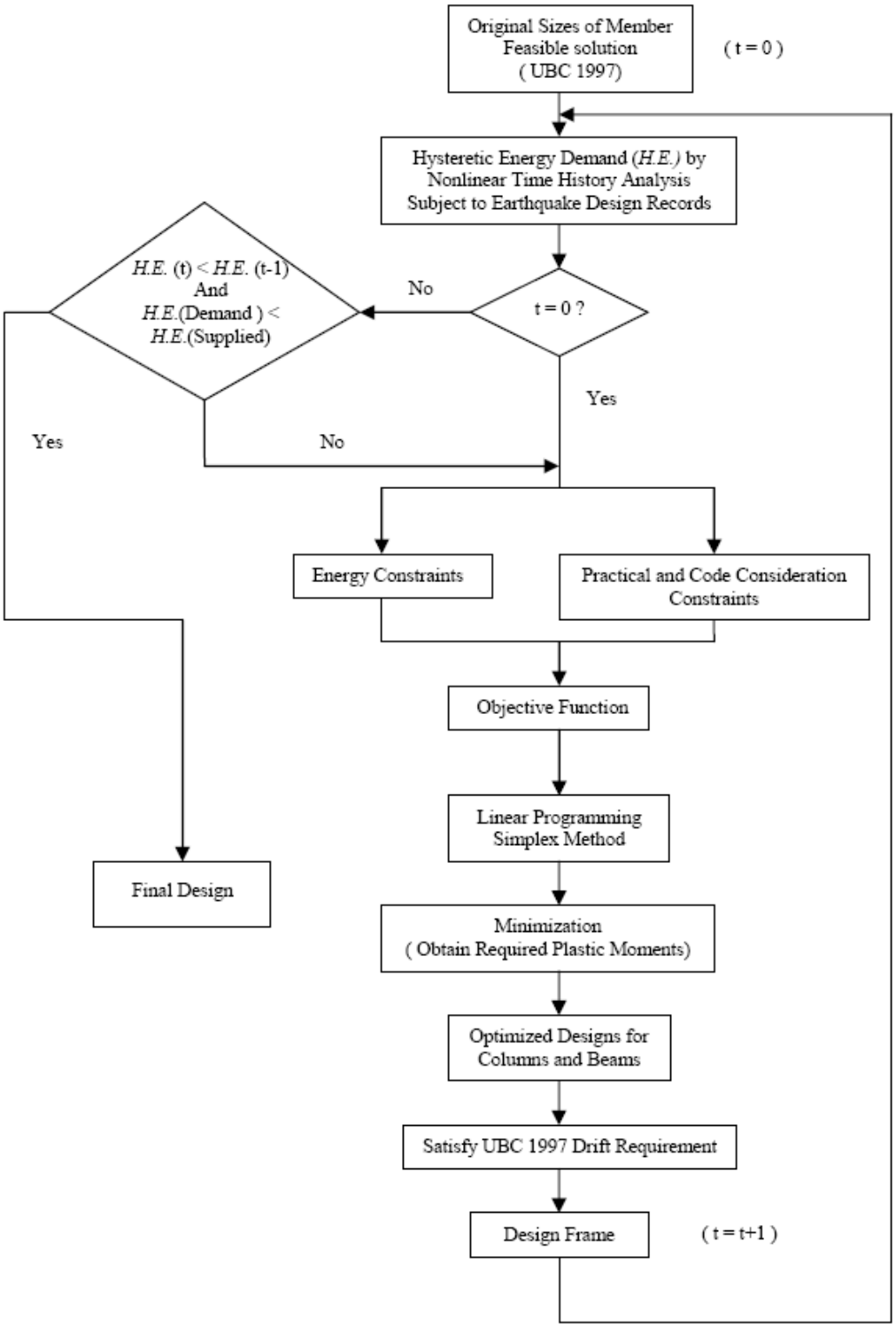

Fig. 4.1: Energy-based design flowchart for RC moment frame

In this thesis, originally RC frame is designed and satisfied subject to the requirement of UBC 1997. To obtain the required hysteretic energy demands used for energy-based design for this RC frame, the frame will be performed nonlinear time history analysis subjects to two sets of records, SAC LA10/50 records and SAC Near Fault records. The SAC LA 10/50 records represent 20 far field modified ground records whose probabilities of exceedence represent 10% in 50 years for the Los Angeles region. The SAC Near Fault records are the set of 20 ground motions corresponding to near-source motion on firm ground, which can be developed in UBC Seismic Zone 4. These sets of records are all derived from historical recordings or from physical simulations. The details of these records are summarized in Tables 4.1 and 4.2 and their corresponding plots in the Appendix, Figs. A.1 and A.2.

Nevertheless, the energy capacity that has been mentioned earlier (see Eqs. 3.7-3.9, 3.11 - 3.13, and 3.15 - 3.17) is based on static energy while the hysteretic energy obtained from nonlinear time history analysis is a cyclic energy. A relationship between these two energies is required. Following ATC 40 for the analysis of existing concrete buildings (ATC, 1996), which develops a methodology for constructing the inelastic response spectra, it recommends:

$$\text{Static Plastic Energy} = \text{Hysteretic Energy} / 4$$

Or

$$\text{Hysteretic Energy} = 4 * \text{Static Plastic Energy}$$

Table 4.1: SAC LA10/50 records

SAC Name	Record	Earthquake Magnitude	Distance (km)
LA01	Imperial Valley, 1940, El Centro	6.9	10
LA02	Imperial Valley, 1940, El Centro	6.9	10
LA03	Imperial Valley, 1979, Array #05	6.5	4.1
LA04	Imperial Valley, 1979, Array #05	6.5	4.1
LA05	Imperial Valley, 1979, Array #05	6.5	1.2
LA06	Imperial Valley, 1979, Array #05	6.5	1.2
LA07	Lenders, 1992, Barstow	7.3	36
LA08	Lenders, 1992, Barstow	7.3	36
LA09	Lenders, 1992, Yermo	7.3	25
LA10	Lenders, 1992, Yermo	7.3	25
LA11	Loma Prieta, 1989, Gilroy	7	12
LA12	Loma Prieta, 1989, Gilroy	7	12
LA13	Northridge, 1994, Newhall	6.7	6.7
LA14	Northridge, 1994, Newhall	6.7	6.7
LA15	Northridge, 1994, Rinaldi RS	6.7	7.5
LA16	Northridge, 1994, Rinaldi RS	6.7	7.5
LA17	Northridge, 1994, Sylmar	6.7	6.4
LA18	Northridge, 1994, Sylmar	6.7	6.4
LA19	North Palm Springs, 1986	6	6.7
LA20	North Palm Springs, 1986	6	6.7

Table 4.2: SAC Near Fault records

SAC Name	Record	Earthquake Magnitude	Distance (km)
NF01	Tabas, 1978	7.4	1.2
NF02	Tabas, 1978	7.4	1.2
NF03	Loma Prieta, 1989, Los Gatos	7	3.5
NF04	Loma Prieta, 1989, Los Gatos	7	3.5
NF05	Loma Prieta, 1989, Lex. Dam	7	6.3
NF06	Loma Prieta, 1989, Lex. Dam	7	6.3
NF07	C. Mendocino, 1992, Petrolia	7.1	8.5
NF08	C. Mendocino, 1992, Petrolia	7.1	8.5
NF09	Erzincan, 1992	6.7	2
NF10	Erzincan, 1992	6.7	2
NF11	Landers, 1992	7.3	1.1
NF12	Landers, 1992	7.3	1.1
NF13	Northridge, 1994, Rinaldi	6.7	7.5
NF14	Northridge, 1994, Rinaldi	6.7	7.5
NF15	Northridge, 1994, Olive View	6.7	6.4
NF16	Northridge, 1994, Olive View	6.7	6.4
NF17	Kobe, 1995	6.9	3.4
NF18	Kobe, 1995	6.9	3.4
NF19	Kobe, 1995, Takatori	6.9	4.3
NF20	Kobe, 1995, Takatori	6.9	4.3

The national guidelines for Prestandard and Commentary for the Seismic Rehabilitation of Buildings (FEMA 356) by Federal Emergency Management Agency (FEMA) has provided the new design criteria and standard procedures for rehabilitation of existing building based on performance-based methodology. Note, FEMA 356 replaced the Guidelines for Seismic Rehabilitation of Buildings (FEMA 273) with converting it into mandatory language. The idea is new which allows the building owner or designer to select their desired building performance level before performing analysis with appropriate earthquake records. The performance is mainly categorized into three levels, 1) Collapse Prevention (CP), 2) Life Safety (LS) and 3) Immediate Occupancy (IO). The descriptions related to each performance level explain in Table 4.3. Each level has specifically acceptance of criteria as a target to be achieved. The criteria are specified by actual laboratory test results along with engineering judgment of various development teams. See Figs. A.3 and A.4 in Appendix section A for the acceptance criteria for nonlinear procedure for reinforced concrete beam and column, respectively. Modeling parameters related to Figs. A.3 and A.4 are obtained from Fig. A.5 in Appendix section A.

Fig. I.5 demonstrates the criteria for deformation-controlled actions in any of the four basic material types. Linear response is depicted between point A and an effective yield point B. The slope from B to C represents phenomena such as strain hardening. C represents strength of the component. Strength degradation starts from point C to point D. Beyond point D, the component responds with substantially reduced strength to point

E. At deformation greater than point E, the component strength is zero. Then parameters a, b, and c can be derived from this deformation-controlled actions.

In this thesis, two design performances, CP and LS are selected and considered. CP is represented by SAC Near Fault and LS is represented by SAC LA 10/50. Referring to Figs. A.3 and A.4, the acceptance criteria for plastic rotation (θ_p) for reinforced concrete columns and beams subject to the Collapse Prevention (CP) performance level is selected and considered. The value of 0.025 radians is a reasonable and suitable choice. Up to now, all parameters for deriving collapse mechanism constraint equations can be obtained.

Table: 4.3: Interpretation of overall damage index (Park et al., 1986)

Type	**Collapse Prevention (CP)**	**Lift Safety (LS)**	**Immediate Occupancy (IO)**
Primary	Extensive cracking and hinge formation in ductile elements. Limited cracking and/or splice failure in some nonductile columns. Severe damage in short columns.	Extensive damage to beams. Spalling of cover and shear cracking (<1/8″ width) for ductile columns. Minor spalling in nonductile columns. Joint cracks <1/8″ wide	Minor hairline cracking. Limited yielding possible at a few locations. No crushing (strains below 0.003).
Secondary	Extensive spalling in columns (limited shortening) and beams. Severe joint damage. Some reinforced buckled.	Extensive cracking and hinge formation in ductile elements. Limited cracking and/or splice failure in some nonductile columns. Severe damage in short columns.	Minor spalling in a few places in ductile columns and beams. Flexural cracking in beams and columns. Shear cracking in joints < 1/16″ width.
Drift	4% transient or permanent	2% transient; 1% permanent	1% transient; negligible permanent

- Practical and Code Constraints

The American Concrete Institute (ACI) has provided the latest Building Code to assist structural engineers in designing and detailing requirements for reinforced concrete structures. As a useful background, it has been extensively adopted by many present building codes. The 1997 Uniform Building Code (UBC) issued by ICBO included and modified some sections of ACI 318-95 for seismic design provision. Beyond the scope of this thesis, it may be necessary to consider and add some sections of these requirements as additional constraints within this optimization.

The combination of high moment capacity at the middle section of the beam with lower moment capacities at the ends may induce inelastic rotations that are too large. This causes cracks at the end of the beam that restricts the use of the high interior moment capacity to utilize the high interior moment capacity. It induces weak in column. To avoid this situation, the moment capacity at the end section should be set to be greater than or equal to the moment capacity at the middle section as indicated below:

$$M_{P,BE_{TOP}} - M_{P,BM} \geq 0 \qquad (4.1)$$

To prevent the total collapse of the structure due to side-sway mechanism, the ACI code limits plastic hinge formation to only occur at the end of beam instead of at the end of column known as strong column-weak beam criteria. The code indicates the following page:

$$\sum M_e \geq (6/5)\sum M_g \qquad \text{(ACI 1921.4.2)}$$

Where $\sum M_e$ is the sum of moments at the center of the joint, relative to the design flexural strength of the columns and $\sum M_g$ is the sum of moments at the center of the joint, relative to the design flexural strength of the girders. To satisfy the current work, the additional constraint equations based on this requirement can be directly included as the follows:

- Roof level (see Fig 4.2)

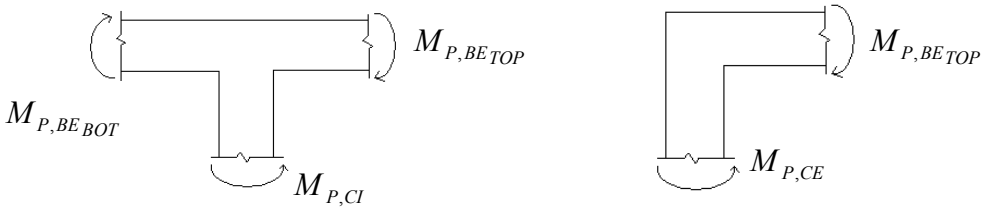

a) At interior column b) At exterior column

Fig. 4.2: Strong column-weak beam criteria at roof level

$$M_{P,CE} - (6/5)M_{P,BE_{TOP}} \geq 0 \qquad (4.2)$$

$$M_{P,CI} - (6/5)(M_{P,BE_{TOP}} + M_{P,BE_{BOT}}) \geq 0 \qquad (4.3)$$

- Inter-story level (see Fig. 4.3)

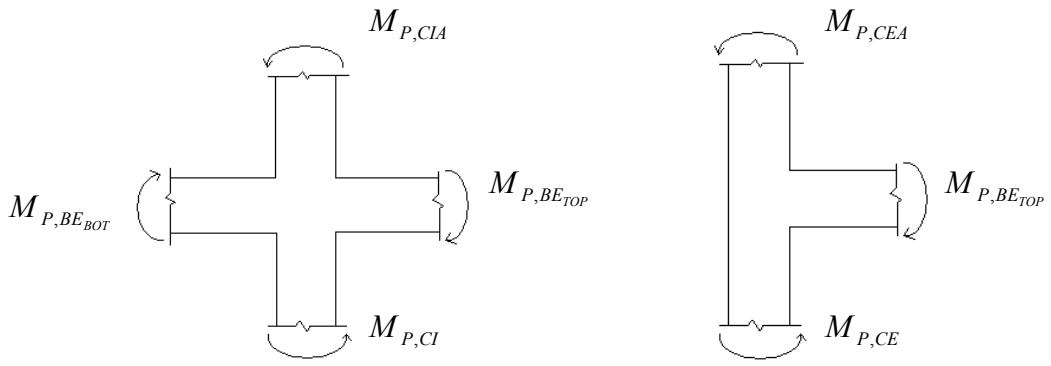

a) At interior column b) At exterior column

Fig. 4.3: Strong column-weak beam criteria at floor level

$$M_{P,CE} + M_{P,CEA} - (6/5)M_{P.BE_{TOP}} \geq 0 \qquad (4.4)$$

$$M_{P,CI} + M_{P,CIA} - (12/5)M_{P.BE_{TOP}} \geq 0 \qquad (4.5)$$

In the case of lateral load controlling, the maximum moments in the span usually occurs at the face of a column. To provide adequate moment resistance, ACI requires additional details according to section 21.3.2 as follows: 1) the positive moment strength at the face of the beam-column joint shall not be less than half the negative moment strength and 2) at every section the positive and negative moment capacity shall not be less than one-forth the maximum moment capacity provided at the face of either joint. Then, the additional constraint equations can be directly derived based on these requirements as shown below:

$$M_{P,BE_{BOT}} - (1/2)M_{P.BE_{TOP}} \geq 0 \qquad (4.6)$$

$$M_{P,BM} - (1/4)M_{P.BE_{TOP}} \geq 0 \qquad (4.7)$$

4.1.2 Objective Equation

Following the works by M.A. Gerlein and F.W. Beaufait (1980), their studies emphasized the optimized design in reinforced concrete frame based on a set of collapse mechanisms. To minimize the cost of the structural frame, they introduced an objective equation in terms of the required bending moments and their relative lengths. In this thesis, the moment capacities of a column (M_{CI}, M_{CE}) are assumed to extend full height at subject story and the moment capacities at the end of a beam (M_{BE}) are assumed to extend over 15% and 25% of span length from the face of exterior column and interior column, respectively. The moment capacities at the middle section of a beam (M_{BM}) controls over 75% of span length. Afterward, the objective equation for each story level can be derived in the following manner:

$$\begin{aligned} Z = {} & (0.30l_i + (N-1)*0.5l_i)*(M_{BE_{TOP}} + M_{BE_{BOT}}) + N(0.75l_i)*M_{BM} \\ & + (N-1)h_i * M_{CI} + 2h_i * M_{CE} \end{aligned} \qquad (4.8)$$

$$\begin{aligned} where \quad & N = number\ of\ bay \\ & l_i = length\ of\ span\ in\ i^{th}\ story\ level \\ & h_i = story\ height\ of\ i^{th}\ level \end{aligned}$$

4.2 Optimized Reinforced Concrete Beam and Column Design

Within this section, the beams and columns will be optimally designed based on the required bending moments and significant nonlinear responses analyzed in section 4.1. The related description will be illustrated as the following:

4.2.1 Optimized RC Beam Design

The optimized beam design will be obtained by setting the minimum costs of the reinforced concrete beam as the objective function with assigned cost of $ 6.75/ft^3 for concrete and $117.6/ft^3 for steel bar while the required bending moment and practical and code requirements for RC beam design as constraint functions are shown in the following list:

1. $\rho_{\min} = 0.003 \leq \rho \leq \rho_{\max} = 0.025$ (ACI 1921.3.2.1)
2. $1.0 \leq$ Beam width / depth ≤ 2.5
3. Beam width $\geq$ 10 in. & beam width $\leq$ column width.
4. 1" min. bar spacing and 1.5"concrete cover.

Iteration will be performed until optimized size is satisfied. At each iteration, ratio of reinforcement (ρ) will be diminutively increased to search for new-satisfied.

$$M = K_n F \tag{4.9}$$

$$F = \frac{bd^2}{12000}, K_n = f_c'\omega(1-\omega/1.7) \tag{4.10}$$

where $\omega = \rho f_y / f_c'$, b is width of beam section, d is depth of beam section, f_y is yield stress of reinforcement, and f_c' is concrete compressive strength.

The optimized design size should be directly obtained and selected from one of the satisfied sizes having a minimum cost. Note that the source code to perform this RC beam design is written in MATLAB and shown as in Appendix section III.

4.2.1 Optimized RC Column Design

The PCACOL program will be used for optimized RC Column design through out this thesis. Within the program, its task can be directly selected either investigation or design subject to specified design codes. In this thesis, design option which takes ACI code into account is elected as our main focus. Minimum and maximum allowable column size and bar size have to be defined together reinforcement pattern before design procedure will be performed. All Sides Equal option, which all the bars of the column are of one size, and the number of bars is the same on all four sides of a rectangular layout, is selected. Factored axial loads and bending moments are input to the program.

The program will automatically optimize the smallest column section with the least amount of reinforcement corresponding to the required bending moment and the axial load. For example, RC column with axial load of 600 kips and 200 ft-kip for bending moment enables to design. The ACI code restricts the maximum and minimum reinforcement to 6% and 1%, respectively. Bar #3 and #10 as min and max allowable bar sizes with clear cover of 1.5’ are defined to the program. The optimized RC column size

is illustrated as in Fig. 4.4. The size of 16"x16" with 10 # 10 bars and a steel percentage of 4.96 are produced.

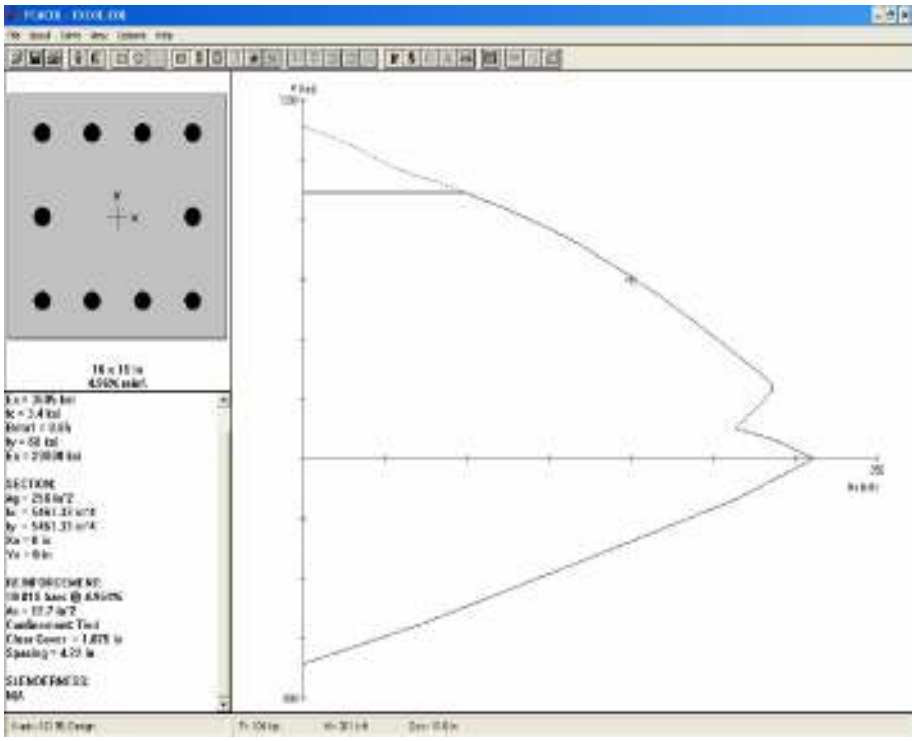

Fig. 4.4: The optimized RC column by PCACOL

4.3 Story Drift Consideration

To satisfy the UBC 97 drift requirements of the designed frame, an appropriate drift-design procedure should be selected and included in the design scheme. In this thesis, since all RC moment frames are restricted to low-rise to mid-rise frame, a significant portion of drift is caused by end rotations of beams and columns as shown in Fig 4.5. This phenomenon is commonly called as bent action.

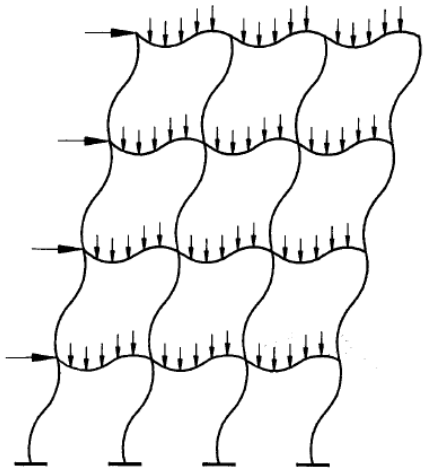

Fig. 4.5: Frame deformation caused by the bent action

Wong H. and El Nimeiri M. (1981) estimated the bent-action, Δ_{bi}, for any level i of a frame as the following:

$$\Delta_{bi} = \frac{(\Sigma V)_i h_i^2}{12E}\left(\frac{1}{(\Sigma K_g)_i} + \frac{1}{(\Sigma K_c)_i}\right) \qquad (4.11)$$

where $(\Sigma V)_i$ is story shear, $(\Sigma K_g)_i$ is summation of I_{gi}/L_{gi} for all girders, $(\Sigma K_c)_i$ is summation of I_{ci}/h_i for all columns, I_{gi} is individual girder moment of inertia, L_{gi} is individual bay length, I_{ci} is individual column moment of inertia, and h_i is story height.

Then, the ratio (Φ) of the actual story drift to the allowable story drift, Δ_a, can be obtained directly as in Eq. 4.12. To satisfy the drift requirement by 1997 UBC, the allowable drift in Eq. 4.12 can be substituted by the one from Eq. 4.13 which is defined

based on period of structure (T) and total structure height (h). Subsequently, the ratio (Φ) will indicate the acceptation on drift of frame, if the ratio (Φ) is less than 1.0, the designed frame is already adequate. Otherwise, the frame requires revising.

$$\Phi = \frac{\Delta_{bi}}{\Delta_a} \tag{4.12}$$

$$\Delta_a \le .025h \qquad for\ T \le 0.7$$

$$\Delta_a \le .020h \qquad for\ T > 0.7 \tag{4.13}$$

4.4 Example for Two-Story RC Moment Frame Design

The RC two-story frame shown in Fig. 4.6 will be revised based on energy-based concept. The original size of roof beam is 10"x 22" with ρ equal to 1.50 % and 0.75 % for top bars and bottom bars, respectively at end section and 0.9% at middle section. For floor beam, 12"x 26" with ρ equal to 1.3 % and 0.65 % for top bars and bottom bars, respectively at end section and 1.0 % at middle section. The size of 18"x18" with ρ = 4.38 % is for column. Uniform dead and live load for roof are 136 psf and 20 psf, respectively. For the 2nd floor level, 180 psf and 50 psf are dead load and live load, respectively. Tributary width is 15 ft. Assuming SAC LA01 (see Table 4.1) as design earthquake ground motion, after performing time history analysis for the frame, hysteretic energy demands become 504 k-in and 1061 k-in for the roof level and the 2nd floor level, respectively. The average axial force in column is 88 k.

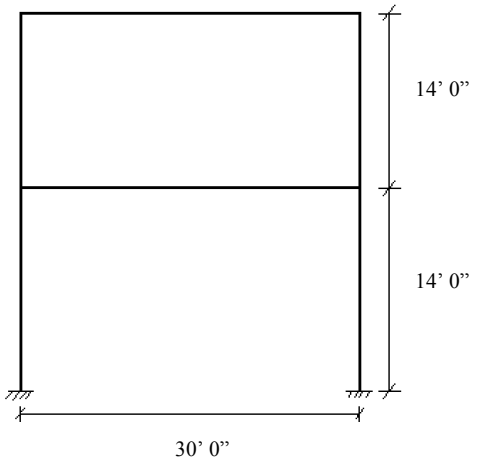

Fig. 4.6: The RC two-story frame

At roof level

The possible collapse mechanisms at this level are illustrated in Fig. 4.7. As the given information: hysteretic energy demand for this level is 504 k-in and 0.025 radians is the limit for plastic rotation, the constraint equations according to Eqs. 3.8 through 3.11of Chapter 3 can be derived as the following:

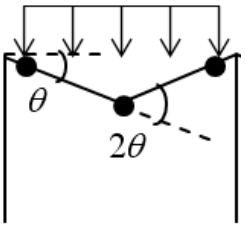

Fig. 4.7a

Fig. 4.7b

Fig. 4.7: Collapse mechanisms at roof level

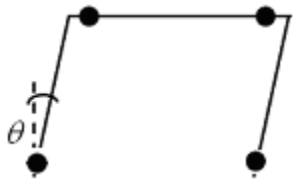

Fig. 4.7c

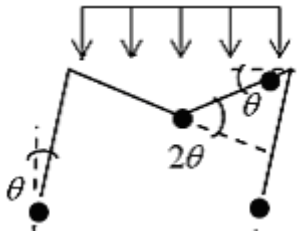

Fig. 4.7d

Fig. 4.7: Continued

Refer to Fig. 4.7a:

$$2M_{P,BE_{TOP}} + 2M_{P,BM} \geq \left((1.4*.136 + 1.7*.020\ ksf) * 15 * \frac{(30)^2}{4} \right)$$

$$M_{P,BE_{TOP}} + M_{P,BM} - 379 \geq 0 \qquad \text{(k-ft)} \qquad (4.14)$$

Refer to Fig. 4.7b:

$$2 * M_{P,CE} * 2(0.025) \geq 504/(4*12)$$

$$M_{P,CE} - 105 \geq 0 \qquad (\text{k-ft}) \qquad (4.15)$$

Refer to Fig. 4.7c:

$$2 * M_{P,CE} * (0.025) + M_{P,BE_{TOP}} * (0.025) + M_{P,BE_{BOT}} * (0.025) \geq 504/(4*12)$$

$$2 * M_{P,CE} + M_{P,BE_{TOP}} + M_{P,BE_{BOT}} - 420 \geq 0 \qquad \text{(k-ft)} \qquad (4.16)$$

Refer to Fig. 4.7d:

$$2 * M_{P,CE} * (0.025) + M_{P,BE_{TOP}} * 2(0.025) + M_{P,BM} * 2(0.025) \geq 504/(4*12) + 757 * 0.025$$

$$M_{P,CE} + M_{P,BE_{TOP}} + M_{P,BM} - 589 \geq 0 \quad \text{(k-ft)} \qquad (4.17)$$

From practical and code consideration, refer to Eqs. 4.2 through 4.7, the additional constraint equations can be derived and included as the following:

$$M_{P,BE_{TOP}} - M_{P,BM} \geq 0 \qquad (4.18)$$

$$M_{P,CE} - (6/5) M_{P,BE_{TOP}} \geq 0 \qquad (4.19)$$

$$M_{P,BE_{BOT}} - (1/2) M_{P.BE_{TOP}} \geq 0 \qquad (4.20)$$

$$M_{P,BM} - (1/4) M_{P.BE_{TOP}} \geq 0 \qquad (4.21)$$

Referring to Eq. 4.8; the objective equation is illustrated as shown below:

$$Z = 0.30 * 30 * (M_{BE_{TOP}} + M_{BE_{BOT}}) + (0.75 * 30) * M_{BM} + 2 * (14) * M_{CE}$$

$$Z = 9 * M_{BE_{TOP}} + 9 * M_{BE_{BOT}} + 22.5 * M_{BM} + 28 * M_{CE} \qquad (4.22)$$

Using the Simplex method as described in Appendix section IV; the initial table can formed subject to the constraint equations as shown in the following table on the next page:

0	-1	0	-1	1	0	0	0	0	0	0	0	-379
-1	0	0	0	0	1	0	0	0	0	0	0	-105
-2	-1	-1	0	0	0	1	0	0	0	0	0	-420
-1	-1	0	-1	0	0	0	1	0	0	0	0	-589
0	-1	1	0	0	0	0	0	1	0	0	0	0
-1	1.2	0	0	0	0	0	0	0	1	0	0	0
0	0.5	-1	0	0	0	0	0	0	0	1	0	0
0	0.25	-1	0	0	0	0	0	0	0	0	1	0
28	9	9	22.5	0	0	0	0	0	0	0	0	0

In this paper, it is written in MATLAB source codes as shown in Appendix section C. MATLAB is a tool for doing numerical computations. It is not easier for modifying and viewing the results as a window based-interactive program but it also allow every computation in matrix form. Obviously, as described in Appendix section B, the simplex method is suitable to be alternatively solved in the form of matrix format. With a large structural system, many more constraint equations must be solved. It really illustrates the effectiveness of MATLAB.

After performing the simplex analysis, the required bending moments which represent optimal solutions are obtained. These are 190 k-ft and 95 k-ft for the beam at the end section that are carried by the top bar and bottom bar, respectively while the beam at the middle section carries 190 k-ft. At column, a moment of 227 k-ft is applied.

Subsequently, the roof beam can be revised according to the above-required bending moments. According to Sec 4.2.1, after iteration is performed, the revised roof beam size will be 10x20 with ρ equal to 1.3 % and 0.65 % for top bars and bottom bars, respectively at the end section. The middle section requires 1.3% for the bottom bars.

Since it is a two-story moment frame, the column should be kept a constant size from the ground up to roof.

Commonly, the required bending moment for the column on the first floor is higher than that on the roof. It is reasonable to retain the column size and corresponding reinforcement.

At 2nd floor level

The possible collapse mechanisms are illustrated in Fig. 4.8. Their constraint equations can be derived as the following equations. Note that Eq. 4.24 requires the bending moment from column above to be considered. Hysteretic energy demand is 1061 k-in.

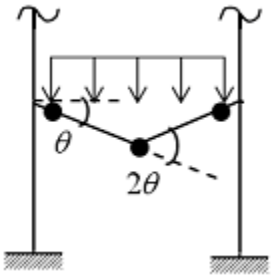

Fig. 4.8a

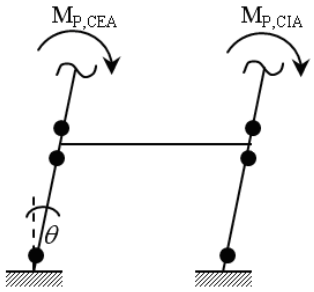

Fig. 4.8b

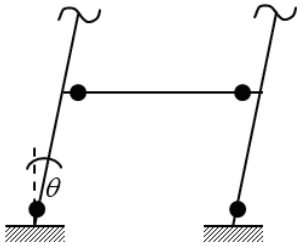

Fig. 4.8c

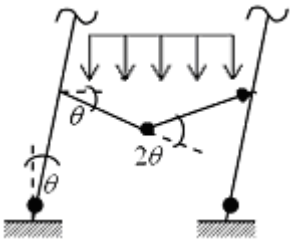

Fig. 4.8d

Fig. 4.8: Collapse mechanisms at 2nd floor level

Refer to Fig. 4.8a:

$$2 * M_{P,BE_{TOP}} + 2 * M_{P,BM} \geq \left((1.4 * .180 + 1.7 * .050\ ksf) * 15 * \frac{(30)^2}{4} \right)$$

$$M_{P,BE_{TOP}} + M_{P,BM} - 569 \geq 0 \qquad \text{(k-ft)} \qquad (4.23)$$

Refer to Fig. 4.8b:

$$4M_{P,CE} * (0.025) - 2(227) * 0.025 \geq 1061/(4 * 12)$$

$$M_{P,CE} - 335 \geq 0 \qquad \text{(k-ft)} \qquad (4.24)$$

Refer to Fig. 4.8c:

$$M_{P,BE_{TOP}} * (0.025) + M_{P,BE_{BOT}} * (0.025) + 2M_{P,CE} * (0.025) \geq 1061/(4 * 12)$$

$$M_{P,BE_{TOP}} + M_{P,BE_{BOT}} + 2M_{P,CE} - 884 \geq 0 \quad \text{(k-ft)} \qquad (4.25)$$

Refer to Fig. 4.8d:

$$M_{P,BM} * 2 * (0.025) + 2M_{P,BE_{TOP}} * (0.025) + 2(M_{P,CE}) * (0.025) \geq 1061/(4 * 12) + 1137 * 0.025$$

$$M_{P,BM} + M_{P,BE_{TOP}} + M_{P,CE} - 1011 \geq 0 \quad \text{(k-ft)} \qquad (4.26)$$

From practical and code consideration, the additional constraint equations are included as the following page:

$$M_{P,BE_{TOP}} - M_{P,BM} \geq 0 \qquad (4.27)$$

$$M_{P,CE} - (6/5)M_{P,BE_{TOP}} \geq -227 \qquad (4.28)$$

$$M_{P,BE_{BOT}} - (1/2)M_{P.BE_{TOP}} \geq 0 \qquad (4.29)$$

$$M_{P,BM} - (1/4)M_{P.BE_{TOP}} \geq 0 \qquad (4.30)$$

Refer to Equation 4.8; objective equation will be directly derived as below:

$$Z = 9 * M_{P,BE_{TOP}} + 9 * M_{P,BE_{BOT}} + 22.5 * M_{P,BM} + 28 * M_{P,CE} \qquad (4.31)$$

Following the Simplex method; the objective equation is minimized based on constraint Eqs. 4.23 through 4.31. The required bending moments will be 289 k-ft and 144 k-ft for the beam at the end section top bar and bottom bar, respectively with 289 k-ft and 360 k-ft for the beam at middle section and column, respectively.

The beam on 2nd floor can be revised for the above required bending moments. Size of 10 in x 25 in with ρ of 1.3 % and 0.65 % for top bars and bottom bars, are results at the end section, respectively while ρ of 1.3 % is used at the middle section.

For column, the required bending moment of 360 k-ft with axial force of 88 k for exterior column can be considered. Refer to section 4.2.1, these data are input to the PCACOL program for optimization purpose and revised size which requires 18 in x 18 with ρ = 3.16 %.

Following the equivalent static load concept in UBC section 16, seismic coefficient of 13 % is selected and assumed for this building. Then, the lateral loads of 11.1 k and 7.4 k are obtained at the roof level and 2nd floor level, respectively.

According to procedure in section 4.3, story drift for this frame can be summarized and calculated as shown in the Table 4.4. Obviously, all ratios (Φ) are less than 1 and the revised frame satisfies drift requirement by 1997 UBC.

Table 4.4: Story drift of revised frame subjects to1997 UBC static equivalent loads.

Level	Story Shear* (k)	ΣK_g (in^3)	ΣK_c (in^3)	hi (ft)	Δ_{bi} * (in)	ϕ **
Roof	11.1	19	104	14	0.45	0.645
2	18.5	36	104	14	0.45	0.646

** Based on linear static seismic lateral force procedures of 1997 UBC.*
*** Subjected to UBC allowable inelastic drift (0.025Δh)*

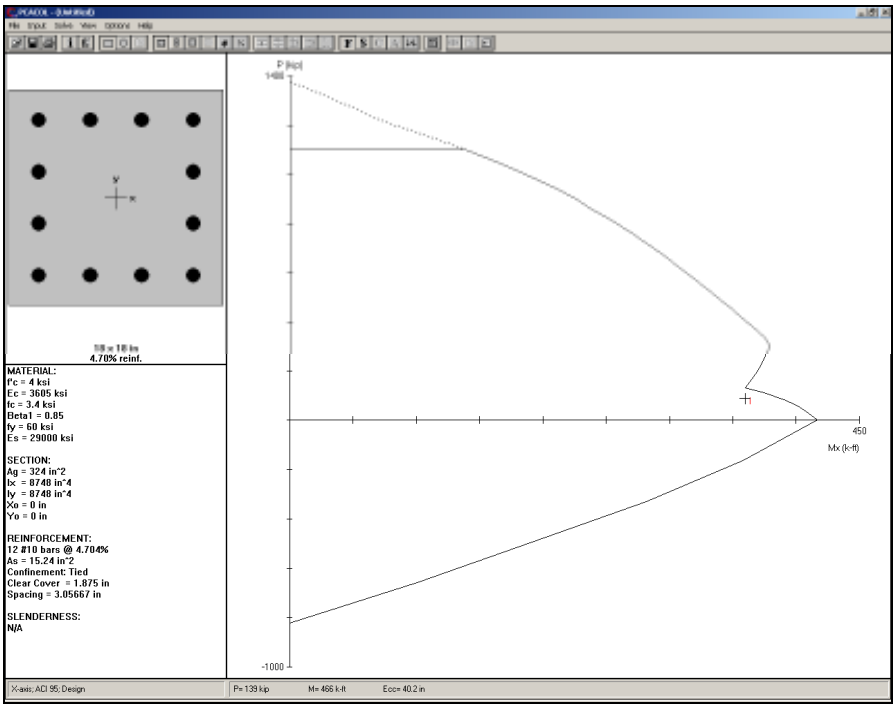

Fig. 4.9: The optimized RC column for two-story frame.

Chapter 5

Design for Three- and Nine- Story RC Moment Frame Buildings

In this chapter, the three-story and nine-story RC moment frame buildings will be revised and examined based on the energy-based design methodology. A layout of the buildings is shown in Figs. 5.1 and 5.2 while their related unit loads are shown in Fig. 5.3. Both buildings are originally designed as special moment resisting frame (SMRF) based on 1997 Uniform Building Code (UBC) and illustrated as in Tables 5.2 through 5.5. Note that the overall dimensions of the buildings are similar to the SAC prototype steel buildings. IDARC 2D version 4.0 is selected to perform the inelastic time history analyses. The IDARC concrete frame model will be created corresponding to the assumptions in section 5.1. The results obtained include hysteretic energy demand, related nonlinear behaviors, and damage induces are evaluated. Afterward, the procedure for energy-based design for RC moment frame structures that was previously described in chapter 4 will be used to optimize the design. The, flow chart summarizing the procedure to revise reinforced concrete moment frame structures based on the energy-based design method is illustrated as in Fig. 4.1 of chapter 4.

Within this chapter, hysteretic energy demands will be obtained by nonlinear time history analysis corresponding to two sets of record, SAC LA10/50 records and SAC Near Fault records. They are used to design both frames. The SAC LA 10/50 records represents 20 far field modified ground records whose probabilities of the exceedence of

10% in 50 years for the Los Angeles region. The SAC Near Fault records are the set of 20 ground motions corresponding to near-source motion on firm ground, which can be developed in UBC Seismic Zone 4. The details of each record and corresponding plots are shown in Tables 4.1 and 4.2 of chapter 4 and Appendix Figs. A.1 and A.2, respectively.

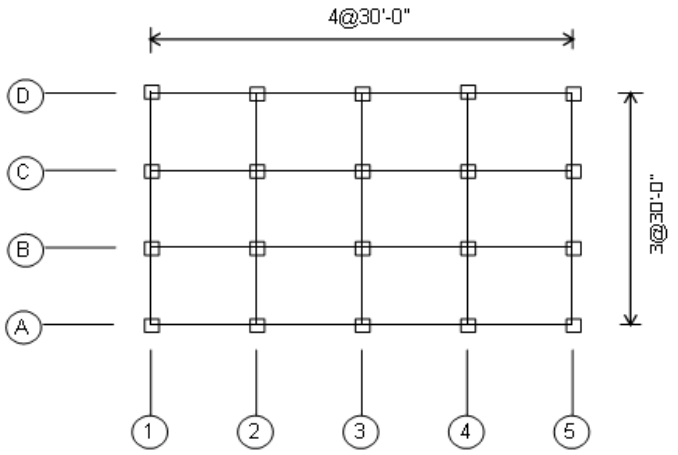

a) Plan View

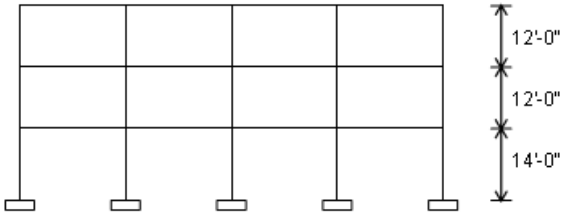

b) Elevation View

Fig. 5.1: Three-story RC moment frame

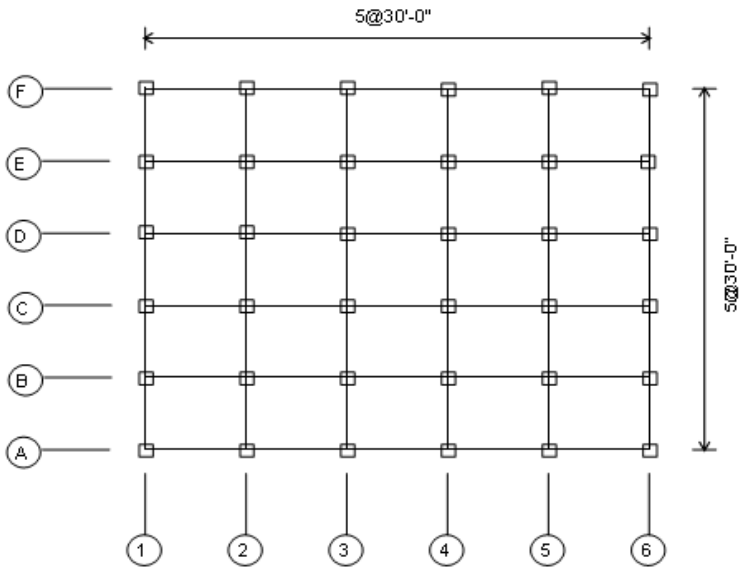

a) Plan View

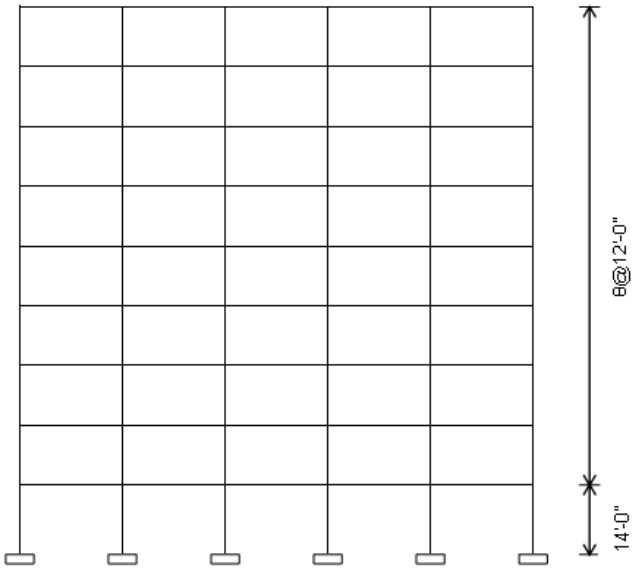

b) Elevation View

Fig. 5.2: Nine-story RC moment frame

5.1 IDARC Reinforced Concrete Frame Model

To obtain the nonlinear responses and hysteretic energy demands, the original three-story and nine-story RC moment frames, which were designed subject to the UBC will be modeled into IDARC RC frame models. The input material properties are set similar to the original design. Compressive strength of the concrete is 4 ksi while yielding strength of the steel rebar is 60,000 ksi. Other material properties such as elastic modulus, strain, and strength are automatically calculated within IDARC 2D program. However, to save analysis time, only the internal frames in the longitudinal direction will be selected and considered for design beyond this chapter. For example, the three-story RC moment frame model shown in Fig. 5.1 will transform to IDARC RC frame model as in Fig. 5.4. Total of 24 beam and 15 column element members are directly input to the program. Each element member is numbered.

Rigid link zones are used for increasing more strength at joint location to simulate real structure. Rigid links at each end of column are set to be half depth of beams that framed to. The half width of column that beams framed to is rigid links at each end of beam. Moreover, P - Δ effect is considered within the analysis. After inputting all element members and their related reinforcing, the program automatically calculates the moment-curvature property subject to each element member. For further information, see the IDARC 2D manual by Kunnath, et al., (1990).

Roof Weights:

Roofing	9.0 psf
Concrete slab (6”)	75.0
Girders	35.0
Columns	4.0
Partitions	5.0
Curtain wall	5.0
Misc.	3.0
	136.0 Psf

Floor Weights:

Concrete slab (8”)	100.0 psf
Girders	48.0
Columns	8.0
Partitions	10.0
Curtain wall	10.0
Misc.	4.0
	180.0 psf

Fig. 5.3: Unit load related to three-story and nine-story RC moment frame buildings

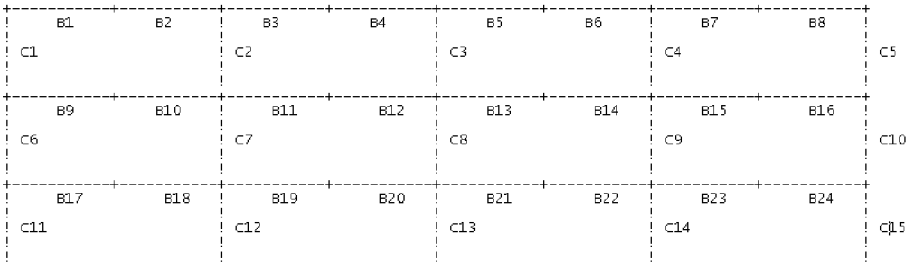

Fig 5.4: IDARC concrete frame model for three-story moment frame

The hysteretic model of each element member incorporates the Three Parameter Park Model; stiffness degrading factor; strength degrading factor; bond slip factor. The model traces the hysteretic behavior as it changes from one linear stage to another, subject to the history of deformations. HC, HBD, HBE and HS are parameters to represent shapes for the stiffness degrading factor, the strength degrading factor, the bond slip factor, respectively. Fig. 5.5 demonstrates the influences of these parameters. However, in this thesis the recommended value of each parameter for a typical RC frame suggested by the IDARC2D manual is used; 8.0 for stiffness degrading factor (HC); 0.1 for strength degrading factor (ductility, HBD); 0.1 for strength degrading factor (energy, HBE); 1.0 for bond slip factor (HS).

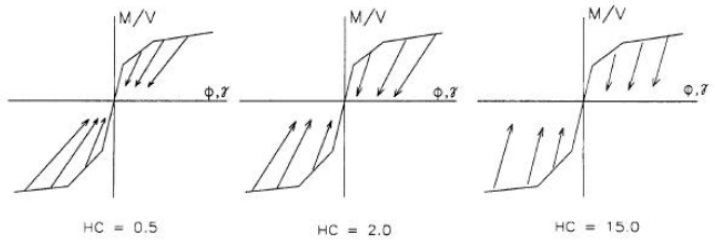

a. Stiffness Degrading Parameter

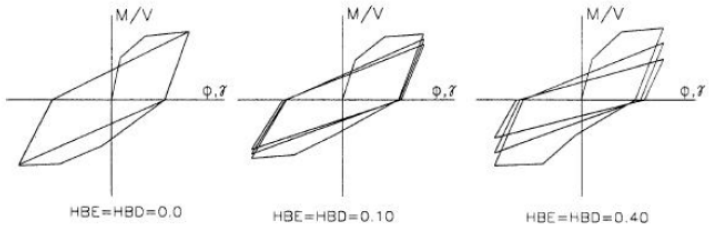

b. Strength Deterioration Parameter

Fig 5.5: Influence of degrading parameters on the hysteretic behavior

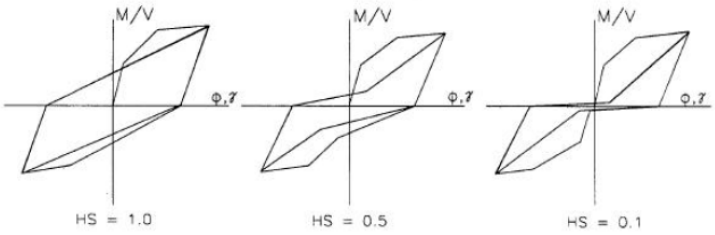

c. Slip Control Parameter

Fig 5.5: Continued

After carefully studying many analyses, the hysteretic energy of the structure is not very sensitive to the values of these parameters. Instead, it depends on the weight of the building, period of building, and the ductility of frame.

5.2 Damage Analysis

This effort measures a qualitative interpretation of the response of structure after dynamic analysis. The Park and Ang damage model was introduced after the original version of IDARC. Both ductility and dissipated hysteretic energy are considered as measures in the damage assessment. Structural damage is expressed as a linear combination of the damage caused by peak deformation and that contributed by hysteretic energy dissipation due to repeated cyclic loading.

$$DI_{p\&A} = \frac{\delta_m}{\delta_u} + \frac{\beta}{\delta_u P_y} \int dE_h \qquad (5.1)$$

Where δ_m is the maximum deformation experienced by the element during the seismic response; δ_u is the ultimate deformation capacity of the element under monotonic loading; P_y is the yield strength of the section; dE_h is incremental absorbed hysteretic energy of the element; and β is a strength deterioration parameter.

The strength deterioration parameter (β) is the ratio of the incremental damage caused by the increase of the maximum response to the normalized incremental hysteretic energy. It is given by the following expression:

$$\beta = \frac{\left(\frac{d\delta_m}{\delta_u}\right)}{\left(\frac{dE}{\delta_u P_y}\right)} = \frac{\delta_m P_y}{dE} \qquad (5.2)$$

However, due to the difficultly to evaluate the deformation at the ends of some element members in which their inelastic behaviors are confined, an additional model was introduced by Kunnath et al., (1992) as given below:

$$DI = \frac{\theta_m - \theta_r}{\theta_u - \theta_r} + \frac{\beta}{M_y \theta_u} E_h \qquad (5.3)$$

Where θ_m is the maximum rotation experienced by the element; θ_u is the ultimate rotational capacity of the element; θ_r is the recoverable rotation when unloading;

M_y is the yield moment. The program selects the biggest values between these two models at element level.

Beyond this point, two additional damage indices; story and overall damage indices, will be derived by a weighted ratio of dissipated energy. They are shown as Eqs. 5.4 and 5.5.

$$DI_{story} = \sum (\lambda_i)_{component} (DI_i)_{component} \tag{5.4}$$

$$DI_{overall} = \sum (\lambda_i)_{story} (DI_i)_{story} \tag{5.5}$$

With:

$$(\lambda_i)_{component} = \left(\frac{E_i}{\sum E_i} \right)_{component} \tag{5.6a}$$

$$(\lambda_i)_{story} = \left(\frac{E_i}{\sum E_i} \right)_{story} \tag{5.6b}$$

Where λ_i are the energy weighting factors; and E_i is the total absorbed energy by the component or story "i". The overall damage index level with explanation is shown as the following page:

Table 5.1: The interpretation of overall Damage Index

Degree of Damage	Physical Appearance	DI	State of Building
Collapse	Partial or total collapse of building	> 1.0	Loss of building
Severe	Extensive crushing of concrete ; disclosure of buckled reinforcement	0.4 - 1.0	Beyond repair
Moderate	Extensive large cracks; spalling of concrete in weaker elements	< 0.4	Repairable
Minor	Minor cracks; partial crushing of concrete in columns		
Slight	Sporadic occurrence of cracking		

5.3 Energy-Based Design for Three-Story RC Moment Frame

Following the procedure previously explained in chapter 4, the three-story RC moment frame is designed. Hysteretic energy demands for each story level subject to SAC LA110/50 and SAC Near Fault acceleration records are illustrated on Figs. 5.9 and 5.10. They are obtained by analyzing the original RC moment frame using the IDARC program and the selected earthquake records. The total hysteretic energy at each level is the sum of all corresponding column and beam hysteretic energies in the particular level as shown in Fig 5.6. Two types of hysteretic energy demand will be obtained and considered in this thesis based on ground motion input; one is the SAC LA 10/50 records

and the other is the SAC Near Fault records. They are illustrated in the following sections:

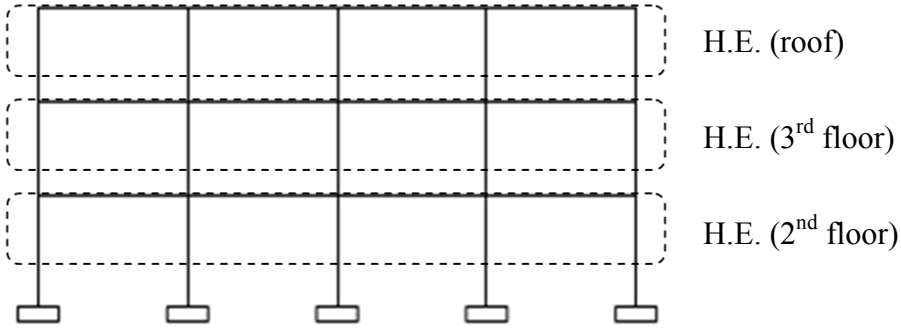

Fig 5.6: The total hysteretic energy of each floor subjects to three-story frame

5.3.1 Energy-based design based on SAC LA10/50 records.

The three-story frame have been performed subjects to the 20 earthquake records of SAC LA10/50, their mean and mean plus standard deviation of energy demand for each level are obtained. However, to smooth the energy demand, their mean plus standard deviation of energy demand will be used. The energy demand in the 2nd floor will be set to the average amount of mean plus standard deviation of energy demand for 2nd floor and for 3rd floor. The smooth energy demand that referred as design energy will be obtained by lining up the energy demand from the 2nd floor toward the roof level. The results are illustrated in Table 5.2 and the plot in Fig. 5.9. The total energy demand is 7593 kip-in is more than 5835 kip-in for the mean of the 20 records. Obviously, the smooth energy demand that obtained and used for design is higher than the mean of energy demand in each story level.

Table 5.2: The hysteretic energy demand for three-story frame subjected to SAC LA10/50

Level	H.E (Mean, kip-in)	H.E (Mean + SD, kip-in)	Smooth H.E. (kip-in)
Roof	160	318	318
3rd floor	1251	2140	2531
2nd floor	4424	7347	4744
Sum	5835	9805	7593

5.3.1.1 The 1st Revised Size Analysis

The hysteretic energy demands obtained from the previous section will be used for design. The procedures to revise the frame are the following:

- Minimize the Required Bending Moments for Each Structural Member

To minimize the required bending moment, the constraint equations, energy constraint equations and practical and code constraint equations along with the objective functions from section 4.1.1 will be selected and derived within this section. Note that M_p is the plastic moment (capacity of the section): subscript (*BE* = section at beam end, *BM* = section at beam middle, *CE* = exterior column, *CI* = interior column, *CEA* = exterior column (above), *CIA* = interior column (above)); super- subscript (TOP = top steel bars, BOT = bottom steel bars). See Fig. 5.7, for their corresponded locations.

Note that the right hand side of the collapse mechanism constraint equations will be replaced with the corresponding energy demands. According to FEMA 356, θ is suitably selected and assigned to a value of 0.025 radians as the performance limit and is substituted on the left hand side. As a result, these equations will transform into the constraint equation format.

At Roof Level:

Refer to Eq. (3.6):

$$2M_{P,BE_{TOP}} + 2M_{P,BM} \geq \left((1.4*.136 + 1.7*.012\ ksf) * 30 * \frac{(30)^2}{4} \right)$$

$$M_{P,BE_{TOP}} + M_{P,BM} - 711 \geq 0 \qquad \text{(k-ft)} \qquad (5.6)$$

Refer to Eq. (3.7):

$$3 * M_{P,CI} * 2(0.025) + 2 * M_{P,CE} * 2(0.025) \geq 318/(4*12)$$

$$3 * M_{P,CI} + 2 * M_{P,CE} - 133 \geq 0 \qquad \text{(k-ft)} \qquad (5.7)$$

Refer to Eq. (3.8):

$$3 * M_{P,CI} * (0.025) + 2M_{P,CE} * (0.025) + 4 * 0.025(M_{P,BE_{TOP}} + M_{P,BE_{BOT}}) \geq 318/(4*12)$$

$$3 * M_{P,CI} + 2M_{P,CE} + 4M_{P,BE_{TOP}} + 4M_{P,BE_{BOT}} - 265 \geq 0 \quad \text{(k-ft)} \qquad (5.8)$$

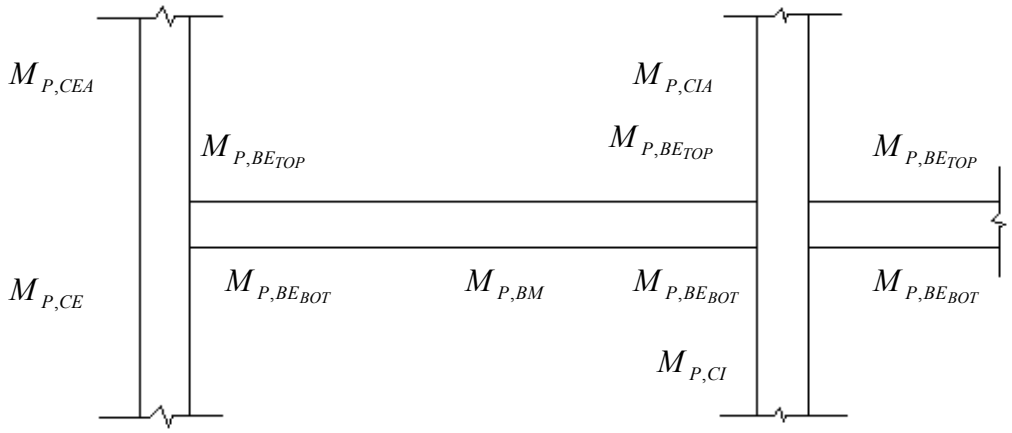

Fig. 5.7: Defined bending moment location

Refer to Eq. (3.9):

$$3*M_{P,CI}*(0.025)+2*M_{P,CE}*(0.025)+4*0.025*(2M_{P,BE_{TOP}}+2M_{P,BM}) = 1422*0.025*4+318/(4*12)$$

$$3*M_{P,CI}+2*M_{P,CE}+8M_{P,BE_{TOP}}+8M_{P,BM}-5957\geq 0 \quad \text{(k-ft)} \qquad (5.9)$$

From practical and code consideration, refer to Eqs. (4.2) through (4.7) of chapter 4, the additional constraint equations can be derived and included as the following:

$$M_{P,BE_{TOP}}-M_{P,BM}\geq 0 \qquad (5.10)$$

$$M_{P,CE}-(6/5)M_{P,BE_{TOP}}\geq 0 \qquad (5.11)$$

$$M_{P,CI}-(12/5)(M_{P,BE_{TOP}}+M_{P,BE_{BOT}})\geq 0 \qquad (5.12)$$

$$M_{P,BE_{BOT}}-(1/2)M_{P.BE_{TOP}}\geq 0 \qquad (5.13)$$

$$M_{P,BM} - (1/4)M_{P.BE_{TOP}} \geq 0 \qquad (5.14)$$

And the objective equation can be derived as the below:

$$Z = (0.30*30 + 3*0.5*30)*(M_{BE_{TOP}} + M_{BE_{BOT}}) + 4(0.75*30)*M_{BM} + 3*12*M_{CI} + 2*12\ *M_{CE}$$

$$Z = 54M_{BE_{TOP}} + 54M_{BE_{BOT}} + 90M_{BM} + 36M_{CI} + 24M_{CE} \qquad (5.15)$$

- Solution

The simplex method is used to optimize the above constraint equations for linear programming according to the example in Chapter 4. The required bending moment capacities for roof level are obtained and illustrated as the following:

$M_{P,CI} \geq 640$ (k-ft) ; $M_{P,CE} \geq 427$ (k-ft)

$M_{P,BE_{TOP}} \geq 355$ (k-ft) ; $M_{P,BE_{BOT}} \geq 178$ (k-ft)

$M_{P,BM} \geq 355$ (k-ft)

<u>At 3rd Floor Level:</u>

Refer to Eq. (3.10):

$$2M_{P,BE_{TOP}} + 2M_{P,BM} \geq \left((1.4*.180 + 1.7*.030\ ksf)*30*\frac{(30)^2}{4}\right)$$

$$M_{P,BE_{TOP}} + M_{P,BM} - 1023 \geq 0 \qquad \text{(k-ft)} \qquad (5.16)$$

Refer to Eq. (3.11):

$$3 * M_{P,CI} * 2(0.025) + 2 * M_{P,CE} * 2(0.025) \geq 2531/(4*12) + 3*640*(0.025) + 2*427*(0.025)$$

$$3 * M_{P,CI} + 2 * M_{P,CE} - 2442 \geq 0 \qquad \text{(k-ft)} \qquad (5.17)$$

Refer to Eq. (3.12):

$$3 * M_{P,CI} * (0.025) + 2M_{P,CE} * (0.025) + 4 * 0.025(M_{P,BE_{TOP}} + M_{P,BE_{BOT}}) \geq 2531/(4*12)$$

$$3 * M_{P,CI} + 2M_{P,CE} + 4M_{P,BE_{TOP}} + 4M_{P,BE_{BOT}} - 2109 \geq 0 \quad \text{(k-ft)} \qquad (5.18)$$

Refer to Eq. (3.13):

$$3 * M_{P,CI} * (0.025) + 2 * M_{P,CE} * (0.025) + 4 * 0.025 * (2M_{P,BE_{TOP}} + 2M_{P,BM}) = 2046 * 0.025 * 4 + 2531/(4*12)$$

$$3 * M_{P,CI} + 2 * M_{P,CE} + 8M_{P,BE_{TOP}} + 8M_{P,BM} - 10293 \geq 0 \qquad \text{(k-ft)} \qquad (5.19)$$

From practical and code consideration, refer to Eqs. (4.2) through (4.7) of chapter 4, the additional constraint equations can be derived and included as the following:

$$M_{P,BE_{TOP}} - M_{P,BM} \geq 0 \qquad (5.20)$$

$$M_{P,CE} - (6/5)M_{P,BE_{TOP}} + 427 \geq 0 \qquad (5.21)$$

$$M_{P,CI} - (12/5)(M_{P,BE_{TOP}} + M_{P,BE_{BOT}}) + 640 \geq 0 \qquad (5.22)$$

$$M_{P,BE_{BOT}} - (1/2)M_{P.BE_{TOP}} \geq 0 \qquad (5.23)$$

$$M_{P,BM} - (1/4)M_{P.BE_{TOP}} \geq 0 \qquad (5.24)$$

And the objective equation can be derived as the below:

$$Z = 54M_{BE_{TOP}} + 54M_{BE_{BOT}} + 90M_{BM} + 36M_{CI} + 24M_{CE} \qquad (5.25)$$

- Solution

The required bending moment capacities for roof level are obtained and illustrated as the following:

$M_{P,CI} \geq 640$ (k-ft); $M_{P,CE} \geq 427$ (k-ft)

$M_{P,BE_{TOP}} \geq 711$ (k-ft) ; $M_{P,BE_{BOT}} \geq 356$ (k-ft)

$M_{P,BM} \geq 312$ (k-ft)

<u>At 2nd Floor Level:</u>

Refer to Eq. (3.14):

$$M_{P,BE_{TOP}} + M_{P,BM} - 1023 \geq 0 \quad \text{(k-ft)} \qquad (5.26)$$

Refer to Eq. (3.15):

$$3 * M_{P,CI} * 2(0.025) + 2 * M_{P,CE} * 2(0.025) \geq 4744/(4*12) + 3*737*(0.025) + 2*491*(0.025)$$

$$3 * M_{P,CI} + 2 * M_{P,CE} - 3364 \geq 0 \qquad \text{(k-ft)} \qquad (5.27)$$

Refer to Eq. (3.16):

$$3 * M_{P,CI} * (0.025) + 2M_{P,CE} * (0.025) + 4 * 0.025 * (M_{P,BE_{TOP}} + M_{P,BE_{BOT}}) \geq 4744/(4*12)$$

$$3 * M_{P,CI} + 2M_{P,CE} + 4M_{P,BE_{TOP}} + 4M_{P,BE_{BOT}} - 3953 \geq 0 \quad \text{(k-ft)} \qquad (5.28)$$

Refer to Eq. (3.17): the equation is substituted as shown in the following:

$$3 * M_{P,CI} * (0.025) + 2 * M_{P,CE} * (0.025) + 4 * 0.025 * (2M_{P,BE_{TOP}} + 2M_{P,BM}) = 2046 * 0.025 * 4 + 4744/(4*12)$$

$$3 * M_{P,CI} + 2 * M_{P,CE} + 8M_{P,BE_{TOP}} + 8M_{P,BM} - 12134 \geq 0 \quad \text{(k-ft)} \qquad (5.29)$$

From practical and code consideration, refer to Eqs. (4.2) through (4.7) of chapter 4, the additional constraint equations can be derived and included as the following:

$$M_{P,BE_{TOP}} - M_{P,BM} \geq 0 \qquad (5.30)$$

$$M_{P,CE} - (6/5)M_{P,BE_{TOP}} + 427 \geq 0 \quad (5.31)$$

$$M_{P,CI} - (12/5)(M_{P,BE_{TOP}} + M_{P,BE_{BOT}}) + 640 \geq 0 \quad (5.32)$$

$$M_{P,BE_{BOT}} - (1/2)M_{P.BE_{TOP}} \geq 0 \quad (5.33)$$

$$M_{P,BM} - (1/4)M_{P.BE_{TOP}} \geq 0 \quad (5.34)$$

And the objective equation can be derived as the below:

$$Z = 54M_{BE_{TOP}} + 54M_{BE_{BOT}} + 90M_{BM} + 36M_{CI} + 24M_{CE} \quad (5.35)$$

- Solution

The required bending moment capacities for roof level are obtained and illustrated as the following:

$M_{P,CI} \geq 866$ (k-ft) ; $M_{P,CE} \geq 578$ (k-ft)

$M_{P,BE_{TOP}} \geq 837$ (k-ft); $M_{P,BE_{BOT}} \geq 419$ (k-ft)

$M_{P,BM} \geq 209$ (k-ft)

- Optimized RC Beam and Column Designs

Referring to the discussion in chapter 4 section 4.2, RC beams and columns will be optimally designed. Based on the required bending moment capacities obtained on the previous section, the optimized interior and exterior columns are designed by PCACOL

program while optimized beams are obtained using the MATLAB source code given in Appendix section C. Subsequently, the revised frame is illustrated as in Tables 5.10 and 5.11.

To evaluate the performances of this frame, the revised sizes and associated reinforcing from Tables 5.10 and 5.11 are input to the IDARC program and analyzed with the design earthquake records. To save analysis time, refer to Fig. 5.9, SAC LA 14 is suitably selected and considered as the design earthquake record since its energy demands are nearest to the values of the mean plus standard deviation of all 20 records. The smooth energy demands for the model before revising are 418 k-in, 2862 k-in, and 5305 k-in, for roof level, 3rd floor level, and 2nd floor level, respectively. The total energy demand is 8585 k-in.

After the analysis is complete, the smooth hysteretic energy demands turn out to be 843 k-in, 2900 k-in, and 4958 k-in, for roof level, 3rd floor level, and 2nd floor level, respectively. The total hysteretic energy demand is 8701 k-in which is greater than 8585 k-in from the previous analysis then 2nd revised analysis is required.

5.3.1.2 The 2nd Revised Analysis

The new smooth hysteretic energy demands from section 5.3.1.1, 843 k-in, 2900 k-in, and 4958 k-in, for roof level, 3rd floor level, and 2nd floor level, respectively are used for revising the sizes. There are illustrated as the following page:

- Minimize the Required Bending Moments for Each Structural Member

Following the procedure on section 5.3.1.1, to obtain hysteretic energy demands, the required bending moments for beams and columns can be attained as the following:

- Solution

After performing Simplex analysis, the required bending moment capacities for the members of each story are the below:

At roof level:

$$M_{P,CI} \geq 640 \quad \text{(k-ft)} ; \qquad M_{P,CE} \geq 427 \quad \text{(k-ft)}$$

$$M_{P,BE_{TOP}} \geq 356 \quad \text{(k-ft)} ; \qquad M_{P,BE_{BOT}} \geq 178 \quad \text{(k-ft)}$$

$$M_{P,BM} \geq 356 \quad \text{(k-ft)}$$

At 3rd Floor level:

$$M_{P,CI} \geq 640 \quad \text{(k-ft)} ; \qquad M_{P,CE} \geq 427 \quad \text{(k-ft)}$$

$$M_{P,BE_{TOP}} \geq 711 \quad \text{(k-ft)} ; \qquad M_{P,BE_{BOT}} \geq 356 \quad \text{(k-ft)}$$

$$M_{P,BM} \geq 312 \quad \text{(k-ft)}$$

At 2nd Floor level:

$$M_{P,CI} \geq 885 \quad \text{(k-ft)} ; \qquad M_{P,CE} \geq 590 \quad \text{(k-ft)}$$

$$M_{P,BE_{TOP}} \geq 848 \quad \text{(k-ft)} ; \qquad M_{P,BE_{BOT}} \geq 424 \quad \text{(k-ft)}$$

$$M_{P,BM} \geq 212 \qquad \text{(k-ft)}$$

• Optimized RC Beam and Column Designs

RC beams and columns will be optimally designed based on these required bending moment capacities. The optimized interior and exterior columns and beams are designed as shown in Tables 5.12 and 5.13.

For acceptance of the frame, the revised sizes and related reinforcing from Tables 5.12 and 5.13 will input to the IDARC program for re-analysis with the design earthquake record, SAC LA 14. After the analysis is complete, modified hysteretic energy demands turn out to be 896 k-in, 2912 k-in, and 4930 k-in, for roof level, 3rd floor level, and 2nd floor level, respectively. The total hysteretic energy demand is near to that from the 1st revised analysis from section 5.3.1.1 therefore no action should be taken. The final design frame is kept as Tables 5.12 and 5.13.

To ensure the story drift requirement by current building code, 1997 UBC, the revised frame is modeled and subjected to the 1997 UBC static equivalent loads. The results are shown as Table 5.14. All ϕ values in the last column are less than 1.0 therefore the new revised frame satisfies the 1997 UBC drift requirement and the design is completed. The result will be compared with 1997 UBC- based design in Chapter 6.

5.3.2 Design based on SAC Near Fault records.

The three-story frame have been analyzed subjects to the 20 earthquake records of SAC near fault, their mean and mean plus standard deviation of energy demand for each level are obtained. However, to smooth the energy demand, their mean plus standard deviation of energy demand will be used. The energy demand in the 2nd floor will be set to the average amount of mean plus standard deviation of energy demand for 2nd floor and for 3rd floor. The smooth energy demand that referred as design energy will be obtained by lining up the energy demand from the 2nd floor toward the roof level. The results are illustrated in Table 5.3 and the plot in Fig. 5.10. The total smooth energy demand is 19305 kip-in is more than 13576 kip-in for the mean of the 20 SAC near fault records.

Table 5.3: The hysteretic energy demand for three-story frame subjected to SAC Near Fault records

Level	H.E (Mean, kip-in)	H.E (Mean + SD, kip-in)	Smooth H.E. (kip-in)
Roof	507	1143	1143
3rd floor	3264	6286	6435
2nd floor	9805	17167	11727
Sum	13576	24596	19305

5.3.2.1 The 1st Revised Size Analysis

The procedures to revise the frame are similar to section 5.2.1.1. There are ill-ustrated as the following page:

- Minimize the Required Bending Moments for Each Structural Member

To minimize the required bending moment, the constraint equations, energy constraint equations and practical and code constraint equations along with the objective function from section 4.1.1 of chapter 4 will be selected and used within this section. Note that the right hand side of the collapse mechanism constraint equations will be replaced with corresponding energy demands. According to FEMA 356, θ is appropriately selected and assigned to 0.025 as performance limit and enables to substitute the left hand side. As a resulted, these equations will transform into the constraint equation format.

- Solution

After performing Simplex analysis, the required bending moment capacities for each story illustrate as the following:

<u>At roof level:</u>

$$M_{P,CI} \geq 640 \quad \text{(k-ft)} ; \qquad M_{P,CE} \geq 427 \quad \text{(k-ft)}$$

$$M_{P,BE_{TOP}} \geq 356 \quad \text{(k-ft)} ; \qquad M_{P,BE_{BOT}} \geq 178 \quad \text{(k-ft)}$$

$$M_{P,BM} \geq 356 \quad \text{(k-ft)}$$

<u>At 3rd Floor level:</u>

$$M_{P,CI} \geq 998 \quad \text{(k-ft)} ; \qquad M_{P,CE} \geq 665 \quad \text{(k-ft)}$$

$$M_{P,BE_{TOP}} \geq 910 \quad \text{(k-ft)} ; \qquad M_{P,BE_{BOT}} \geq 455 \quad \text{(k-ft)}$$

$$M_{P,BM} \geq 228 \qquad \text{(k-ft)}$$

At 2nd Floor level:

$$M_{P,CI} \geq 1906 \quad \text{(k-f)} ; \qquad M_{P,CE} \geq 665 \qquad \text{(k-ft)}$$

$$M_{P,BE_{TOP}} \geq 1091 \text{ (k-ft)} ; \qquad M_{P,BE_{BOT}} \geq 545 \quad \text{(k-ft)}$$

$$M_{P,BM} \geq 273 \qquad \text{(k-ft)}$$

- Optimized RC Beam and Column Designs

RC beams and columns will be optimally designed. Based on the required bending moment capacities, the optimized interior and exterior columns, and beams are designed as shown in Tables 5.15 and 5.16. To confirm the seismic performance of the frame, the revised sizes and corresponding reinforcing from Tables 5.15 and 5.16 will be input to the IDARC program and subjected to the design earthquake records. To save analysis time, SAC NF 05 is suitably selected and considered as the design earthquake record since its energy demands are nearest to values of the mean plus standard deviation of all 20 records. Their smooth energy demands for the frame before revising are 739 k-in, 5637 k-in, and 10534 k-in, for roof level, 3rd floor level, and 2nd floor level, respectively. The total energy demand is 16910 k-in.

After the analysis is complete, smooth hysteretic energy demands turn out to be 1746 k-in, 5185 k-in, and 8625 k-in, for roof level, 3rd floor level, and 2nd floor level,

respectively. The total smooth energy demand, 15556 k-in, is less than the previous one, 16910 k-in, and then no action should be taken. The final design frame will keep as Tables 5.15 and 5.16. It should be noted that the energy demands of the near fault records for this building are 81 % larger than for the 10/50 records.

To ensure the story drift requirement by current building code, 1997 UBC, the revised frame is modeled and acted subject to the 1997 UBC static equivalent loads. The results are shown as Table 5.17. All ϕ values in last column are less than 1.0 then the new revised frame satisfies the 1997 UBC drift requirement.

5.4 Energy-Based Design for Nine-Story RC Moment Frame

Following the procedure that was in the previous section, the design of the nine-story RC moment frame is obtained. Hysteretic energy demand for this building under the SAC LA110/50 and SAC Near Fault records are illustrated in Figs. 5.11 and 5.12. They are obtained by analyzing original RC moment frame by IDARC program to corresponding earthquake records. The total hysteretic energy at each level is the sum of all corresponding column and beam hysteretic energies as shown in Fig. 5.8. One of the designed nine-story RC moment frames is subjected to SAC LA 10/50 records and the other to the SAC Near Fault records.

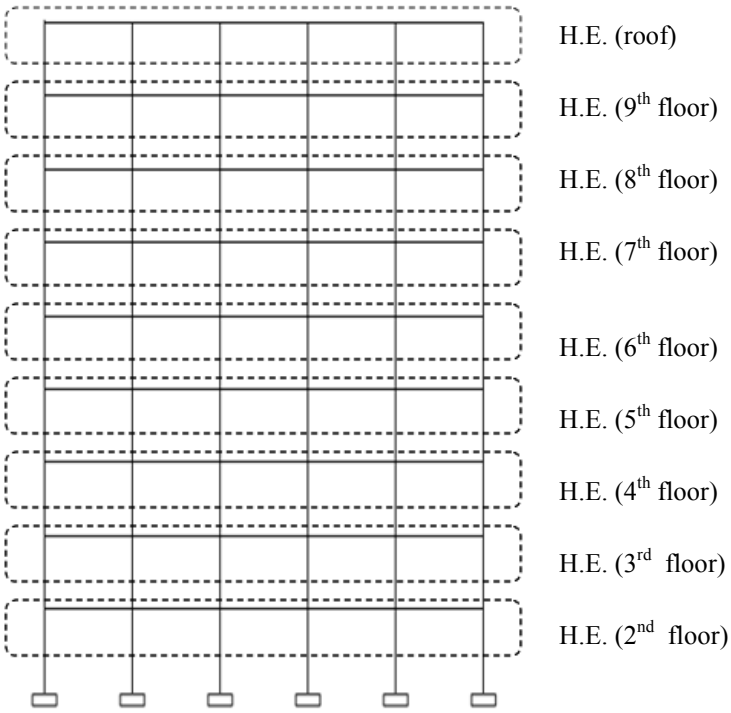

Fig 5.8: The total hysteretic energy of each floor subjects to nine-story frame

5.4.1 Design based on SAC LA10/50 records.

As discussed previously, the smooth energy demands for design are applicable. Subsequently, the results are illustrated in Table 5.4 and the plot in Fig. 5.11. The total smooth energy demand is 44024 kip-in is more than 29757 kip-in for the mean of the 20 SAC LA10/50 records. Obviously, the smooth energy demand that obtained and used for design is higher than the mean of energy demand in each story level.

5.4.1.1 The 1st Revised Size Analysis

The procedures to revise the frame are similar to section 5.2.1.1. There are ill-ustrated as the following:

Table 5.4: The hysteretic energy demand for nine-story frame subjected to SAC LA10/50 records

Level	H.E (Mean, kip-in)	H.E (Mean + SD, kip-in)	Smooth H.E. (kip-in)
Roof	123	279	279
9th floor	418	764	1432
8th floor	1092	1806	2585
7th floor	1991	3195	3738
6th floor	3228	5028	4892
5th floor	4464	6859	6045
4th floor	5301	7852	7198
3rd floor	5879	8336	8351
2nd floor	7261	10672	9504
Sum	29757	44791	44024

- Minimize the Required Bending Moments for Each Structural Member

To minimize the required bending moment, the constraint equations, energy constraint equations and practical and code constraint equations along with objective equations from section 4.1.1 of chapter 4 will be suitably selected and derived within this section. Note that the right hand side of the collapse mechanism constraint equations will be replaced with corresponding energy demands. According to FEMA 356, θ is

appropriately selected and assigned to 0.025 as performance limit and enables to substitute the left hand side. As resulted, these equations will transform into constraint equation format.

- Solution

After performing the Simplex analysis, the required bending moment capacities for each story are as follow:

At roof level:

$$M_{P,CI} \geq 640 \quad \text{(k-ft)} ; \quad M_{P,CE} \geq 427 \quad \text{(k-ft)}$$

$$M_{P,BE_{TOP}} \geq 356 \quad \text{(k-ft)} ; \quad M_{P,BE_{BOT}} \geq 178 \quad \text{(k-ft)}$$

$$M_{P,BM} \geq 356 \quad \text{(k-ft)}$$

At 9^{th} – 7^{th} Floor levels:

$$M_{P,CI} \geq 640 \quad \text{(k-ft)} ; \quad M_{P,CE} \geq 427 \quad \text{(k-ft)}$$

$$M_{P,BE_{TOP}} \geq 711 \quad \text{(k-ft)} ; \quad M_{P,BE_{BOT}} \geq 356 \quad \text{(k-ft)}$$

$$M_{P,BM} \geq 312 \quad \text{(k-ft)}$$

At 6^{th} Floor level:

$$M_{P,CI} \geq 764 \quad \text{(k-ft)} ; \quad M_{P,CE} \geq 509 \quad \text{(k-ft)}$$

$$M_{P,BE_{TOP}} \geq 780 \quad \text{(k-ft)} ; \quad M_{P,BE_{BOT}} \geq 390 \quad \text{(k-ft)}$$

$$M_{P,BM} \geq 243 \quad \text{(k-ft)}$$

At 5th Floor level:

$$M_{P,CI} \geq 880 \quad \text{(k-ft)}; \quad M_{P,CE} \geq 519 \quad \text{(k-ft)}$$

$$M_{P,BE_{TOP}} \geq 857 \quad \text{(k-ft)}; \quad M_{P,BE_{BOT}} \geq 428 \quad \text{(k-ft)}$$

$$M_{P,BM} \geq 214 \quad \text{(k-ft)}$$

At 4th Floor level:

$$M_{P,CI} \geq 1054 \quad \text{(k-ft)}; \quad M_{P,CE} \geq 532 \quad \text{(k-ft)}$$

$$M_{P,BE_{TOP}} \geq 876 \quad \text{(k-ft)}; \quad M_{P,BE_{BOT}} \geq 438 \quad \text{(k-ft)}$$

$$M_{P,BM} \geq 219 \quad \text{(k-ft)}$$

At 3rd Floor level:

$$M_{P,CI} \geq 1264 \quad \text{(k-ft)}; \quad M_{P,CE} \geq 532 \quad \text{(k-ft)}$$

$$M_{P,BE_{TOP}} \geq 885 \quad \text{(k-ft)}; \quad M_{P,BE_{BOT}} \geq 443 \quad \text{(k-ft)}$$

$$M_{P,BM} \geq 221 \quad \text{(k-ft)}$$

At 2nd Floor level:

$$M_{P,CI} \geq 1487 \quad \text{(k-ft)}; \quad M_{P,CE} \geq 536 \quad \text{(k-ft)}$$

$$M_{P,BE_{TOP}} \geq 890 \text{ (k-ft)}; \quad M_{P,BE_{BOT}} \geq 445 \quad \text{(k-ft)}$$

$$M_{P,BM} \geq 223 \quad \text{(k-ft)}$$

- Optimized RC Beam and Column Designs

RC beams and columns will be optimally designed. Based on the required bending moment capacities, the optimized interior and exterior columns, and beams are designed as shown in Tables 5.18 and 5.19. After the revised frame is obtained, story drift analysis using the 1997 UBC static equivalent loads is conducted. The results are shown as Table 5.20. It illustrates that ϕ value for 2nd floor is greater than 1.0 then only beams on 2nd floor are required to increase the sizes to satisfy the 1997 UBC requirement. The revised frame should be modified as shown in Tables 5.21 but for column sizes are kept as Table 5.19.

To ensure their performances, the revised sizes and associated reinforcing from Tables 5.19 and 5.21 are input to the IDARC program and the response is evaluated with the design earthquake records. The SAC LA01 is selected as the design earthquake record since its energy demands are nearest to the values of the mean plus standard deviation considering all 20 records. The smooth energy demands for the frame are 245 kip-in, 1339 kip-in, 2434 kip-in, 3528 kip-in, 4623 kip-in, 5718 kip-in, 6813 kip-in, 7907 kip-in, and 9002 kip-in for roof level down through 2nd floor level, respectively. The total energy demand is 41611 k-in.

After the analysis is complete, hysteretic energy demands become 185 kip-in, 1170 kip-in, 2155 kip-in, 3140 kip-in, 4125 kip-in, 5110 kip-in, 6095 kip-in, 7080 kip-in, and 8065 kip-in for roof level down through 2nd floor level, respectively. The total hysteretic energy demand is 37125 kip-in which less than 41611 kip-in from the previous

analysis. No action should be taken. The final design frame is kept as Tables 5.19 and 5.21.

5.4.2 Design based on SAC Near Fault records.

As discussed previously, the smooth energy demands for design are applicable. Subsequently, the results are illustrated in Table 5.5 and the plot in Fig. 5.12. The total modified energy demand is 81383 kip-in is more than 47431 kip-in for the mean of the 20 SAC near fault records.

Table 5.5: The hysteretic energy demand for nine-story frame subjected to SAC Near Fault records

Level	H.E (Mean, kip-in)	H.E (Mean + SD, kip-in)	Smooth H.E. (kip-in)
Roof	118	304	304
9th floor	473	1165	2489
8th floor	1736	3643	4673
7th floor	3464	6679	6858
6th floor	5320	9730	9043
5th floor	7175	12516	11227
4th floor	8061	13527	13412
3rd floor	8459	13987	15596
2nd floor	12625	21885	17781
Sum	47431	83126	81383

5.4.2.1 The 1st Revised Size Analysis

There are the procedures to revise the frame as the below:

- Minimize the Required Bending Moments for Each Structural Member

To minimize the required bending moment, the constraint equations, energy constraint equations and practical and code constraint equations along with objective equations from section 4.1.1 of chapter 4 will be suitably determined and derived within this section. Note that the right hand side of the collapse mechanism constraint equations will be replaced with corresponding energy demands. According to FEMA 356, θ is appropriately selected and assigned to a value of 0.025 radians as a performance limit. As resulted, these equations will transform into constraint equation format.

- Solution

After performing Simplex analysis, the required bending moment capacities for each story illustrate as the following:

<u>At roof level:</u>

$$M_{P,CI} \geq 640 \quad \text{(k-ft)} ; \qquad M_{P,CE} \geq 427 \quad \text{(k-ft)}$$

$$M_{P,BE_{TOP}} \geq 356 \quad \text{(k-ft)} ; \qquad M_{P,BE_{BOT}} \geq 176 \quad \text{(k-ft)}$$

$$M_{P,BM} \geq 356 \quad \text{(k-ft)}$$

At 9th Floor level:

$M_{P,CI} \geq 640$ (k-ft) ; $M_{P,CE} \geq 427$ (k-ft)

$M_{P,BE_{TOP}} \geq 711$ (k-ft) ; $M_{P,BE_{BOT}} \geq 356$ (k-ft)

$M_{P,BM} \geq 312$ (k-ft)

At 8th Floor level:

$M_{P,CI} \geq 729$ (k-ft) ; $M_{P,CE} \geq 486$ (k-ft)

$M_{P,BE_{TOP}} \geq 761$ (k-ft) ; $M_{P,BE_{BOT}} \geq 380$ (k-ft)

$M_{P,BM} \geq 262$ (k-ft)

At 7th Floor level:

$M_{P,CI} \geq 909$ (k-ft) ; $M_{P,CE} \geq 583$ (k-ft)

$M_{P,BE_{TOP}} \geq 891$ (k-ft) ; $M_{P,BE_{BOT}} \geq 446$ (k-ft)

$M_{P,BM} \geq 223$ (k-ft)

At 6th Floor level:

$M_{P,CI} \geq 1251$ (k-ft) ; $M_{P,CE} \geq 583$ (k-ft)

$M_{P,BE_{TOP}} \geq 927$ (k-ft) ; $M_{P,BE_{BOT}} \geq 464$ (k-ft)

$M_{P,BM} \geq 232$ (k-ft)

At 5th Floor level:

$$M_{P,CI} \geq 1649 \quad \text{(k-ft)} ; \quad M_{P,CE} \geq 583 \quad \text{(k-ft)}$$

$$M_{P,BE_{TOP}} \geq 946 \quad \text{(k-ft)} ; \quad M_{P,BE_{BOT}} \geq 473 \quad \text{(k-ft)}$$

$$M_{P,BM} \geq 236 \quad \text{(k-ft)}$$

At 4th Floor level:

$$M_{P,CI} \geq 2076 \quad \text{(k-ft)} ; \quad M_{P,CE} \geq 583 \quad \text{(k-ft)}$$

$$M_{P,BE_{TOP}} \geq 955 \quad \text{(k-ft)} ; \quad M_{P,BE_{BOT}} \geq 477 \quad \text{(k-ft)}$$

$$M_{P,BM} \geq 239 \quad \text{(k-ft)}$$

At 3rd Floor level:

$$M_{P,CI} \geq 2517 \quad \text{(k-ft)} ; \quad M_{P,CE} \geq 583 \quad \text{(k-ft)}$$

$$M_{P,BE_{TOP}} \geq 959 \quad \text{(k-ft)} ; \quad M_{P,BE_{BOT}} \geq 480 \quad \text{(k-ft)}$$

$$M_{P,BM} \geq 240 \quad \text{(k-ft)}$$

At 2nd Floor level:

$$M_{P,CI} \geq 2965 \quad \text{(k-ft)} ; \quad M_{P,CE} \geq 583 \quad \text{(k-ft)}$$

$$M_{P,BE_{TOP}} \geq 961 \quad \text{(k-ft)} ; \quad M_{P,BE_{BOT}} \geq 481 \quad \text{(k-ft)}$$

$$M_{P,BM} \geq 240 \quad \text{(k-ft)}$$

- Optimized RC Beam and Column Designs

RC beams and columns will be optimally designed. Based on the required bending moment capacities, the optimized interior and exterior columns, and beams are designed as shown in Tables 5.22 and 5.23. After the revised frame is obtained, story drift analysis subjects to 1997 UBC static equivalent loads applies. The results are shown as Table 5.24. It illustrates clearly that the new revised frame satisfies the 1997 UBC drift requirement.

To ensure their performances, the revised sizes and corresponding reinforcing from Tables 5.22 and 5.23 were input to the IDARC program and the frame was analyzed with the design earthquake records. SAC NF 17 is suitably selected as the design earthquake record since its energy demands are nearest to values of the mean plus standard deviation of all 20 records. The smooth energy demands for the frame before revising are 381 kip-in, 2515 kip-in, 4649 kip-in, 6783 kip-in, 8917 kip-in, 11051 kip-in, 13184 kip-in, 15318 kip-in, and 17452 kip-in for roof level down through 2nd floor level, respectively. The total energy demand is 80249 k-in.

After the analysis is complete, the smooth hysteretic energy demand become 3311 kip-in, 4535 kip-in, 5759 kip-in, 6983 kip-in, 8207 kip-in, 9431 kip-in, 10655 kip-in, 11879 kip-in, and 13104 kip-in for the roof level down through the 2nd floor level, respectively. Total hysteretic energy demand is 73864 k-in less than 80249 k-in. However, the energy demands on 9th floor and 8th floor levels are increased for the revised model compares with the original model. The related sizes will remain due to

governing of gravity mechanism. No action should be taken. The final design frame is similar to Tables 5.22 and 5.23.

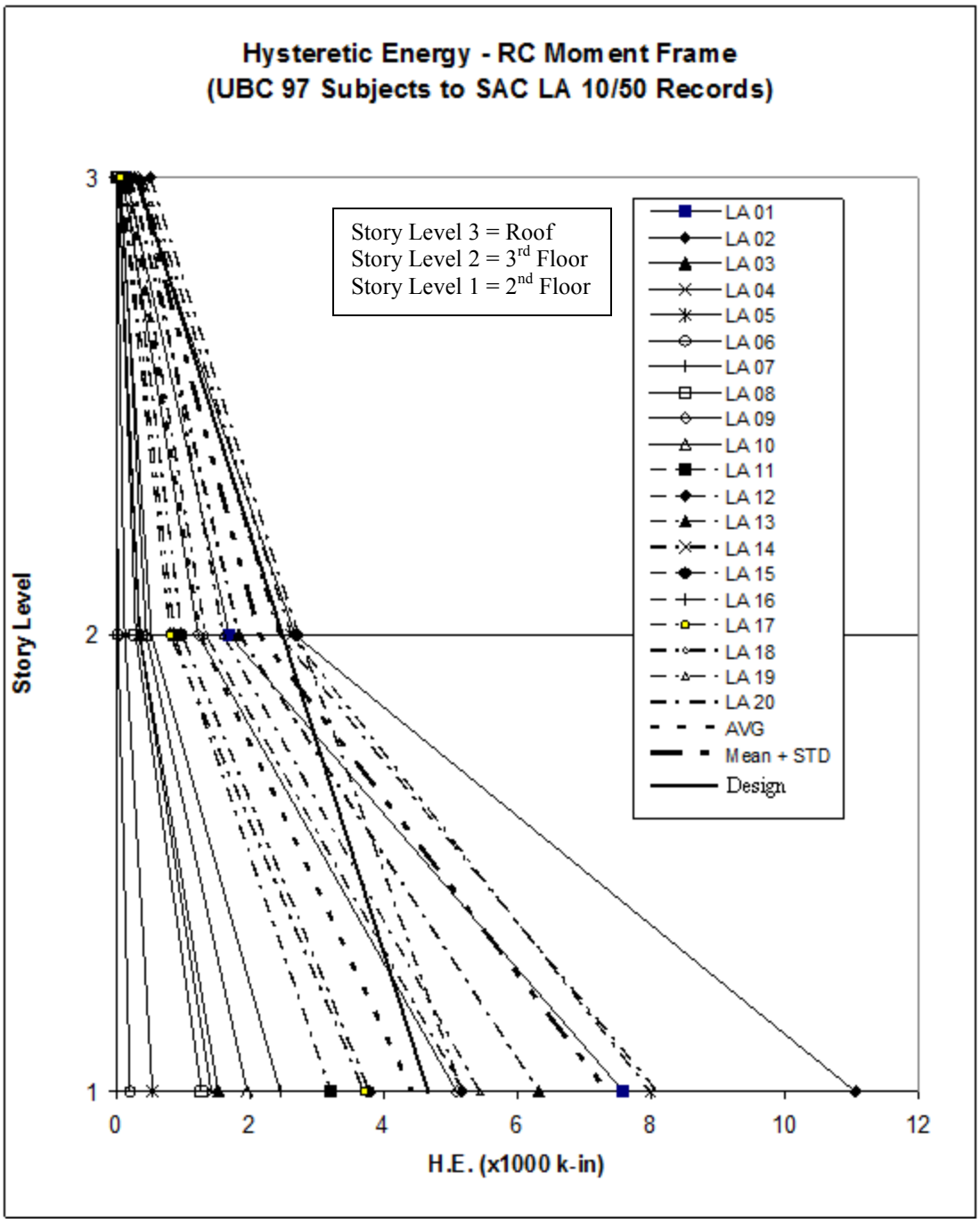

Fig. 5.9: Summation of hysteretic energy each story level, SAC LA10/50 records (20)

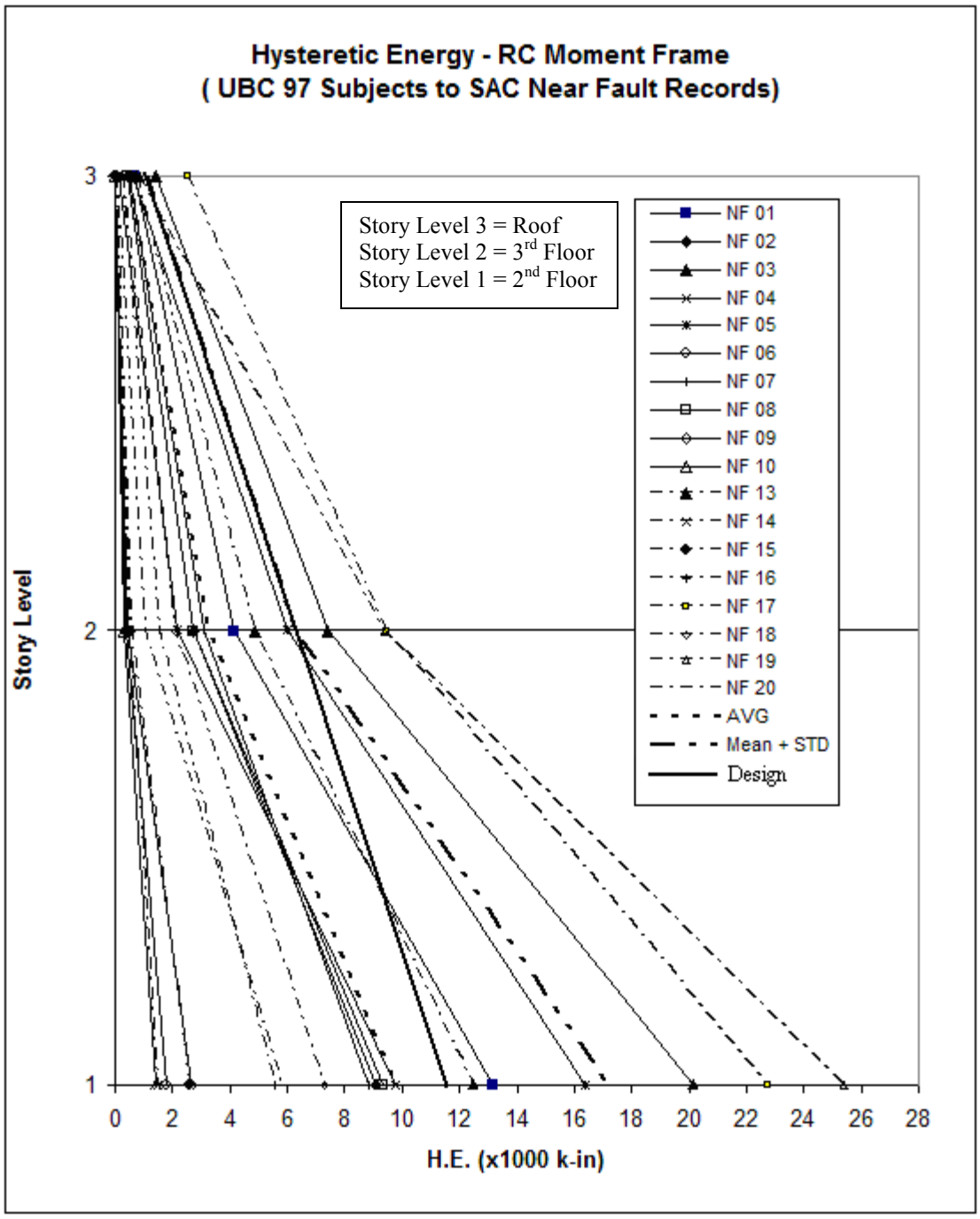

Fig. 5.10: Summation of hysteretic energy each story level, SAC Near Fault records (20)

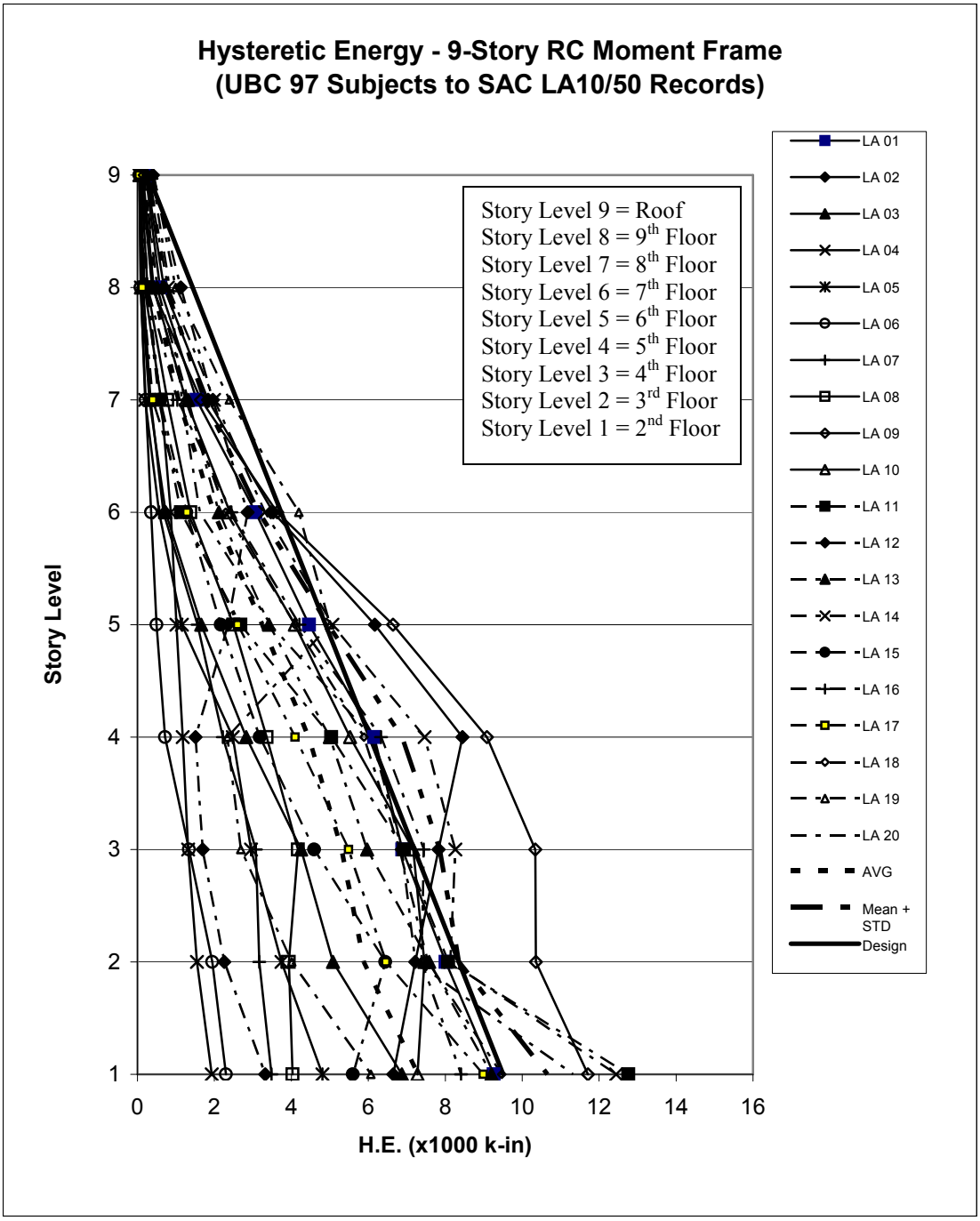

Fig. 5.11: Summation of hysteretic energy each story level, SAC LA10/50 records (20)

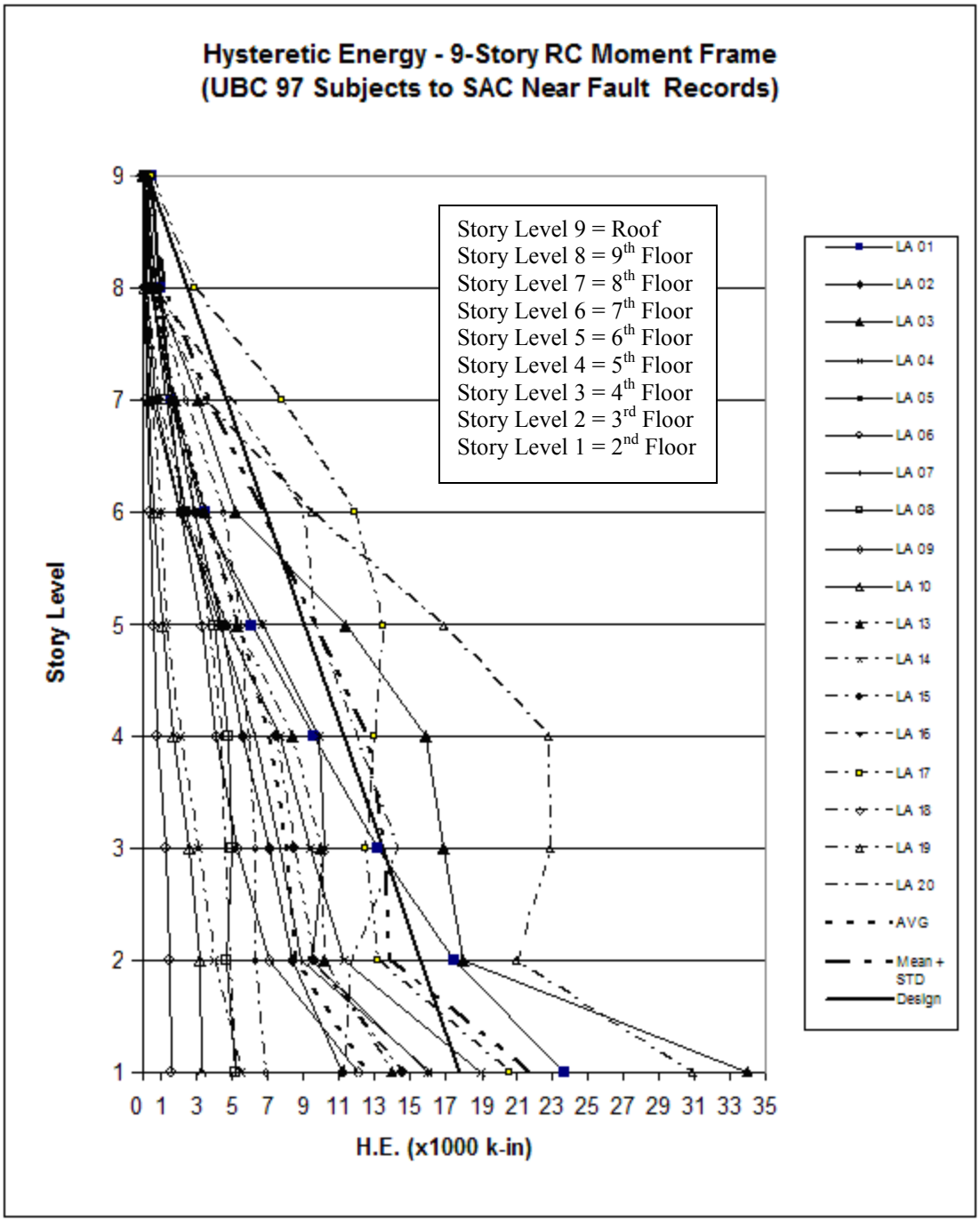

Fig. 5.12: Summation of hysteretic energy each story level, SAC Near Fault records (20)

Table 5.6: Original beam sizes and their reinforcing of 3-story RC MF based on 1997 UBC

	Size	Exterior Beam Section		Midspan Beam Section		Interior Beam Section	
Level	b x h (in x in)	Top Bar (in^2)	Bot. Bar (in^2)	Top Bar (in^2)	Bot. Bar (in^2)	Top Bar (in^2)	Bot. Bar (in^2)
Roof	14 x 29	3.7	1.9	2.2	2.2	4.8	2.4
3rd Floor	16 x 36	4.9	2.5	2.3	2.3	5.9	3.0
2nd Floor	16 x 40	4.4	2.2	2.1	2.1	5.4	2.7

Table 5.7: Original column sizes and their reinforcing of 3-story RC MF based on 1997 UBC

	Exterior Column		Interior Column	
Level	b x h (in x in)	ρ (%)	b x h (in x in)	ρ (%)
3 - Roof	20 x 20	4.45	26 x 26	3.38
2 - 3	20 x 20	4.45	26 x 26	3.38
1 - 2	20 x 20	4.45	26 x 26	3.38

Table 5.8: Original beam sizes and their reinforcing of 9-story RC MF based on 1997 UBC

	Size	Exterior Beam Section		Midspan Beam Section		Interior Beam Section	
Level	b x h (in x in)	Top Bar (in^2)	Bot. Bar (in^2)	Top Bar (in^2)	Bot. Bar (in^2)	Top Bar (in^2)	Bot. Bar (in^2)
Roof	12 x 32	4.0	2.0	2.2	2.2	4.0	2.0
9 th Floor	16 x 34	5.7	2.9	2.8	2.8	5.7	2.9
8 th Floor	16 x 40	5.6	2.8	2.3	2.3	5.6	2.8
7 th Floor	16 x 42	5.8	2.9	2.3	2.3	5.8	2.9
6 th Floor	18 x 42	6.5	3.3	2.5	2.5	6.5	3.3
5 th Floor	18 x 44	6.9	3.5	2.6	2.6	6.9	3.5
4 th Floor	18 x 45	7.0	3.5	2.8	2.8	7.0	3.5
3rd Floor	18 x 45	7.0	3.5	2.9	2.9	7.0	3.5
2nd Floor	18 x 45	7.0	3.5	3.0	3.0	7.0	3.5

Table 5.9: Original column sizes and their reinforcing of 9-story RC MF based on 1997 UBC

	Exterior Column		Interior Column	
Level	b x h (in x in)	ρ (%)	b x h (in x in)	ρ (%)
9 –Roof	24 x 24	2.19	30 x 30	1.00
8 – 9	24 x 24	2.19	30 x 30	1.00
7 – 8	24 x 24	2.19	30 x 30	1.00
6 - 7	24 x 24	2.19	30 x 30	1.00
5 – 6	24 x 24	3.00	30 x 30	2.28
4 – 5	24 x 24	3.00	30 x 30	2.63
3 - 4	24 x 24	4.87	30 x 30	3.0
2 - 3	24 x 24	5.96	30 x 30	3.45
1 - 2	24 x 24	5.96	30 x 30	4.16

Table 5.10: The 1st revised beam sizes and their reinforcing of 3-story RC MF based on SAC LA10/50

	Size	Exterior Beam Section		Midspan Beam Section		Interior Beam Section	
Level	b x h (in x in)	Top Bar (in^2)	Bot. Bar (in^2)	Top Bar (in^2)	Bot. Bar (in^2)	Top Bar (in^2)	Bot. Bar (in^2)
Roof	12 x 25	3.5	2.0	3.5	3.5	3.5	2.0
3rd Floor	14 x 35	5.0	2.6	3.3	3.3	5.0	2.6
2nd Floor	16 x 35	5.7	3.1	2.3	2.3	5.7	3.1

Table 5.11: The 1st revised column sizes and their reinforcing of 3-story RC MF based on SAC LA10/50

	Exterior Column		Interior Column	
Level	b x h (in x in)	ρ (%)	b x h (in x in)	ρ (%)
3 - Roof	20 x 20	5.72	24 x 24	3.97
2 - 3	20 x 20	5.72	24 x 24	3.97
1 - 2	20 x 20	5.72	24 x 24	3.97

Table 5.12: The 2nd revised beam sizes and their reinforcing of 3-story RC MF based on SAC LA10/50

	Size	Exterior Beam Section		Midspan Beam Section		Interior Beam Section	
Level	b x h (in x in)	Top Bar (in^2)	Bot. Bar (in^2)	Top Bar (in^2)	Bot. Bar (in^2)	Top Bar (in^2)	Bot. Bar (in^2)
Roof	12 x 25	3.5	2.0	3.5	3.5	3.5	2.0
3rd Floor	14 x 35	5.0	2.6	3.3	3.3	5.0	2.6
2nd Floor	16 x 35	5.7	3.1	1.7	1.7	5.7	3.1

Table 5.13: The 2nd revised column sizes and their reinforcing of 3-story RC MF based on SAC LA10/50

	Exterior Column		Interior Column	
Level	b x h (in x in)	ρ (%)	b x h (in x in)	ρ (%)
3 - Roof	20 x 20	5.72	24 x 24	4.87
2 - 3	20 x 20	5.72	24 x 24	4.87
1 - 2	20 x 20	5.72	24 x 24	4.87

Table 5.14: Story drift of revised frame (SAC LA10/50) subjects to1997 UBC static equivalent loads

Level	Story Shear* (k)	ΣK_g (in^3)	ΣK_c (in^3)	hi (ft)	Δ_{bi}^{*} (in)	ϕ^{**}
Roof	96	174	761	12	0.33	0.543
3rd Floor	183	556	761	12	0.27	0.456
2nd Floor	230	635	652	14	0.47	0.667

** Based on linear static seismic lateral force procedures of 1997 UBC.*
*** Subjected to UBC allowable inelastic drift (0.025Δh)*

Table 5.15: Revised beam sizes and their reinforcing of 3-story RC MF based on SAC Near Fault

		Exterior Beam Section		Midspan Beam Section		Interior Beam Section	
Level	b x h (in x in)	Top Bar (in^2)	Bot. Bar (in^2)	Top Bar (in^2)	Bot. Bar (in^2)	Top Bar (in^2)	Bot. Bar (in^2)
Roof	12 x 25	3.5	2.0	3.5	3.5	3.5	2.0
3rd Floor	16 x 37	6.0	3.2	1.8	1.8	6.0	3.2
2nd Floor	18 x 38	7.0	3.7	2.1	2.1	7.0	3.7

Table 5.16: Revised column sizes and their reinforcing of 3-story RC MF based on SAC Near Fault

	Exterior Column		Interior Column	
Level	b x h (in x in)	ρ (%)	b x h (in x in)	ρ (%)
3 - Roof	22 x 22	4.72	32 x 32	3.96
2 - 3	22 x 22	4.72	32 x 32	3.96
1 - 2	22 x 22	4.72	32 x 32	3.96

Table 5.17: Story drift of revised frame (SAC Near Fault) subjects to1997 UBC static equivalent loads

Level	Story Shear* (k)	ΣK_g (in^3)	ΣK_c (in^3)	hi (ft)	Δ_{bi}^{*} (in)	ϕ^{**}
Roof	96	174	2092	12	0.29	0.479
3rd Floor	183	750	2092	12	0.16	0.265
2nd Floor	230	915	1793	14	0.25	0.354

** Based on linear static seismic lateral force procedures of 1997 UBC.*
*** Subjected to UBC allowable inelastic drift (0.025Δh)*

Table 5.18: Revised beam sizes and their reinforcing of 9-story RC MF based on SAC LA10/50

	Size	Exterior Beam Section		Midspan Beam Section		Interior Beam Section	
Level	b x h (in x in)	Top Bar (in^2)	Bot. Bar (in^2)	Top Bar (in^2)	Bot. Bar (in^2)	Top Bar (in^2)	Bot. Bar (in^2)
Roof	12 x 25	3.5	2.0	3.5	3.5	3.5	2.0
9 th Floor	14 x 35	5.0	2.6	2.3	2.3	5.0	2.6
8 th Floor	14 x 35	5.0	2.6	2.3	2.3	5.0	2.6
7 th Floor	14 x 35	5.0	2.6	2.3	2.3	5.0	2.6
6 th Floor	16 x 34	5.6	3.0	2.0	2.0	5.6	3.0
5 th Floor	16 x 35	5.7	3.2	1.8	1.8	5.7	3.2
4 th Floor	16 x 36	5.9	3.1	1.8	1.8	5.9	3.1
3rd Floor	16 x 36	5.9	3.2	1.8	1.8	5.9	3.2
2nd Floor	16 x 36	5.9	3.3	1.8	1.8	5.9	3.3

Table 5.19: Revised column sizes and their reinforcing of 9-story RC MF based on SAC LA10/50

	Exterior Column		Interior Column	
Level	b x h (in x in)	ρ (%)	b x h (in x in)	ρ (%)
9 -Roof	22 x 22	2.10	30 x 30	1.00
8 – 9	22 x 22	2.10	30 x 30	1.00
7 – 8	22 x 22	2.10	30 x 30	1.00
6 - 7	22 x 22	2.10	30 x 30	1.00
5 – 6	22 x 22	2.89	30 x 30	1.00
4 – 5	22 x 22	3.72	30 x 30	1.71
3 - 4	22 x 22	4.20	30 x 30	2.55
2 - 3	22 x 22	4.72	30 x 30	3.39
1 - 2	22 x 22	5.77	30 x 30	4.23

Table 5.20: Story drift subjects to revised frame (SAC LA10/50) 1997 UBC static equivalent loads

Level	Story Shear* (k)	ΣK_g (in^3)	ΣK_c (in^3)	hi (ft)	Δ_{bi}^{*} (in)	ϕ^{**}
Roof	144	217	2146	12	0.35	0.585
9	260	695	2146	12	0.24	0.396
8	362	695	2146	12	0.33	0.552
7	450	695	2146	12	0.41	0.686
6	524	728	2146	12	0.46	0.771
5	583	794	2146	12	0.48	0.805
4	628	864	2146	12	0.49	0.805
3	659	864	2146	12	0.51	0.816
2	676	864	1840	14	0.75	1.073

** Based on linear static seismic lateral force procedures of 1997 UBC.*
*** Subjected to UBC allowable inelastic drift (0.02Δh)*

Table 5.21: Revised beam sizes and their reinforcing of 9-story RC MF based on SAC LA10/50

	Size	Exterior Beam Section		Midspan Beam Section		Interior Beam Section	
Level	b x h (in x in)	Top Bar (in^2)	Bot. Bar (in^2)	Top Bar (in^2)	Bot. Bar (in^2)	Top Bar (in^2)	Bot. Bar (in^2)
Roof	12 x 25	3.5	2.0	3.5	3.5	3.5	2.0
9 th Floor	14 x 35	5.0	2.6	2.3	2.3	5.0	2.6
8 th Floor	14 x 35	5.0	2.6	2.3	2.3	5.0	2.6
7 th Floor	14 x 35	5.0	2.6	2.3	2.3	5.0	2.6
6 th Floor	16 x 34	5.6	3.0	2.0	2.0	5.6	3.0
5 th Floor	16 x 35	5.7	3.2	1.8	1.8	5.7	3.2
4 th Floor	16 x 36	5.9	3.1	1.8	1.8	5.9	3.1
3rd Floor	16 x 36	5.9	3.2	1.8	1.8	5.9	3.2
2nd Floor	16 x 37	6.0	3.0	2.0	2.0	6.0	3.0

Table 5.22: Revised beam sizes and their reinforcing of 9-story RC MF based on SAC Near Fault

	Size	Exterior Beam Section		Midspan Beam Section		Interior Beam Section	
Level	b x h (in x in)	Top Bar (in^2)	Bot. Bar (in^2)	Top Bar (in^2)	Bot. Bar (in^2)	Top Bar (in^2)	Bot. Bar (in^2)
Roof	12 x 25	3.5	2.0	3.5	3.5	3.5	2.0
9 th Floor	14 x 35	5.0	2.6	2.3	2.3	5.0	2.6
8 th Floor	16 x 31	6.0	3.2	2.2	2.2	6.0	3.2
7 th Floor	16 x 36	5.9	3.2	1.8	1.8	5.9	3.2
6 th Floor	16 x 40	5.4	2.9	2.0	2.0	5.4	2.9
5 th Floor	18 x 38	5.8	3.2	2.1	2.1	5.8	3.2
4 th Floor	18 x 38	5.8	3.2	2.1	2.1	5.8	3.2
3rd Floor	18 x 39	5.9	3.1	2.2	2.2	5.9	3.1
2nd Floor	18 x 39	5.9	3.1	2.2	2.2	5.9	3.1

Table 5.23: Revised column sizes and their reinforcing of 9-story RC MF based on SAC Near Fault

	Exterior Column		Interior Column	
Level	b x h (in x in)	ρ (%)	b x h (in x in)	ρ (%)
9 -Roof	22 x 22	2.80	36 x 36	1.00
8 – 9	22 x 22	2.80	36 x 36	1.00
7 – 8	22 x 22	2.80	36 x 36	1.00
6 - 7	22 x 22	3.31	36 x 36	1.00
5 – 6	22 x 22	3.67	36 x 36	1.21
4 – 5	22 x 22	4.20	36 x 36	1.93
3 - 4	22 x 22	4.72	36 x 36	2.65
2 - 3	22 x 22	5.25	36 x 36	3.37
1 - 2	22 x 22	5.77	36 x 36	4.09

Table 5.24: Story drift subjects to revised frame (SAC Near Fault) 1997 UBC static equivalent loads

Level	Story Shear* (k)	ΣK_g (in^3)	ΣK_c (in^3)	hi (ft)	Δ_{bi}^{*} (in)	ϕ^{**}
Roof	144	217	4159	12	0.34	0.559
9	260	695	4159	12	0.21	0.349
8	362	552	4159	12	0.36	0.595
7	450	864	4159	12	0.30	0.503
6	524	1185	4159	12	0.27	0.454
5	583	1143	4159	12	0.31	0.520
4	628	1143	4159	12	0.34	0.560
3	659	1236	4159	12	0.33	0.553
2	676	1236	3565	14	0.48	0.686

** Based on linear static seismic lateral force procedures of 1997 UBC.*
*** Subjected to UBC allowable inelastic drift (0.02Δh)*

Chapter 6

Conclusions and Recommendations

- Beyond this chapter, the behavior of reinforced concrete moment frames which were designed subject to the energy-based design (EBD) concept in chapter 5 will be compared with 1997 uniform building code (UBC 97) concept. Two sources of hysteretic energy demands, SAC LA10/50 and SAC Near Fault ground motion records are employed for EBD. LA 09 and LA 14 represent mean and mean plus standard deviation for SAC LA10/50 records, respectively while NF 08 and NF 05 represent mean and mean plus standard deviation for SAC Near Fault records**,** respectively**.** Story level details for three and nine-story fames are shown in Fig. 6.1 and Fig. 6.2.

- Refer to Park and Ang's overall damage index as shown in Table 6.1, three-story RC moment frame buildings designed based on UBC 97 and EBD perform well when subjected to the SAC LA10/50 records. Their indexes are less than 0.4 which is categorized as moderate damage (see Table 5.1 of chapter 5). Extensive large cracks and spalling of some concrete elements are predicted to occur, however, they are repairable. This type of behavior is consistent with both design conditions.

- Subject to SAC Near Fault records, for NF 08 which represents their mean of the records, all designs perform well as seen in Table 6.1. But for stronger record like NF 05 which represents their mean plus standard deviation of the records, the frame that is designed based on UBC 97 indicates severe damage with extensive crushing of concrete or disclosure of buckled reinforcement may occur. The frame that is designed based on EBD with SAC Near Fault shows a clear advantage under the NF 05 ground motion. It demonstrates only minor to moderate damage.

- Refer to model analysis of three-story frame as shown in Table 6.2, the frame that is designed based on EBD with SAC LA10/50 records is more flexible since having a period that is 15% longer compared to the frame that is designed based on UBC97 while for the 9-story frame that is designed based on EBD with SAC LA10/50 records provides 28% longer period compared to the relative frame as shown in Table 6.4. Obviously, EBD tends to redistribute the hysteretic energy demand from higher demand in lower story to lower demand in upper story.

- For the nine-story RC moment frame building, as illustrated in Table 6.3, all designs perform well subject to SAC records except record NF 17 which is strong earthquake record and represents mean plus standard deviation of the SAC Near Fault records, UBC 97 based-design indicates the most damage to the structure while EBD with SAC Near Fault record has the lowest damage index.

- Hysteretic energy demands for the three-story moment frame building used for EBD are shown in Figs. 6.3 through 6.6. Obviously, the graph indicates the optimal design because the difference of hysteretic energy demand between the 2^{nd} revised sizes (after the 2^{nd} iteration for frame design) and the 3^{rd} revised sizes (after the 3^{rd} iteration of frame design) is less than between the 1^{st} revised sizes (after the 1^{st} iteration of frame design) and the 2^{nd} revised sizes. For roof level, although energy demands are increasing as more revising performed, it is not considered since the beam mechanism control the design not sway mechanism.

- Figs. 6.5 through 6.8 demonstrate the maximum plastic rotations in beam subjects to the selcted SAC LA10/50 records and Near Fault records. The value of 0.025 radians is limited for Collapse Prevention Performance by FEMA 356 (see Table A.3 of Appendix A). The results, shown in Figs. 6.5, 6.6 and 6.8, indicate that the three-story RC moment frame buildings designed based on 1997 UBC and EBD perform well when subjected to the SAC LA10/50 records. For the stronger NF records such a NF 05 (Fig. 6.7), only the EBD NF designed frame satisfies the require maximum plastic rotations that are within the limit.

- Considering the recommended maximum rotation of 0.025 radians for columns (Table A.4 of Appendix A), the results shown in Figs. 6.9 and 6.10, indicate that the three-story RC moment frame buildings designed based on UBC 97 and EBD perform well when subjected to the selected SAC LA10/50 records. However,

considering a strong, near fault earthquake record like NF 05 as shown in Fig. 6.11, only the designed frame subjected to EBD (NF) perform well.

- Refer to the requirement of interstory drift limitation by UBC 97 which indicates the maximum allowable interstory drift is 0.25*h (note: h = story height) . The interstory drift results shows as in Fig. 6.13. It clearly demonstrates the interstory drifts relate to the EBD frame are within the acceptable limit.

- Refer to Figs. 6.14 through 6.17; the interstory drifts of designed three-story building subjects to the selected SAC records are illustrated. Obviously, all of them are within the limit of 4%, which recommended as collapse prevention performance by FEMA 356 (see Table 4.3 of chapter 4). They are acceptable.

- Subject to the element damage index as in Figs. 6.18 through 6.21; all values are within 1.0 then it indicates no total collapse of beams or columns is occurred subjects to Park and Ang's damage concept. However, for strong earthquake record, NF 05, as shown in Fig. 6.20, several beams on 2^{nd} floor of frame of designed frame by UBC 97 produce the most damage indexes, nearly to 1.0 while the designed frame by EBD subjects to Near Fault records performs every well. Apparently, at every joint, damage indexes for beams are higher than columns. It may conclude that the three-story moment frame buildings designed according to EBD concept beyond this thesis satisfy the strong column–weak beam criteria.

- Hysteretic energy demands for nine-story moment frame building used for EBD are shown in Figs. 6.22 and 6.23. For SAC LA10/50 records, the hysteretic demands as shown in Fig. 6.22 are decreasing while more iteration is performed. It clearly represents the reaching of optimized design in EBD then the design process enables to discontinue. For SAC Near Fault record as shown in Fig. 6.23, although in 2^{nd} iteration, the hysteretic energy demands are increasing for 6^{th} level up to roof level, they are not considered since their demands still are less than the demands from gravity loads. Then, the more iteration is not necessary.

- Figs. 6.24 through 6.27 demonstrate the maximum plastic rotations in beam subjects to selected SAC LA10/50 records and Near Fault records of designed nine-story moment frame buildings. The value of 0.025 radians is limited for Collapse Prevention performance by FEMA. Fig. 6.24 shows more advantage in design of EBD than UBC 97 based-design. UBC 97 based-design produces excessive plastic rotation, 0.034 radians while EBD works well. For strong earthquake, NF17, all designed frames provide plastic rotations over than 0.025 radians in the 2^{nd} floor, 3^{rd} floor, and 4^{th} floor levels as shown in Fig. 6.27. However, EBD subjects to SAC Near Fault records is suitable since it produces the smallest values.

- Subject to the recommended value of 0.025 radians for column rotation, refer to Figs. 6.28 through 6.351, it typically enables to conclude that UBC 97 based-

design and EBD are suitable for nine-story RC moment frame buildings subjects to SAC LA10/50 records. But for strong earthquake record such SAC Near Fault records, NF 17, as in Fig. 6.31, only EBD subjects to SAC Near Fault record is appropriate which their maximum plastic rotations are within the limit.

- To satisfy drift requirement by 1997 UBC, the designed nine-story moment frame buildings are applied the corresponding static equivalent loads which defined by 1997 UBC. The results are demonstrated as in Fig. 6.32. It clearly demonstrates the interstory drifts by EBD are within the limit of 0.25h then they are acceptable.

- Subjects to Figs. 6.33 through 6.36; the interstory drift of designed nine-story building subjects to the selected SAC records is illustrated. Obviously, all of them satisfy the limit of 4%, which recommended as collapse prevention performance by FEMA 356.

- Figs. 6.37 through 6.40 illustrate the element damage index corresponding to SAC records. The most designed frames produce the damage indexes within the limit of 1.0. However, for strong earthquake record, NF17, the designed frame subjects to EBD with SAC Near Fault records is the most suitable, all damage indexes are less than UBC based-design as shown in Fig. 6.40. Apparently, at every joint, damage indexes for beams are higher than columns. It may reasonably conclude

that the nine-story moment frame buildings designed according to EBD concept beyond this thesis satisfy the strong column–weak beam criteria.

- For RC three-story moment frames subject to EBD, member sizes and their reinforcement are illustrate in Tables 5.12, 5.13, 5.15, and 5.16 of chapter 5. It concludes that for SAC LA10/50 records, the gravity mechanism governs the roof level and 3rd floor level while sway mechanism controls the 2nd floor level. But for SAC Near Fault records, stronger earthquakes provide more inelastic deformation in structural members bring more hysteretic energy demands. It results in the 1st floor and the 2nd floor levels are controlled by sway mechanism. However, roof level is still governed by gravity mechanism.

- For RC nine-story moment frames subject to EBD, member sizes and their reinforcement are illustrated in Tables 5.19, 5.21, 5.22, and 5.23 of chapter 5. It concludes that for SAC LA10/50 records, the gravity mechanism govern the roof level down to 7th floor level otherwise sway mechanism controls. For SAC Near Fault records, stronger earthquakes provide more inelastic deformation in structural members bring higher hysteretic energy demands. Only the roof and 9th floor levels are only controlled by gravity mechanism.

- Cost comparisons between UBC 97 and EBD according to the three-story and nine moment frame buildings are illustrated in Figs. 6.41 and 6.42. For three-story

building, EBD designed subjects to SAC LA10/50 records provides 20 % cheaper in cost than UBC 97 while EBD designed subjects to SAC Near Fault records allow 6.4 % higher in cost. Nine-story building, EBD designed subjects to SAC LA10/50 records produces 17.8 % cheaper but EBD designed subjects to SAC Near Fault records gives 4.0 % higher in cost than UBC 97.

- Based on the study beyond this thesis, it reasonably concludes that to sustain the far-field earthquake ground motion, the frames subjects to UBC's design, EBD (LA10/50), EBD (NF) satisfy all requirements such plastic rotation and interstory drift by FEMA356. The EBD (LA10/50) produces a design comparable to the UBC97's design. But for strong ground motion, only EBD (NF) satisfies the requirements. Large plastic rotations for beams and columns occur in EBD (LA10/50) and UBC's design.

- The EBD procedure developed in this thesis is a viable alternative for earthquake resistant design of moment frames. The use of energy also has the advantage of incorporating the effect of duration and cumulative energy dissipation. it enables to modify for different hysteretic energy levels representative of different performance levels.

Table 6.1: Overall Damage Index of 3-story building subjects to SAC records

	Overall Damage Index			
Design Concept	LA 09	LA 14	NF 05	NF 08
1997 UBC	0.163	0.232	0.416	0.235
EBD (SAC LA10/50)	0.183	0.217	0.440	0.234
EBD (SAC Near Fault)	0.085	0.160	0.173	0.168

Table 6.2: Modal analysis of 3-story building

Mode	Period (sec)		
	1997 UBC	EBD (SAC LA 10/50)	EBD (SAC Near Fault)
1	0.47	0.54	0.41
2	0.16	0.18	0.14
3	0.08	0.09	0.06

Table 6.3: Overall Damage Index of 9- story buildings subjects to SAC records

	Overall Damage Index			
Design Concept	LA 01	LA 03	NF 02	NF 17
1997 UBC	0.333	0.279	0.256	0.513
EBD (SAC LA10/50)	0.253	0.394	0.367	0.428
EBD (SAC Near Fault)	0.237	0.311	0.265	0.418

Table 6.4: Modal analysis of 9- story buildings

Mode	Period (sec)		
	1997 UBC	EBD (SAC LA 10/50)	EBD (SAC Near Fault)
1	1.10	1.41	1.24
2	0.40	0.49	0.44
3	0.23	0.28	0.25
4	0.15	0.18	0.15
5	0.11	0.13	0.10
6	0.08	0.10	0.07
7	0.06	0.07	0.05
8	0.05	0.06	0.04
9	0.04	0.05	0.03

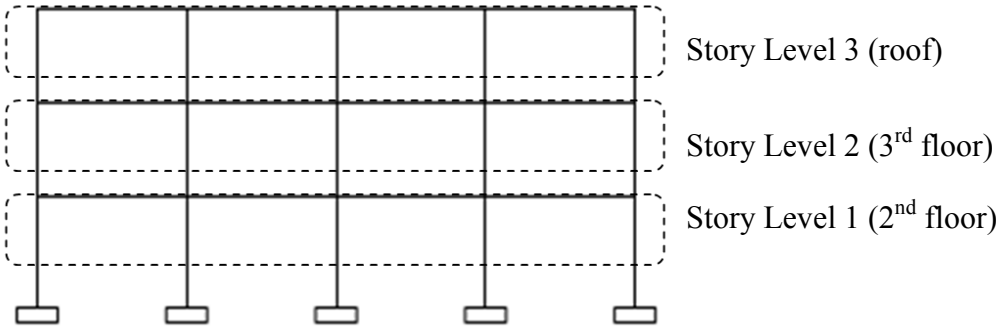

Fig 6.1: Story level for three-story frame

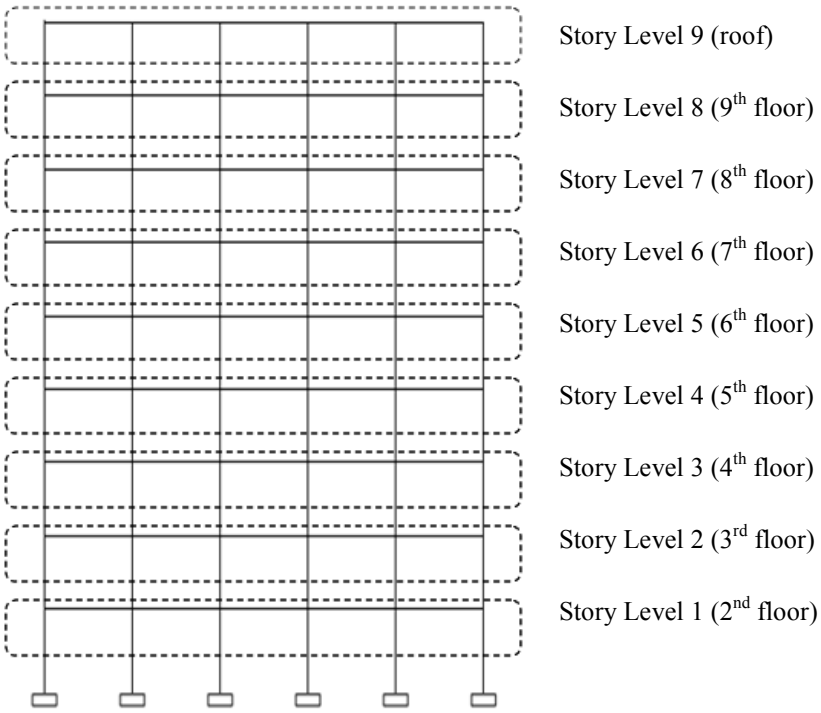

Fig 6.2: Story level for nine-story frame

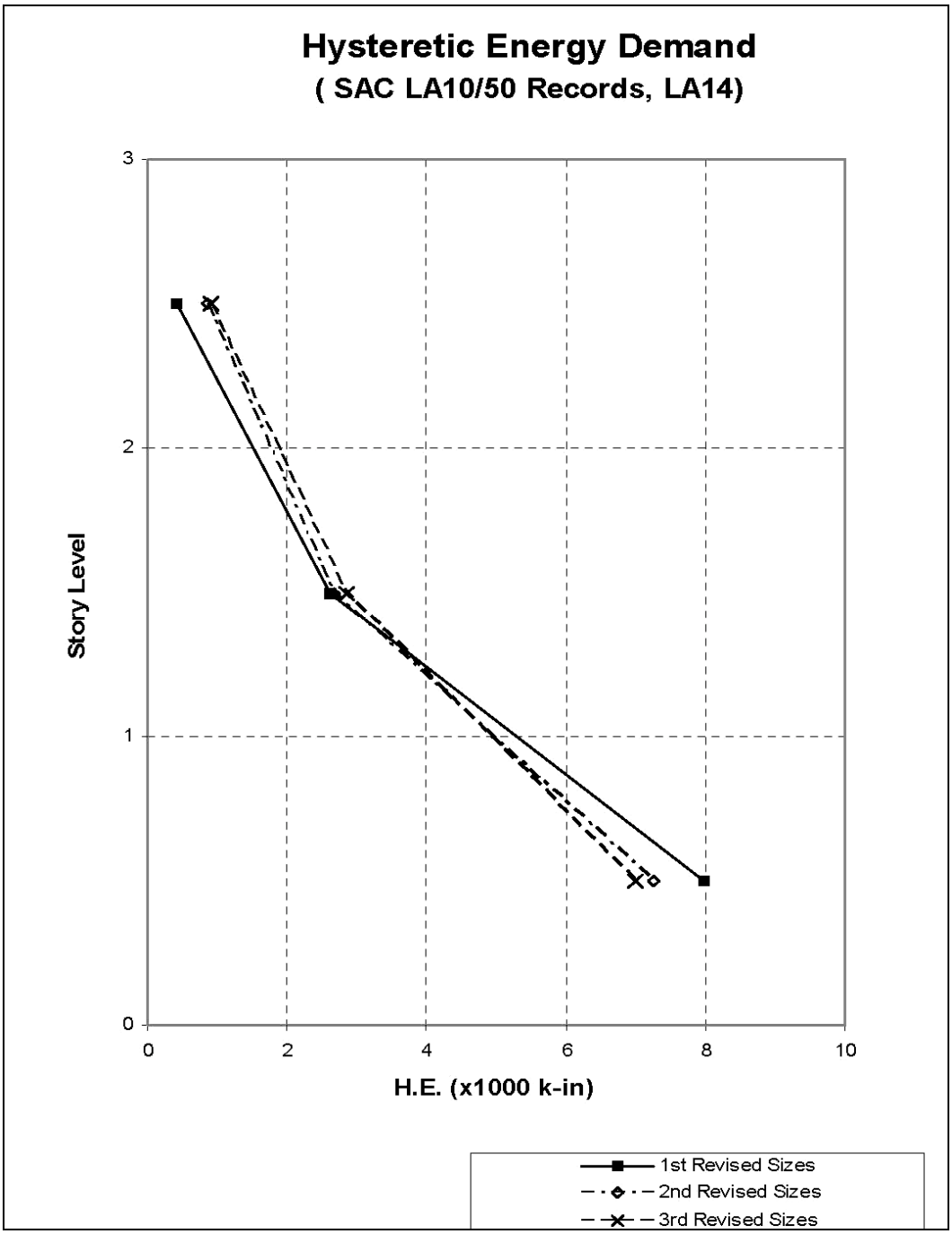

Fig. 6.3: Hysteretic energy demand for 3-story building subjects to SAC LA10/50 records, LA14

** The i^{th} revised sizes = sizes after the i^{th} iteration for frame design*

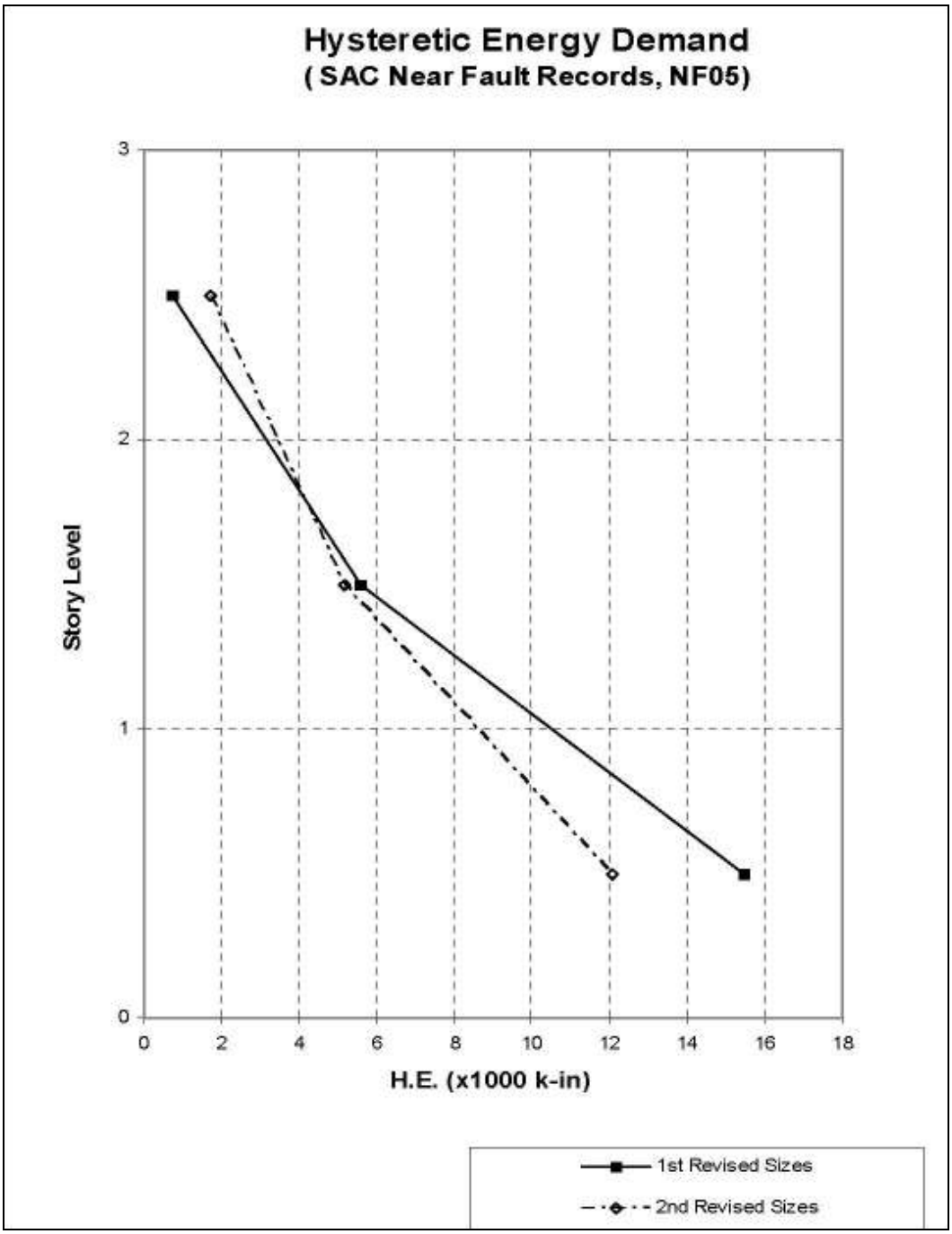

Fig. 6.4: Hysteretic energy demand for 3-story building subjects to SAC Near Fault records, NF05

** The i^{th} revised sizes = sizes after the i^{th} iteration for frame design*

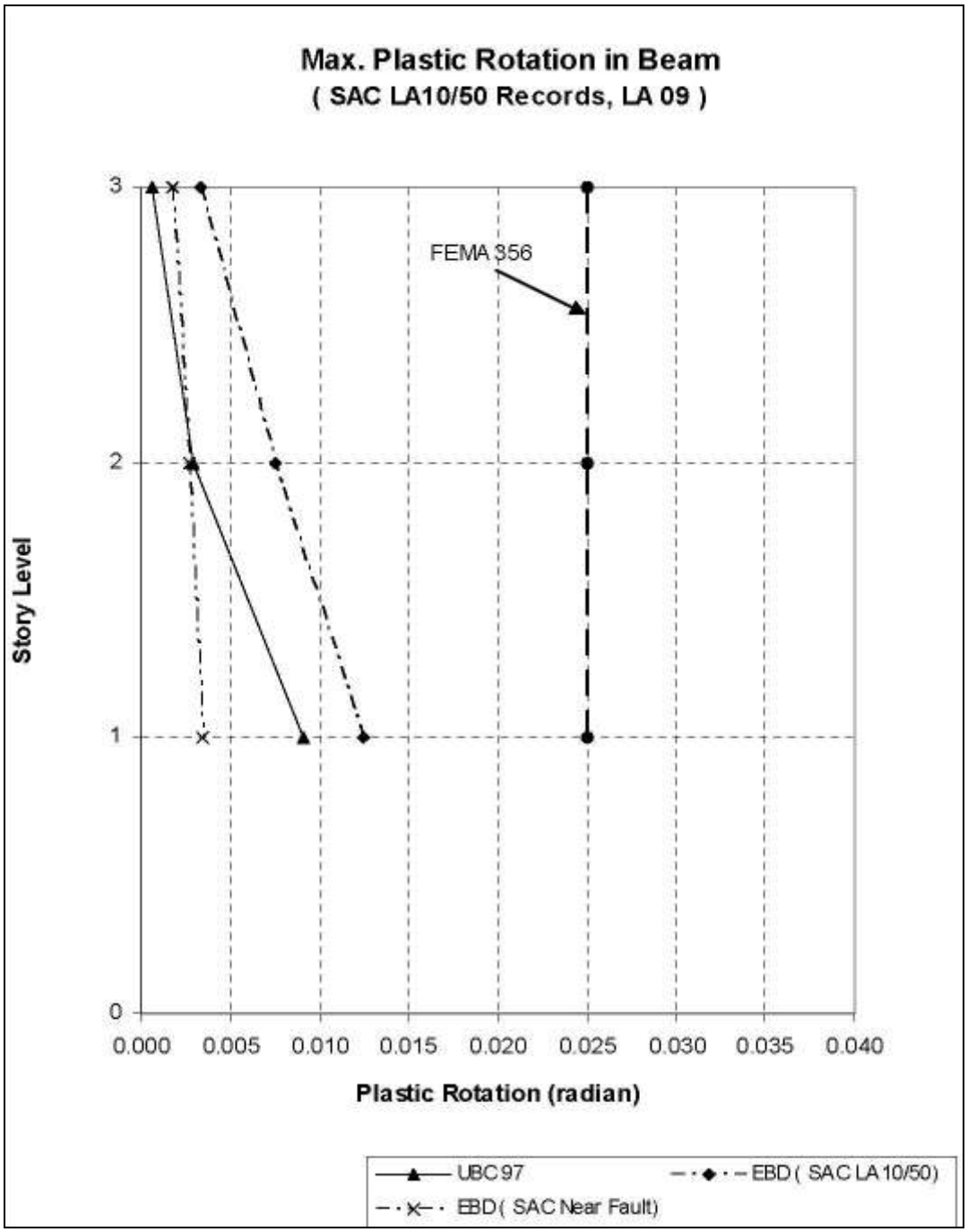

Fig. 6.5: Max plastic rotation in beam subjects to SAC LA 09

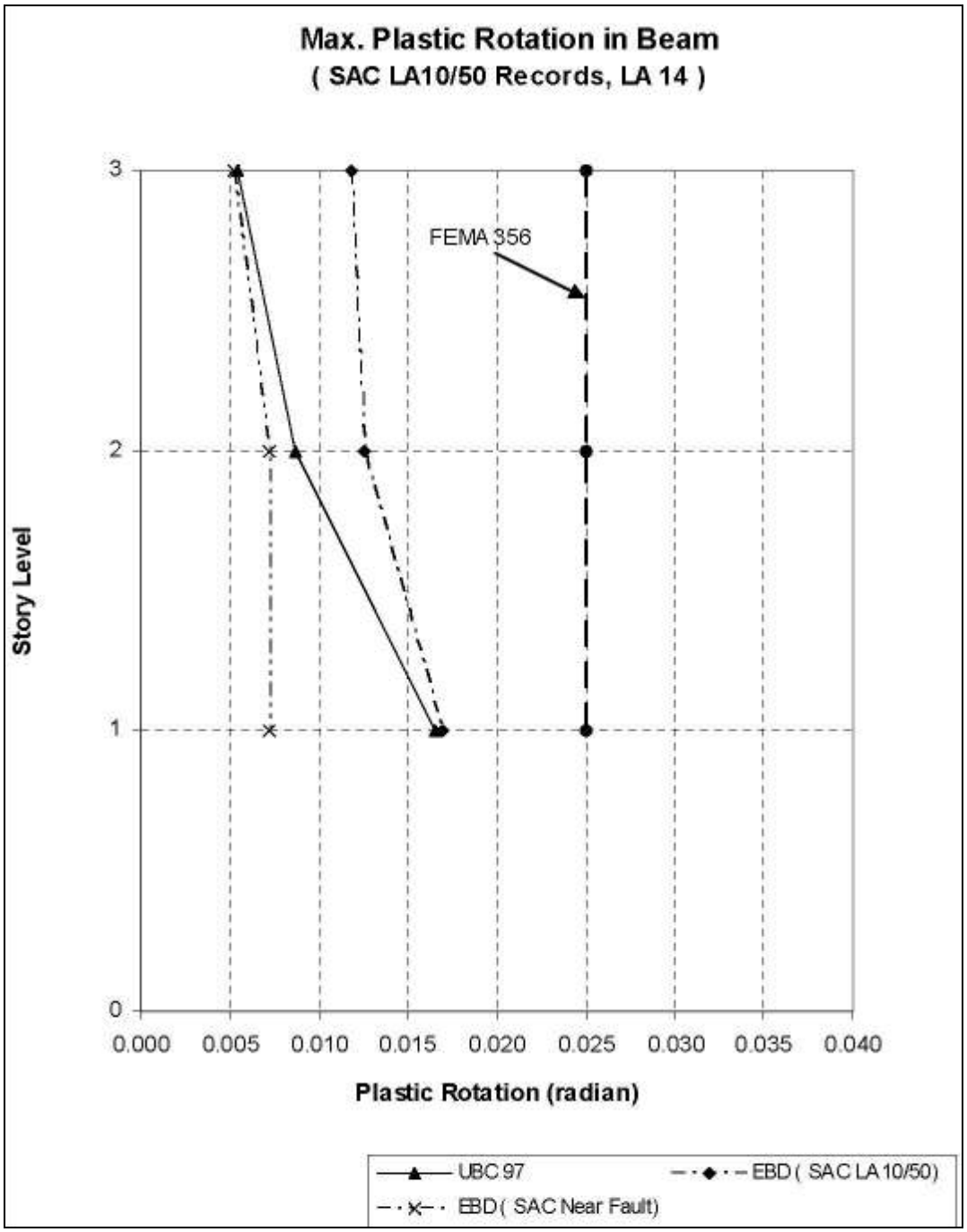

Fig. 6.6: Max plastic rotation in beam subjects to SAC LA 14

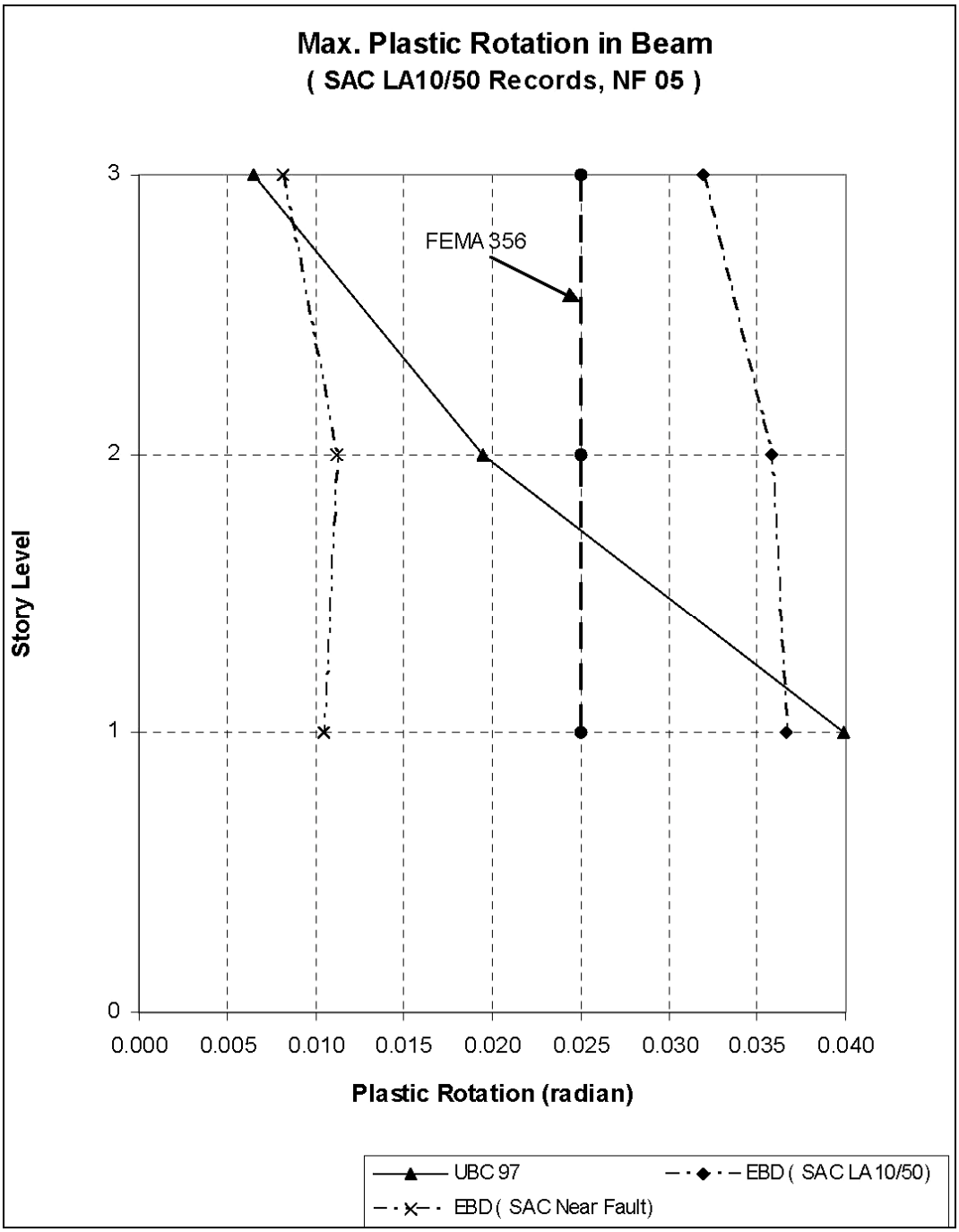

Fig. 6.7: Max plastic rotation in beam subjects to SAC NF 05

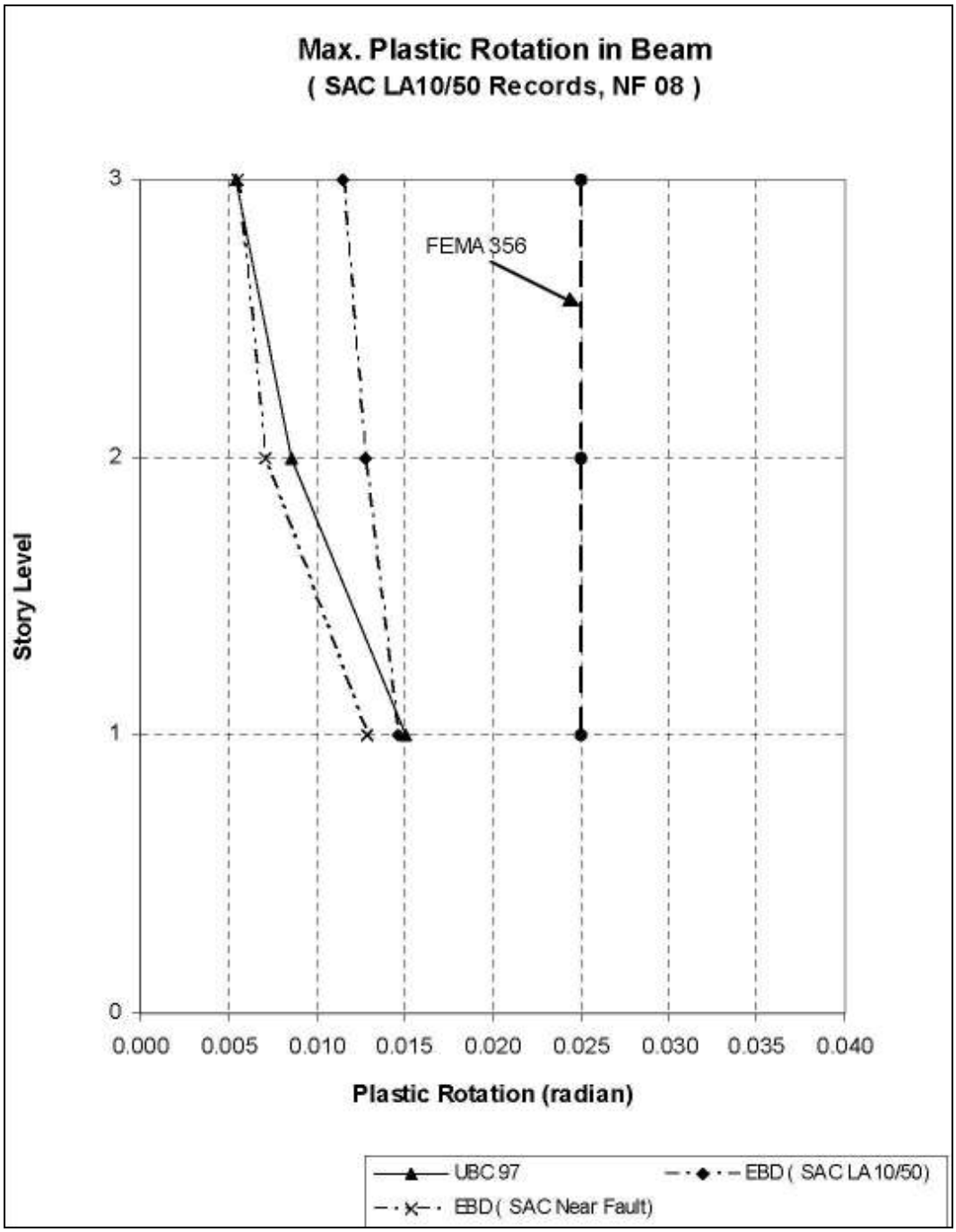

Fig. 6.8: Max plastic rotation in beam subjects to SAC NF 08

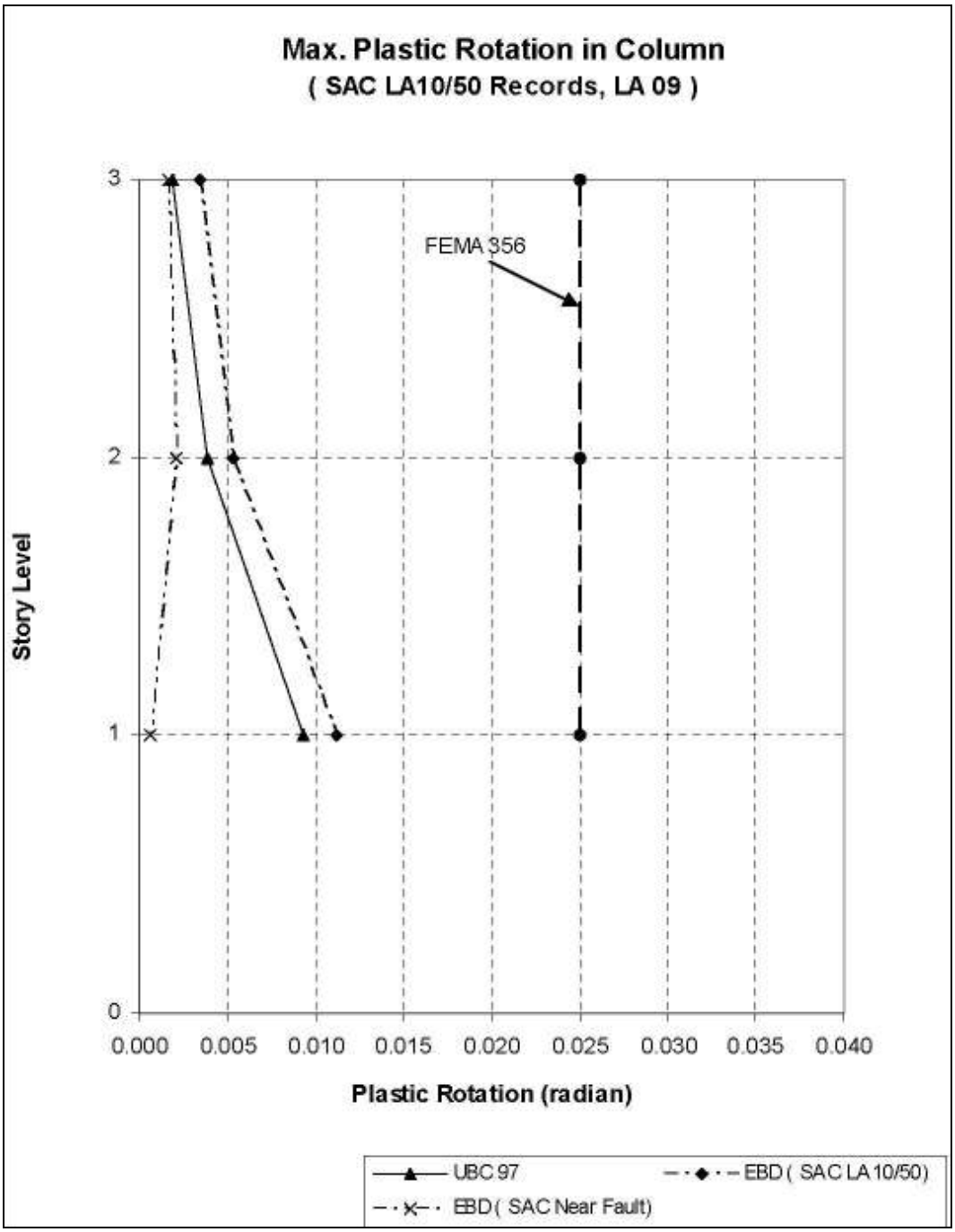

Fig. 6.9: Max plastic rotation in column subjects to SAC LA 09

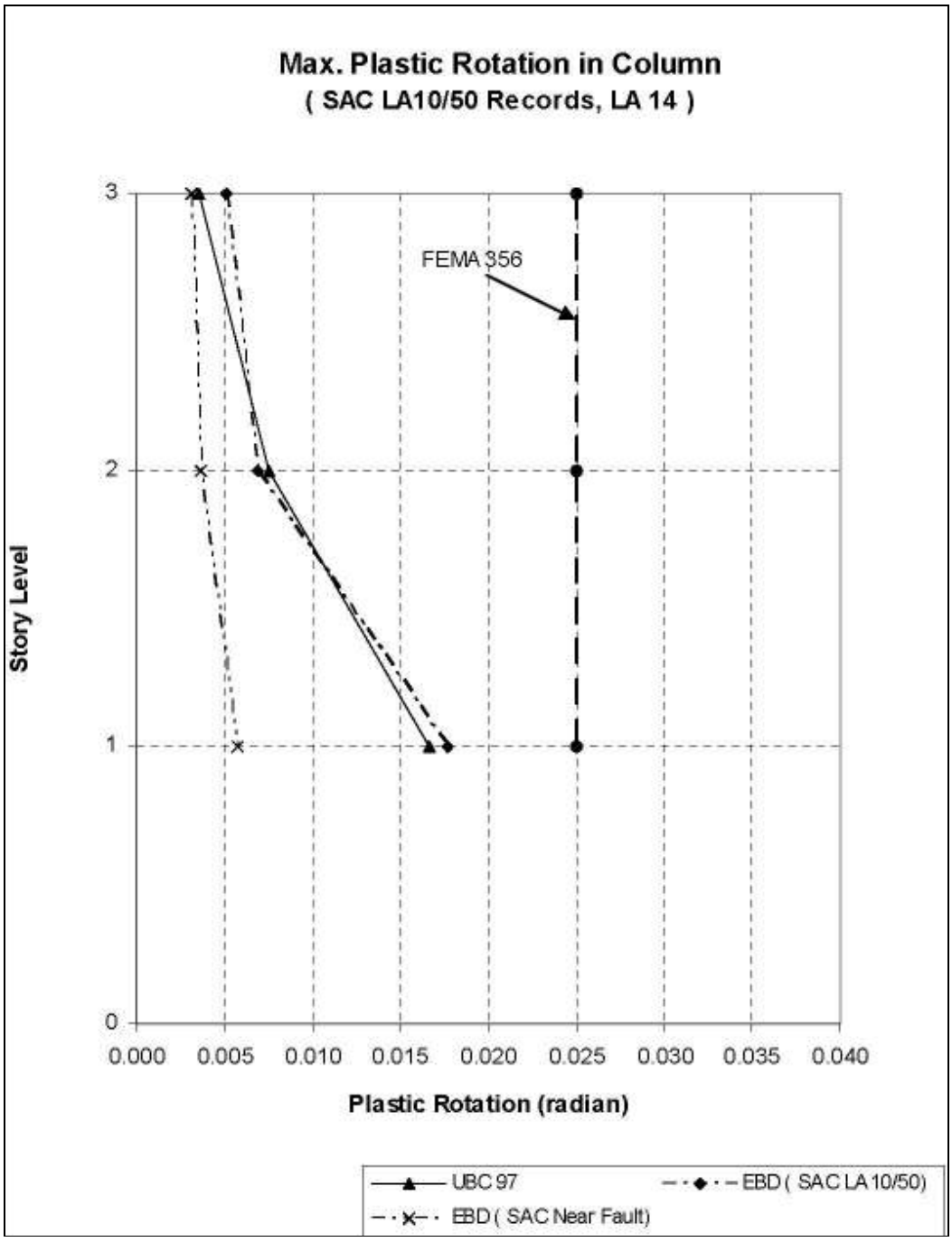

Fig. 6.10: Max plastic rotation in column subjects to SAC LA 14

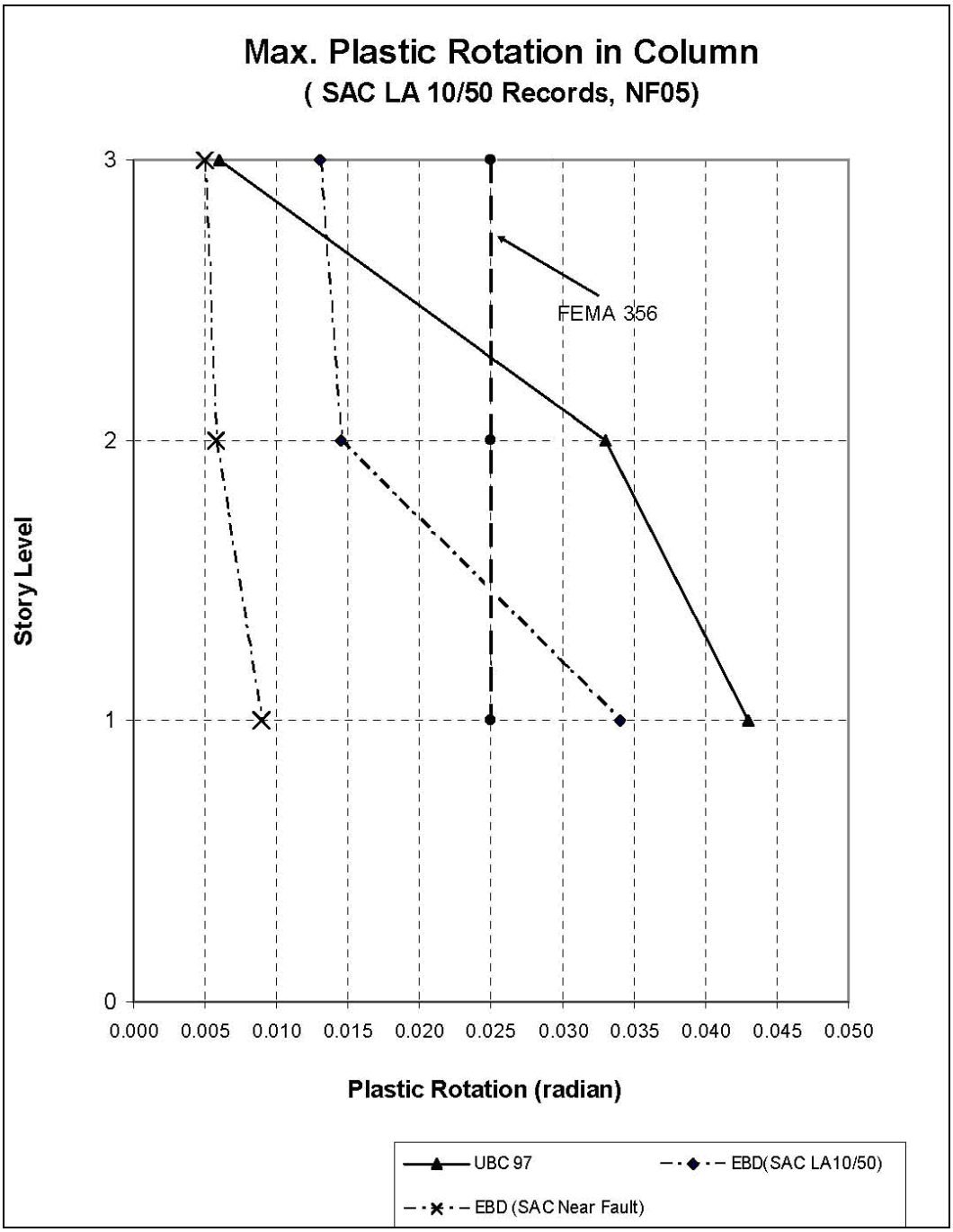

Fig. 6.11: Max plastic rotation in column subjects to SAC NF 05

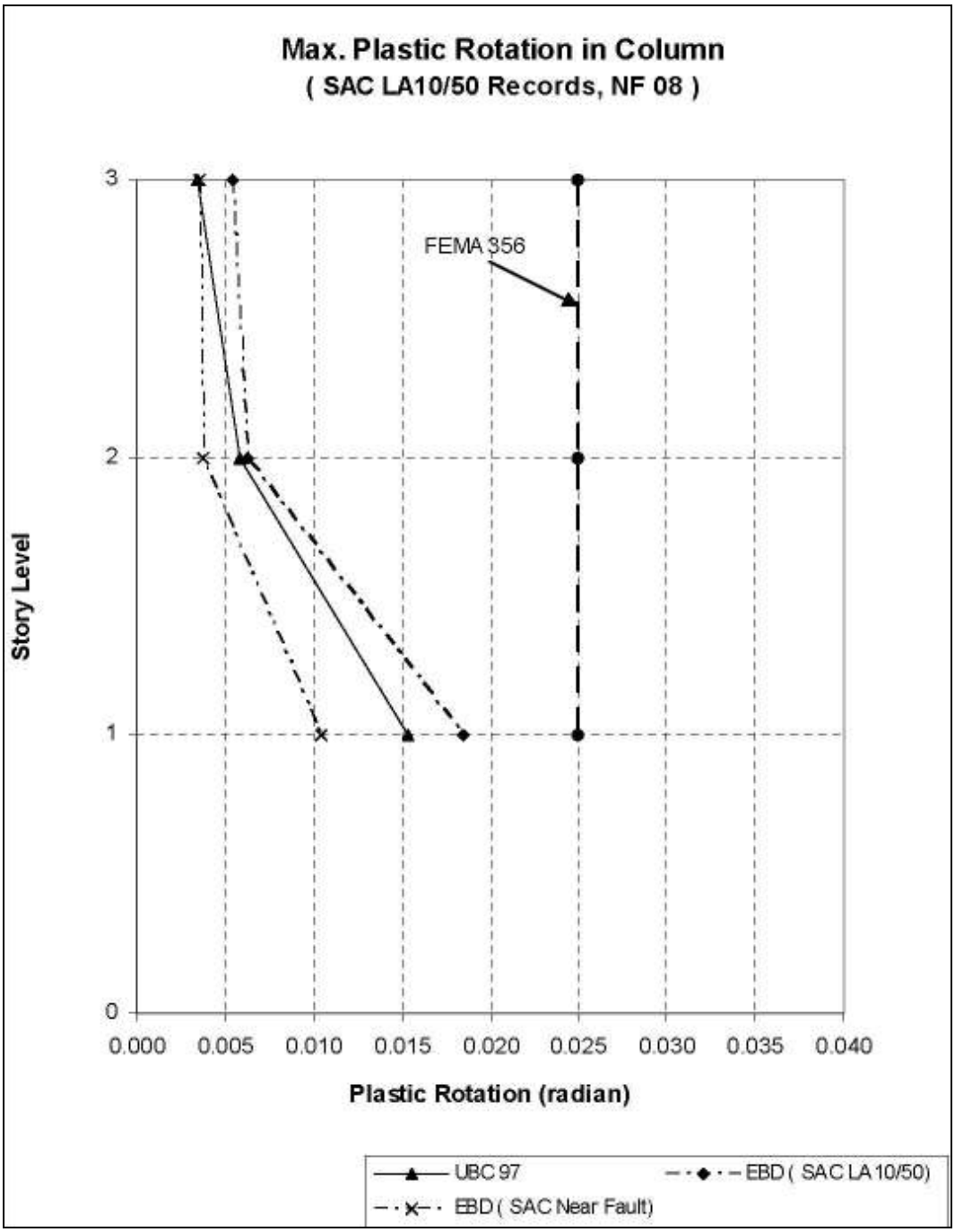

Fig. 6.12: Max plastic rotation in column subjects to SAC NF 08

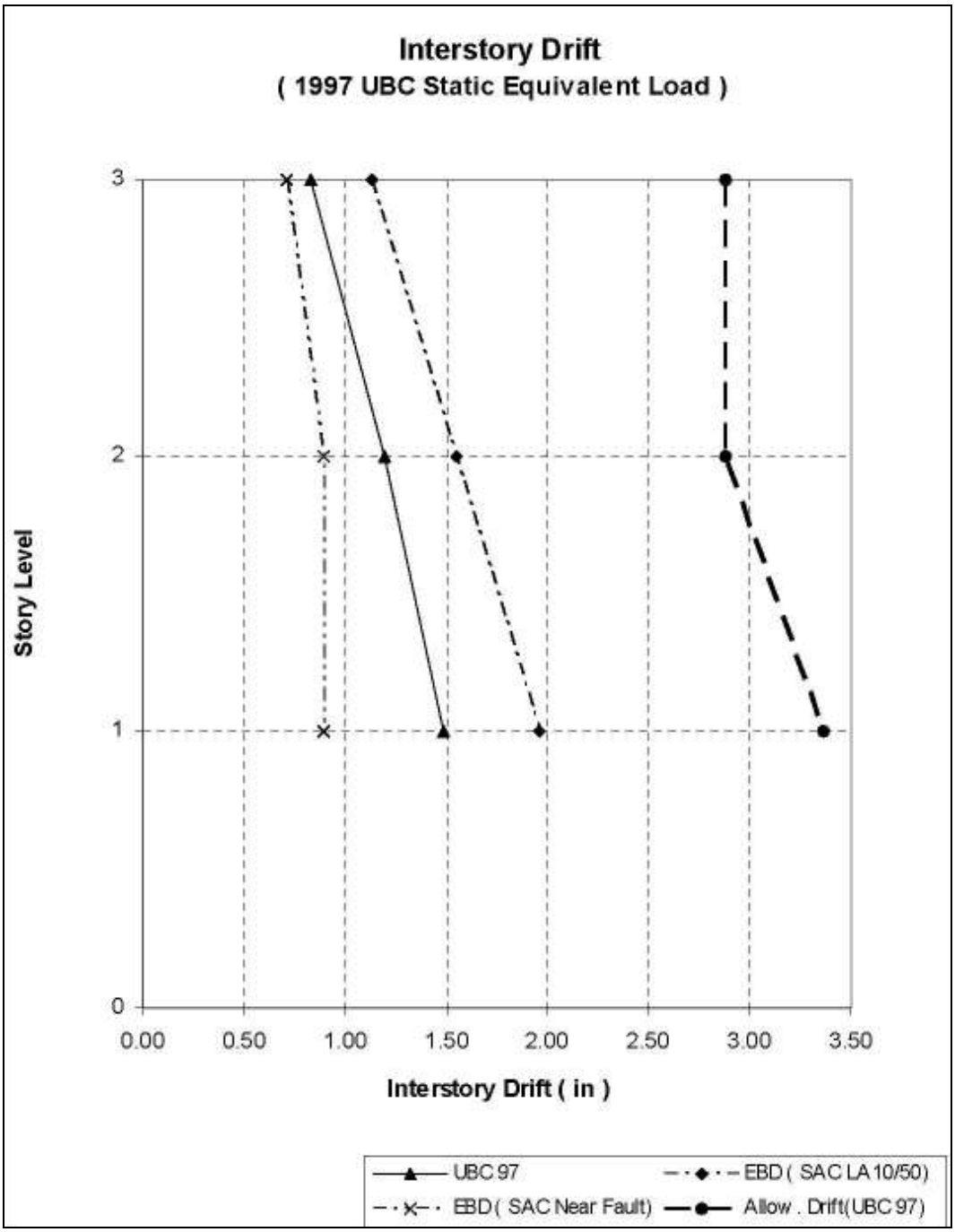

Fig. 6.13: Interstory drift subjects to 1997 UBC static equivalent load

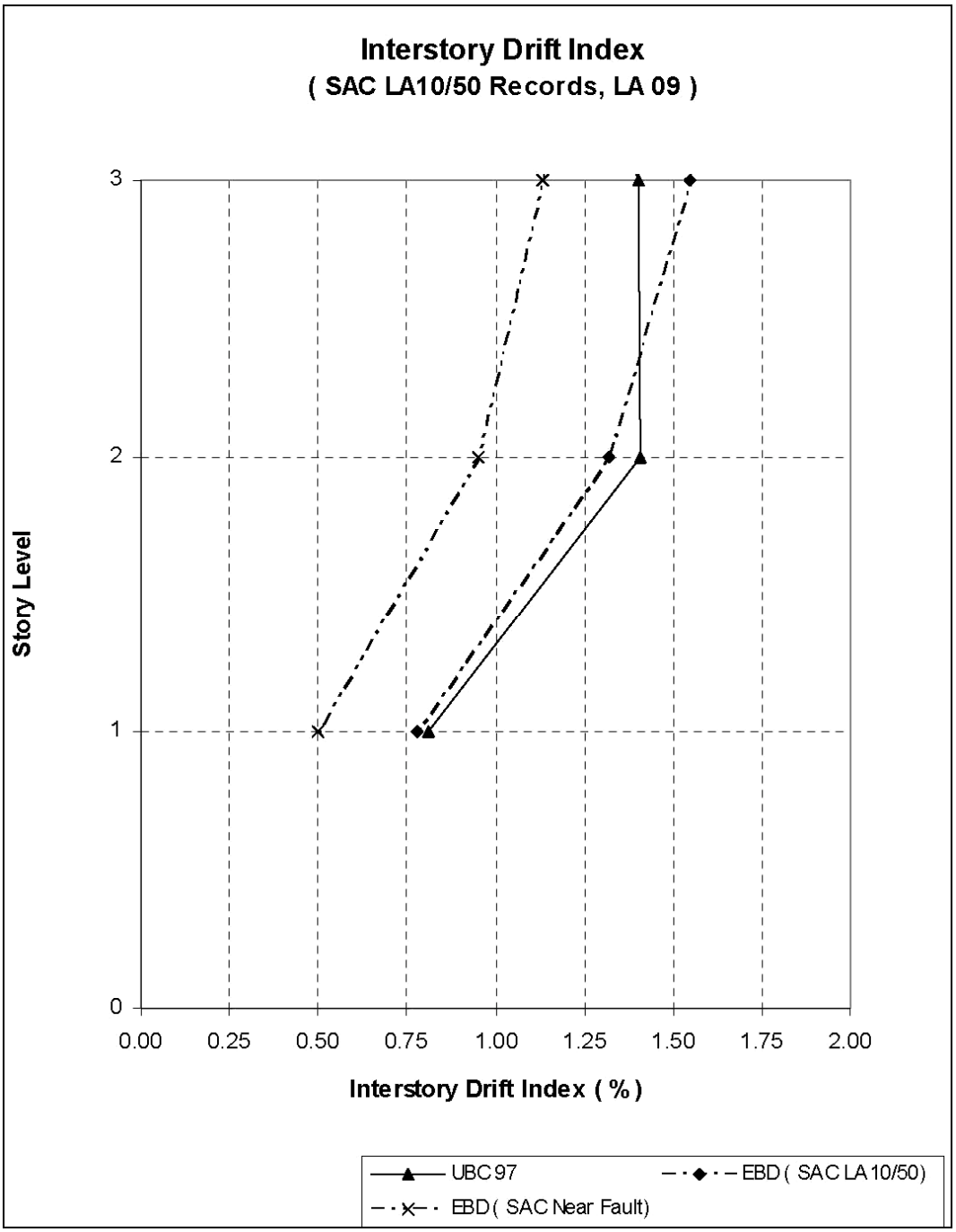

Fig. 6.14: Interstory drift index subjects to SAC LA 09

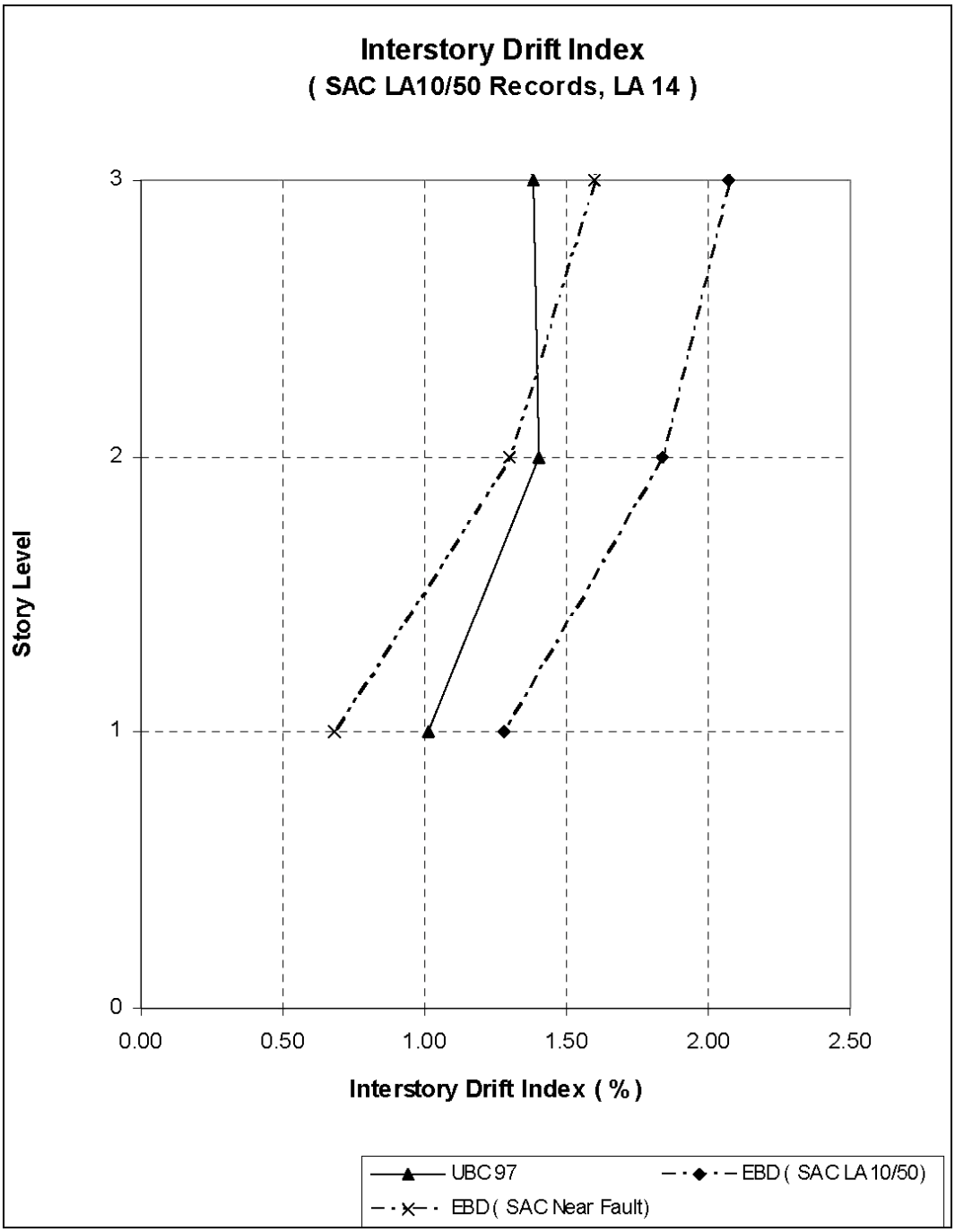

Fig. 6.15: Interstory drift index subjects to SAC LA 14

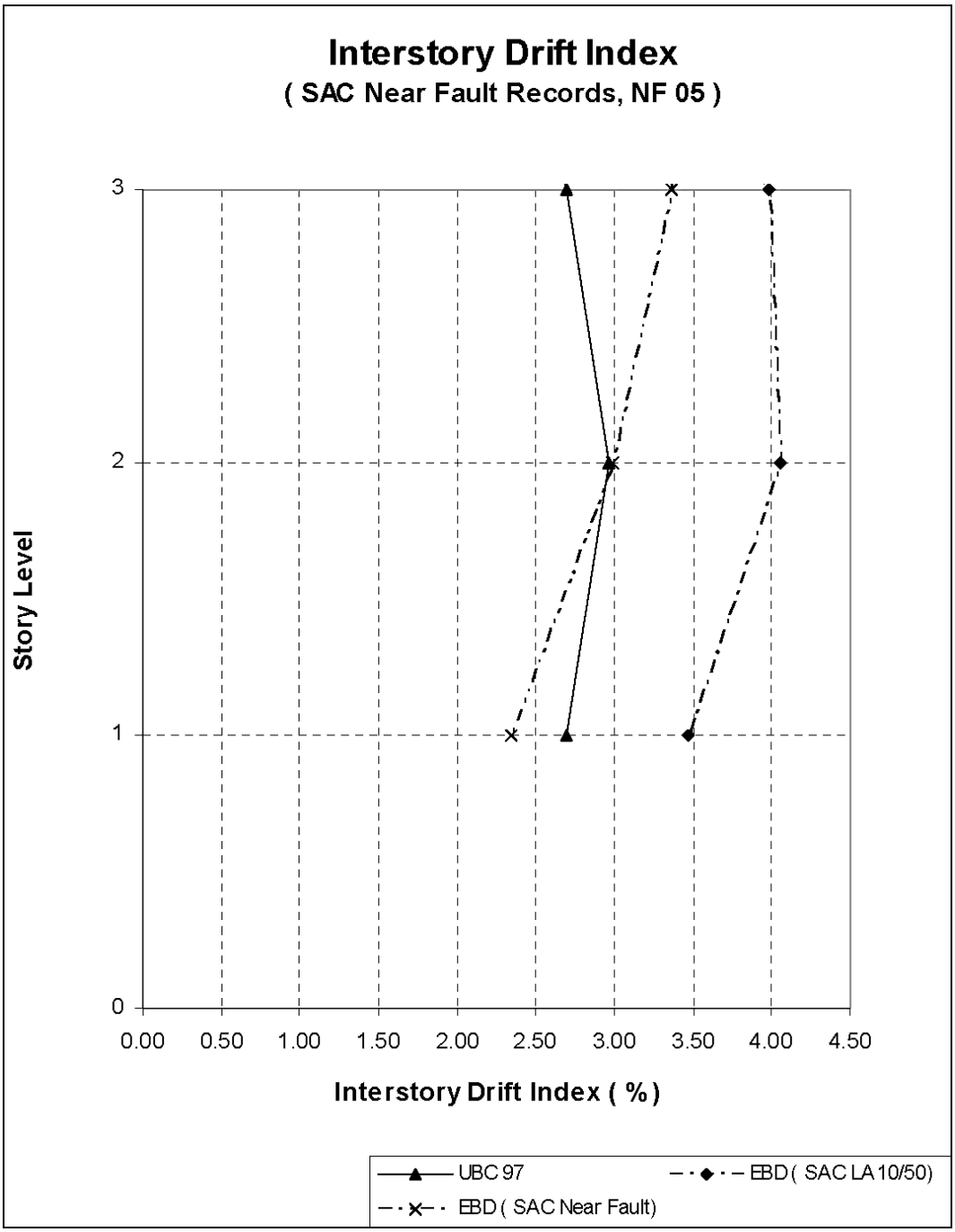

Fig. 6.16: Interstory drift index subjects to SAC NF 05

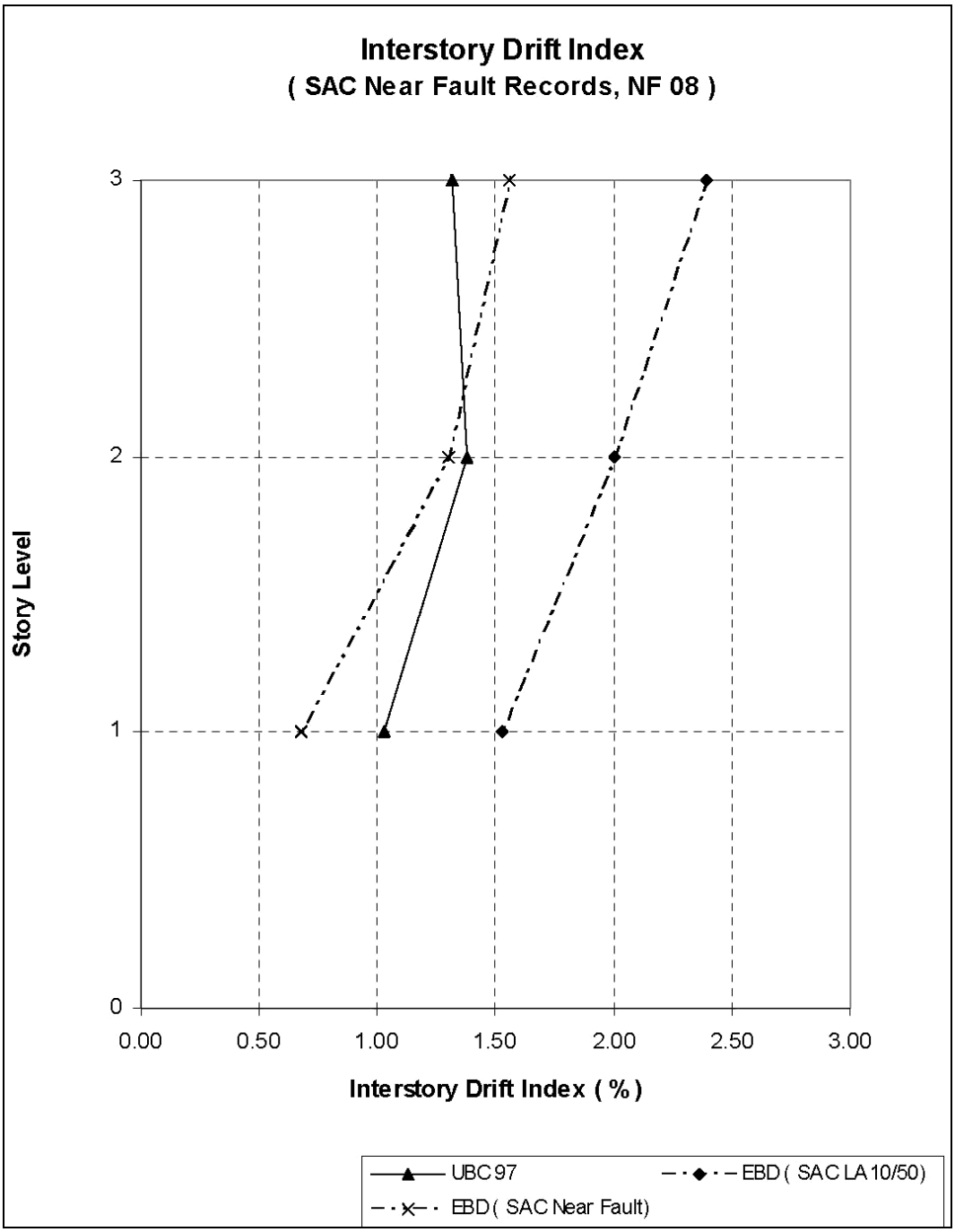

Fig. 6.17: Interstory drift index subjects to SAC NF 08

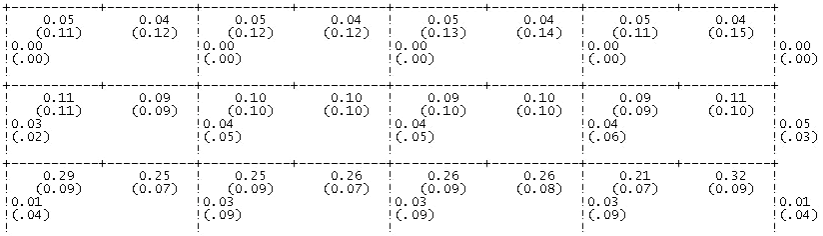

a) UBC LA09

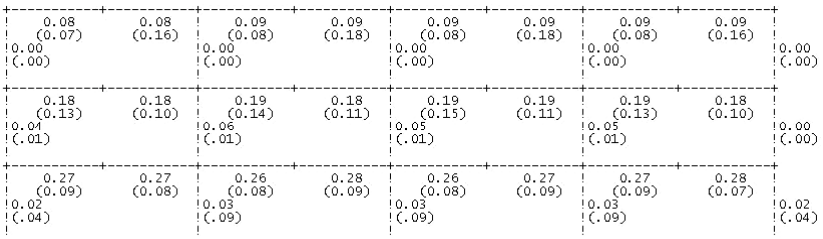

b) EBD (LA 10/50)

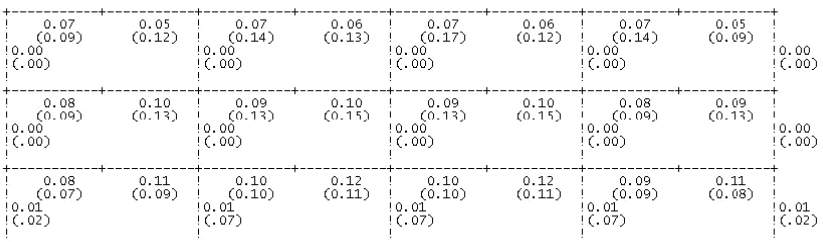

C) EBD (NF)

(< 0.4 = Repairable; 0.4-1.0 = Beyond repair; > 1.0 = Loss of building)
*** Value in parenthesis is Energy ratio (see 2nd part of Eq. 5.1 of Chapter 5)

Fig. 6.18: Damage index for beams and columns subjects to SAC LA09

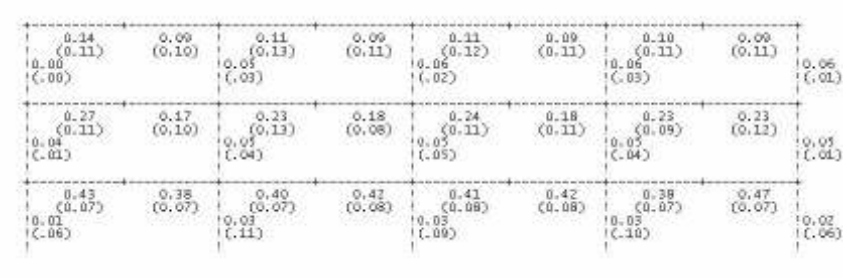

a) UBC 97

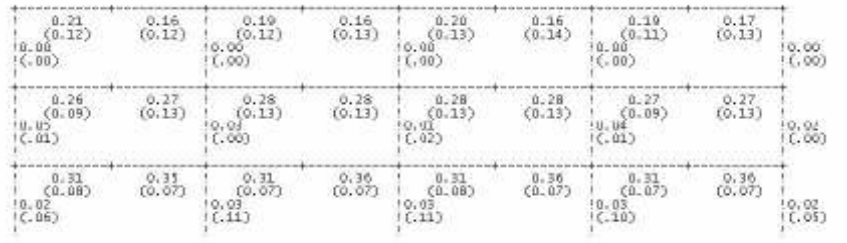

b) EBD (SAC LA10/50)

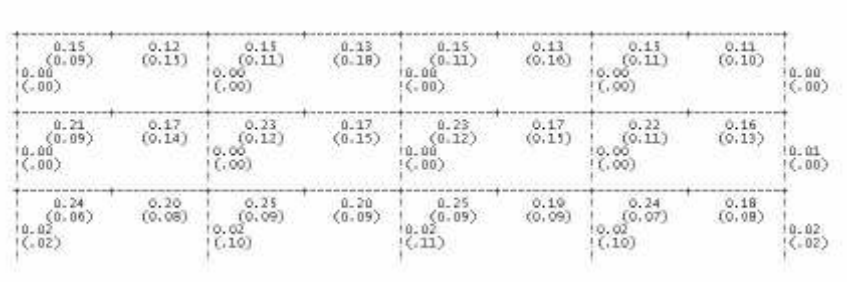

c) EBD (SAC NF)

(< 0.4 = Repairable; 0.4-1.0 = Beyond repair; > 1.0 = Loss of building)
*** Value in parenthesis is Energy ratio (see 2nd part of Eq. 5.1 of Chapter 5)

Fig. 6.19: Damage index for beams and columns subjects to SAC LA14

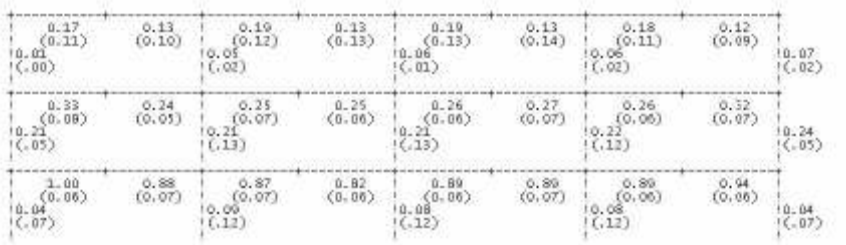

a) UBC 97

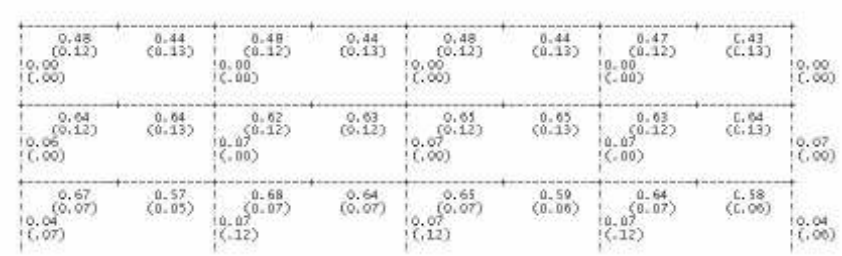

b) EBD (SAC LA10/50)

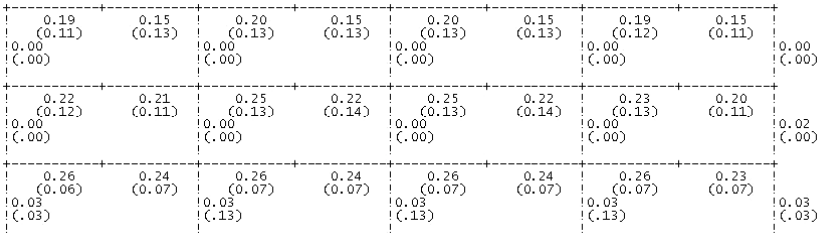

c) EBD (SAC NF)

(< 0.4 = Repairable; 0.4-1.0 = Beyond repair; > 1.0 = Loss of building)
*** Value in parenthesis is Energy ratio (see 2nd part of Eq. 5.1 of Chapter 5)

Fig. 6.20: Damage index for beams and columns subjects to SAC NF 05

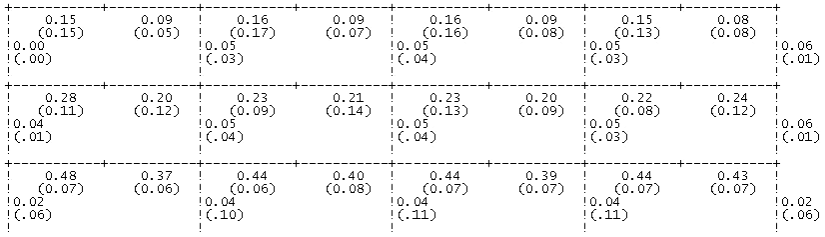

a) UBC 97

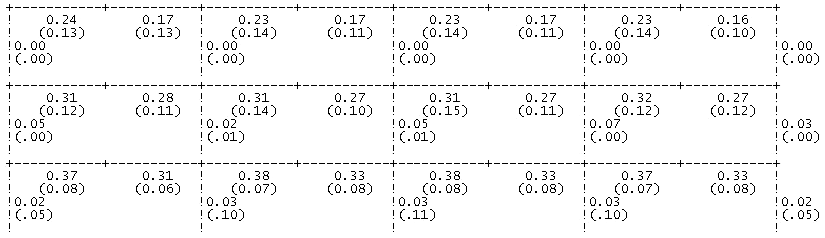

b) EBD (SAC LA10/50)

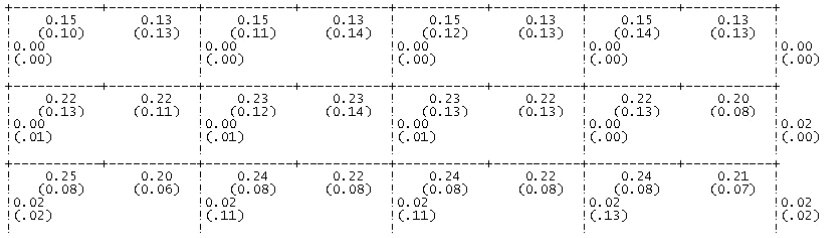

c) EBD (SAC NF)

(< 0.4 = Repairable; 0.4-1.0 = Beyond repair; > 1.0 = Loss of building)
*** Value in parenthesis is Energy ratio (see 2nd part of Eq. 5.1 of Chapter 5)

Fig. 6.21: Damage index for beams and columns subjects to SAC NF 08

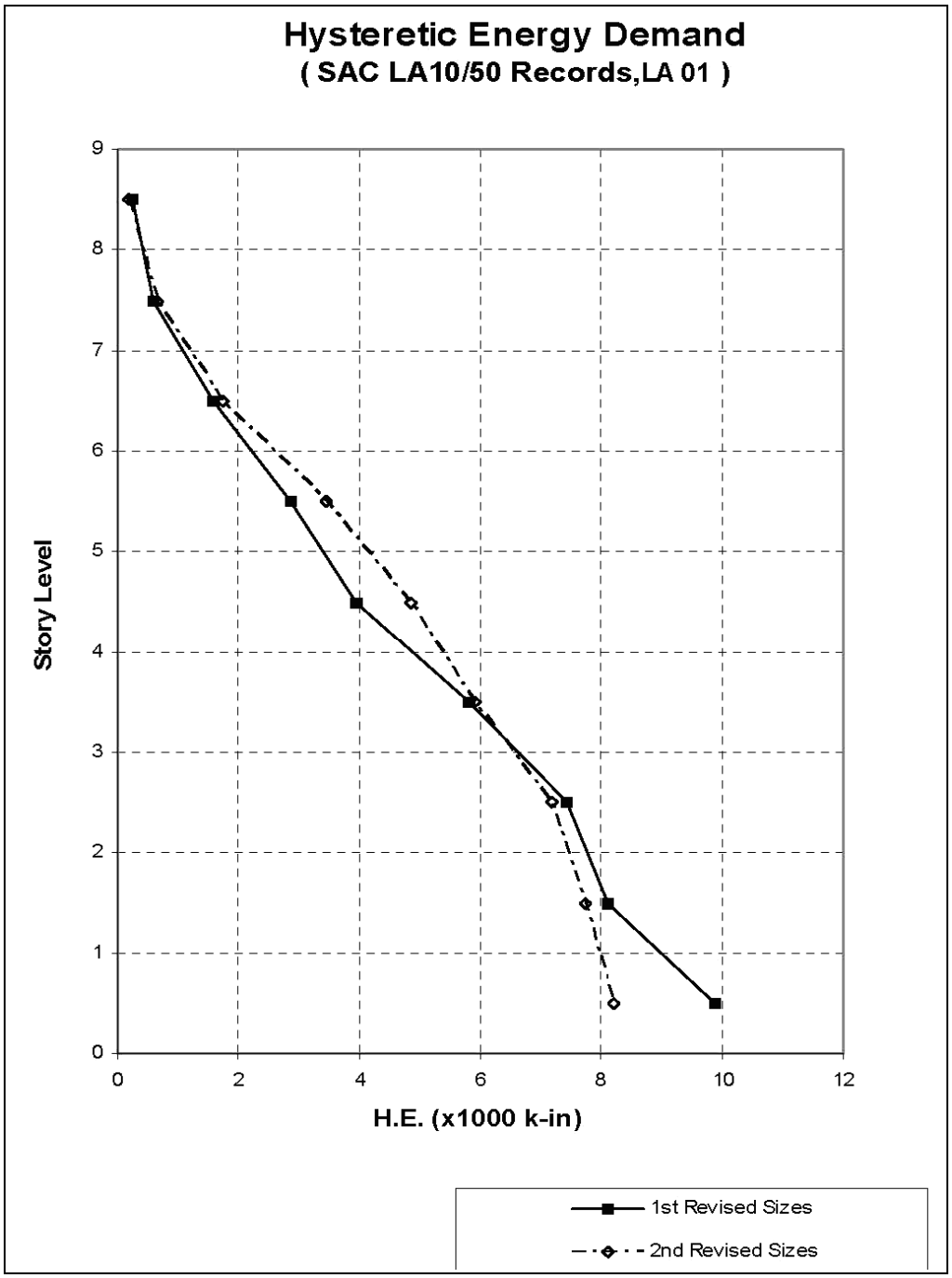

Fig. 6.22: Hysteretic energy demand for 9-story building subjects to SAC LA10/50 records, LA01

** The i^{th} revised sizes = sizes after the i^{th} iteration for frame design*

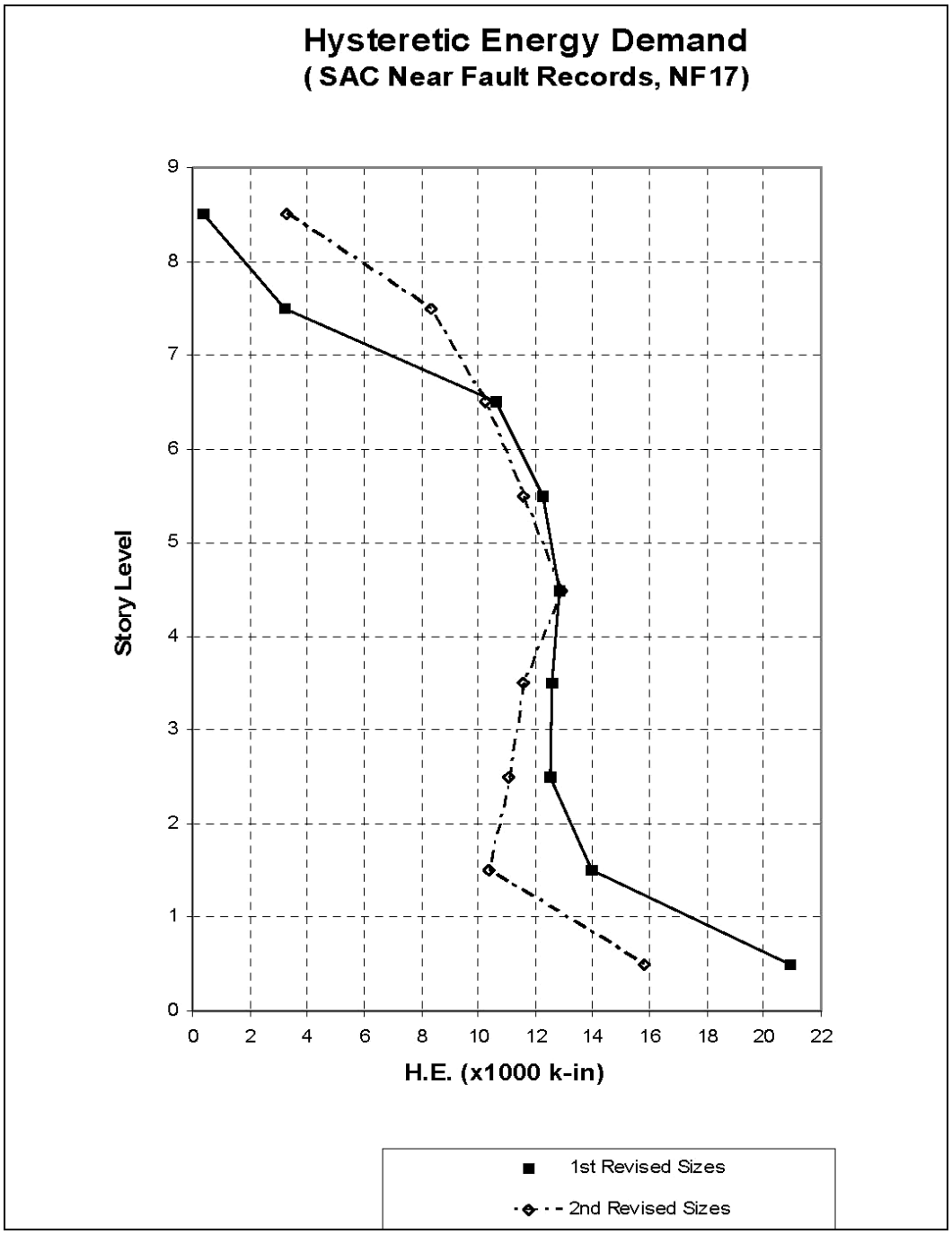

Fig. 6.23: Hysteretic energy demand for 9-story building subjects to SAC Near Fault records, NF17

** The i^{th} revised sizes = sizes after the i^{th} iteration for frame design*

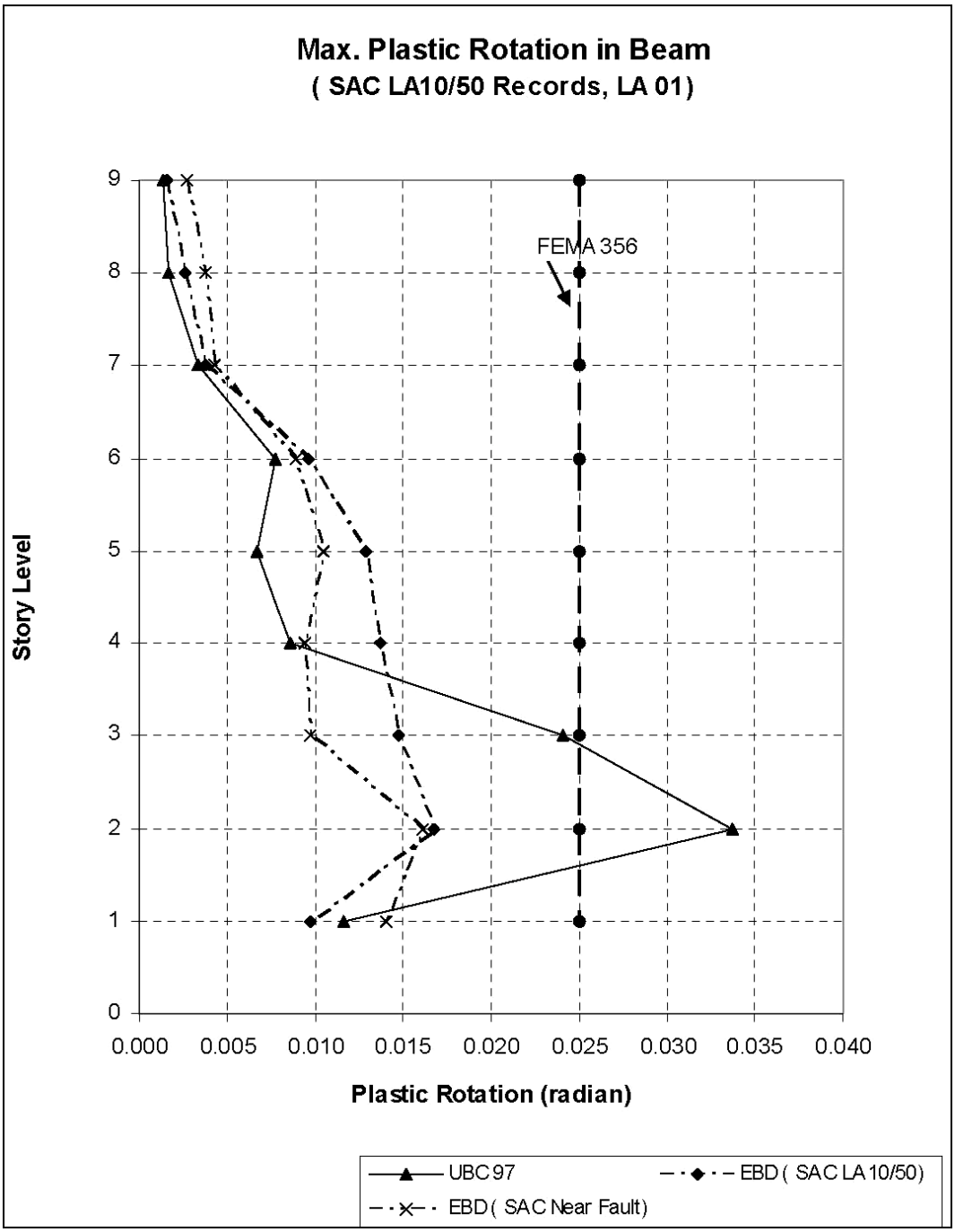

Fig. 6.24: Max plastic rotation in beam subjects to SAC LA01

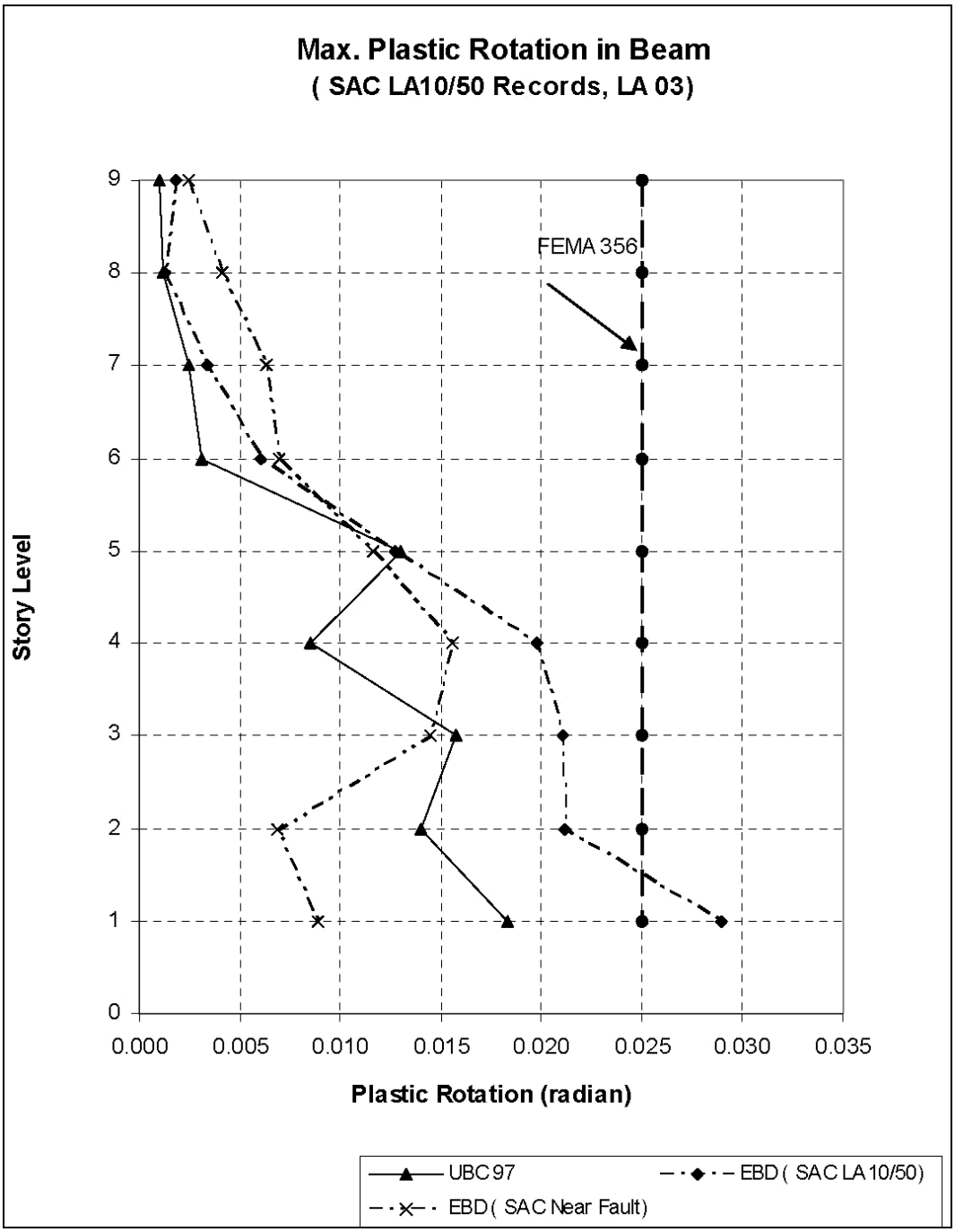

Fig. 6.25: Max plastic rotation in beam subjects to SAC LA 03

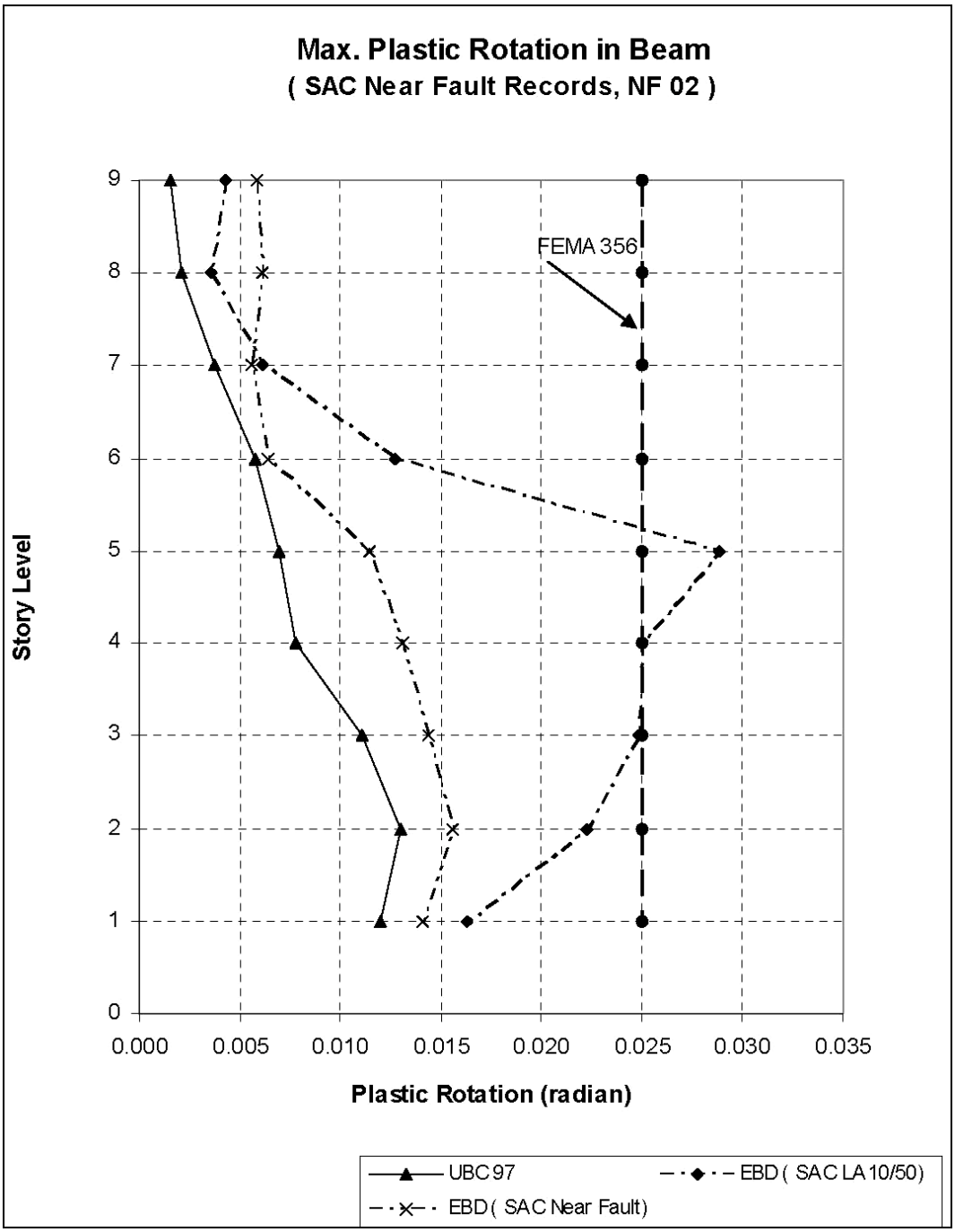

Fig. 6.26: Max plastic rotation in beam subjects to SAC NF 02

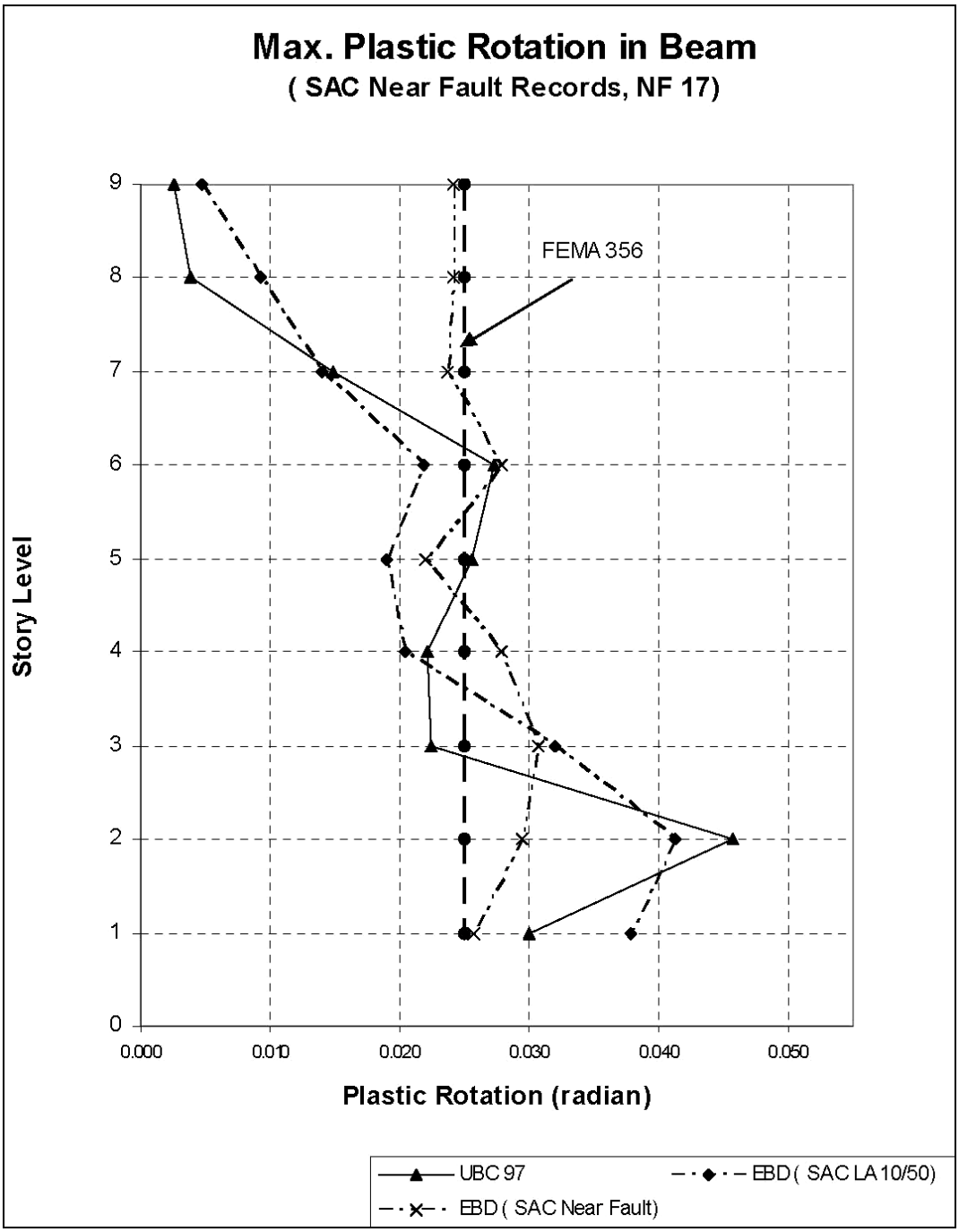

Fig. 6.27: Max plastic rotation in beam subjects to SAC NF 17

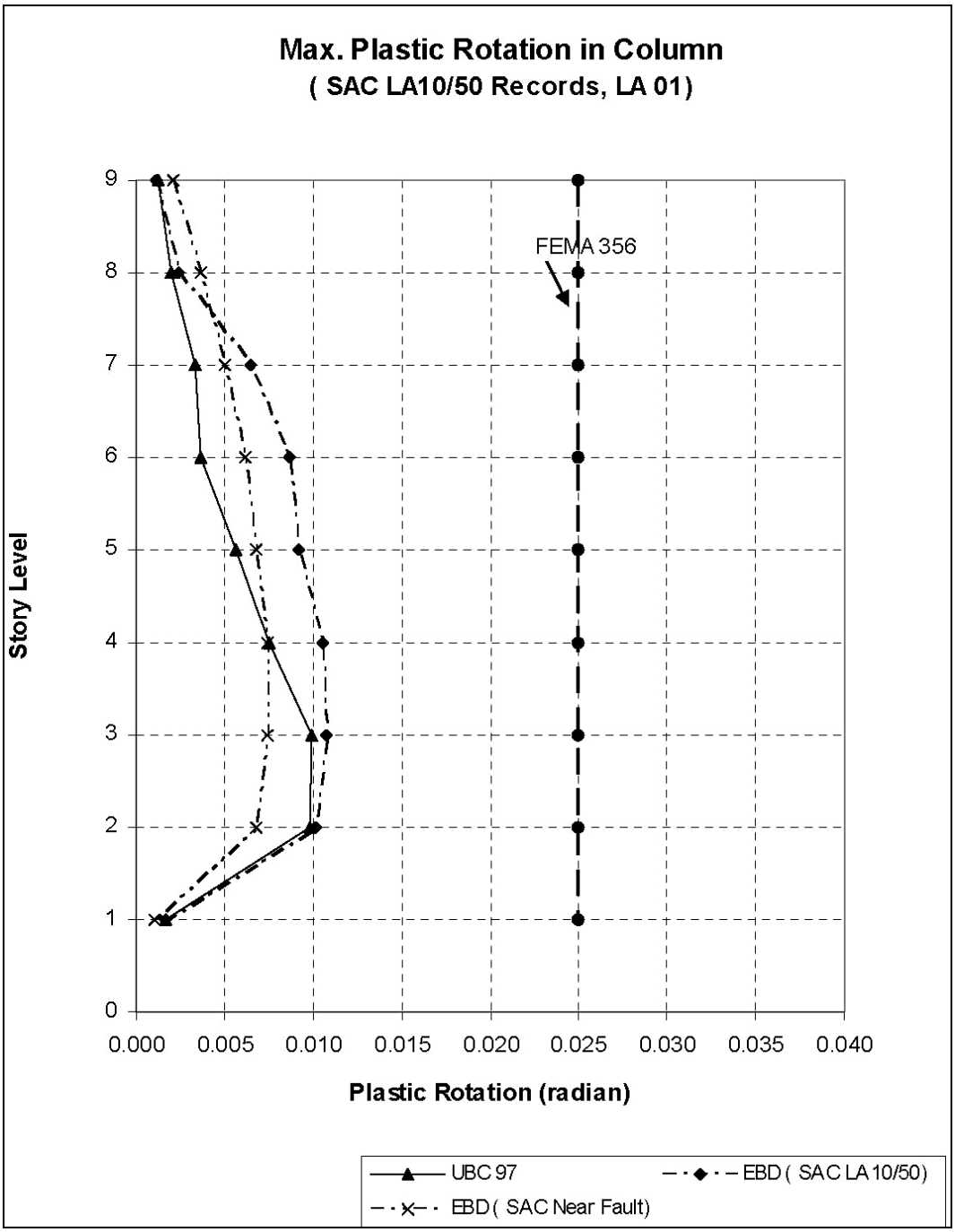

Fig. 6.28: Max plastic rotation in column subjects to SAC LA 01

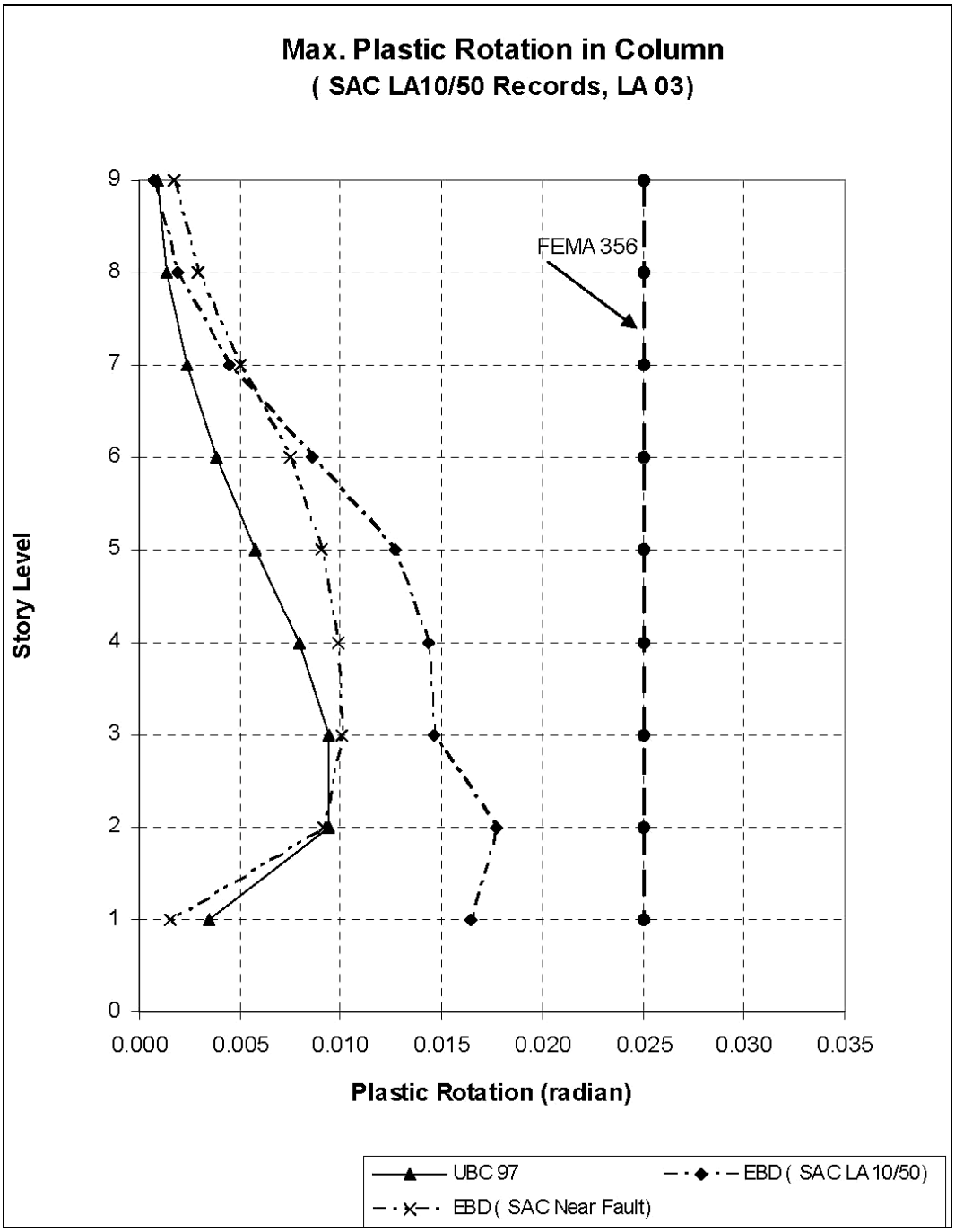

Fig. 6.29: Max plastic rotation in column subjects to SAC LA 03

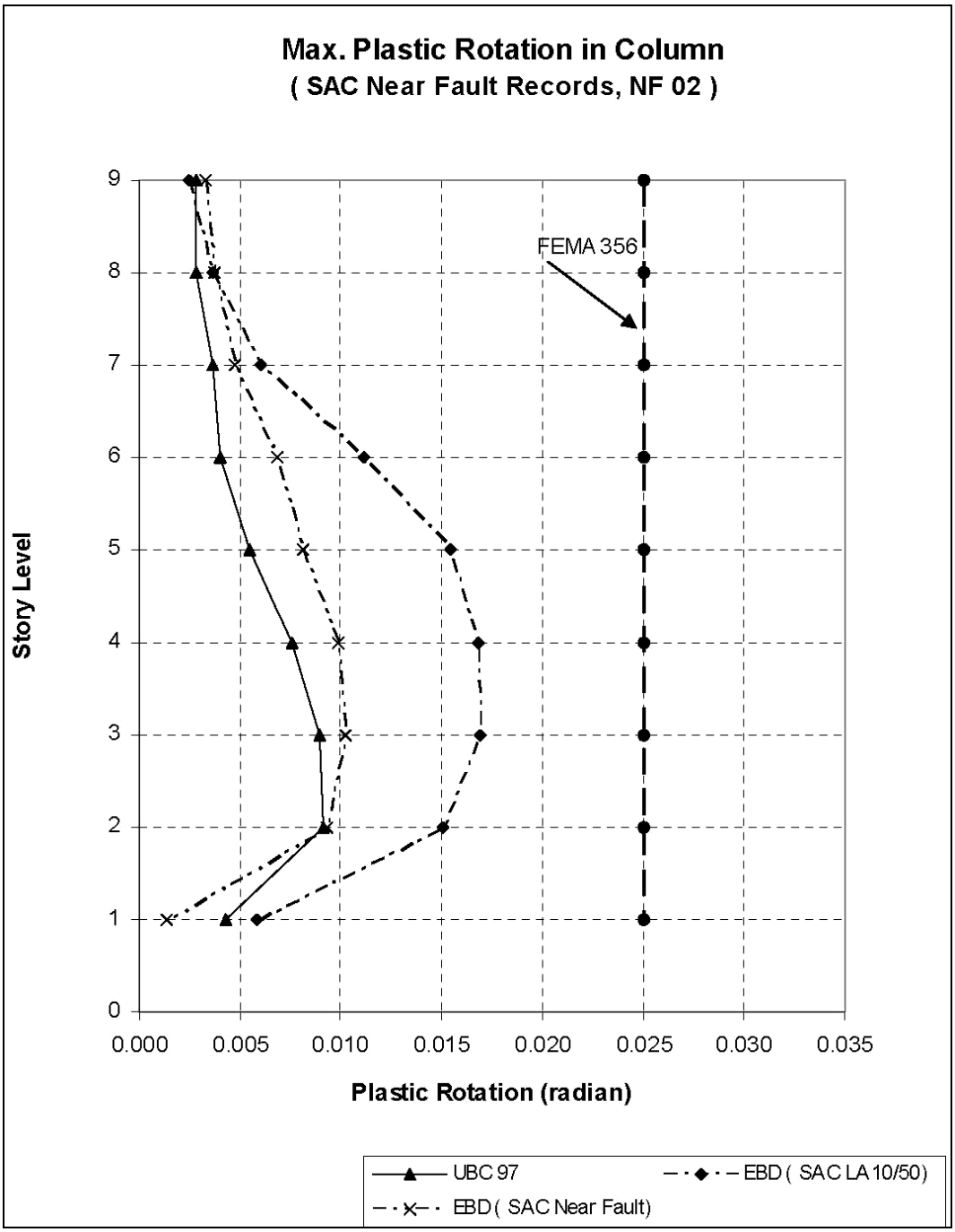

Fig. 6.30: Max plastic rotation in column subjects to SAC NF 02

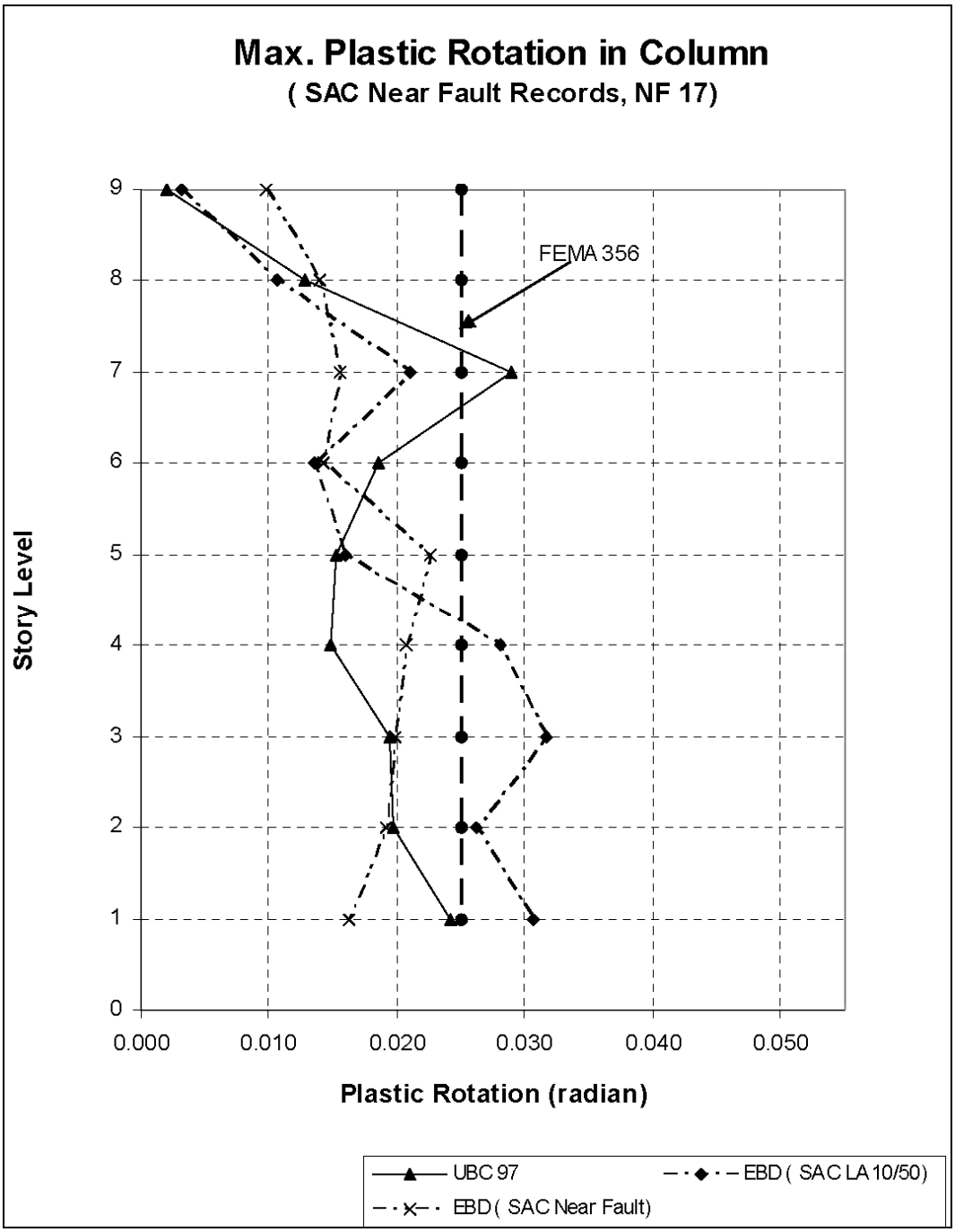

Fig. 6.31: Max plastic rotation in column subjects to SAC NF 17

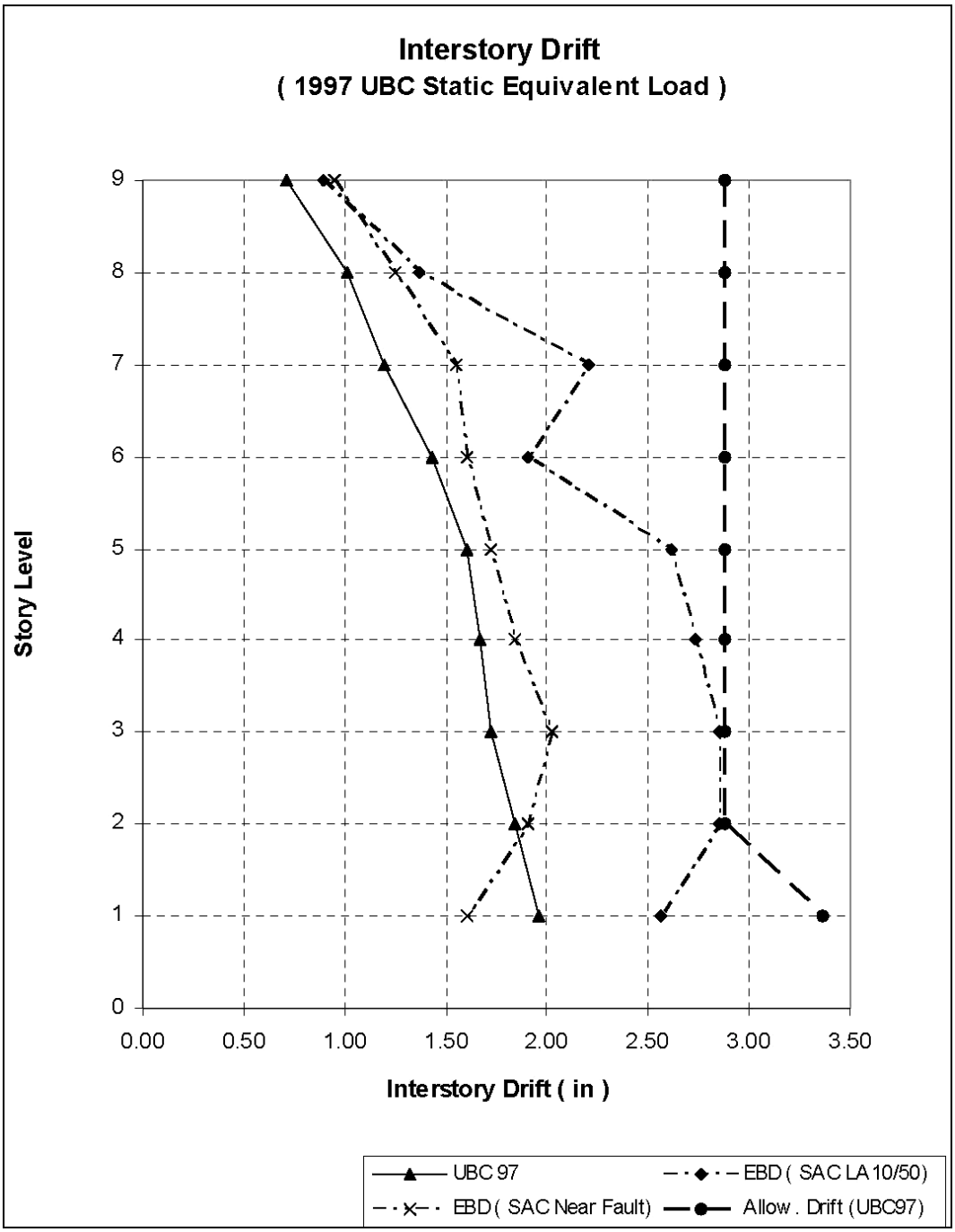

Fig. 6.32: Inter-story drift subjects to 1997 UBC static equivalent load

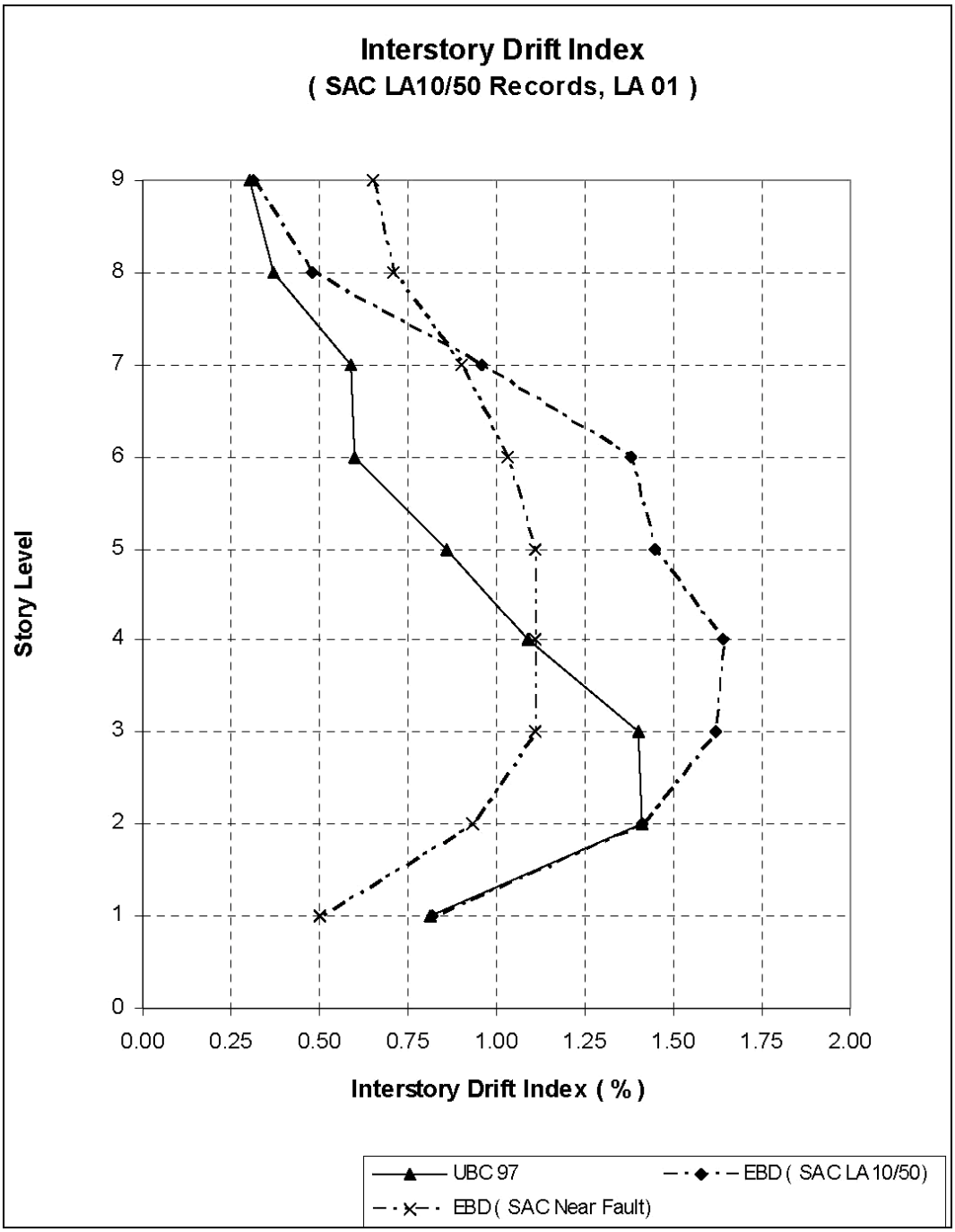

Fig. 6.33: Interstory drift index subjects to SAC LA 01

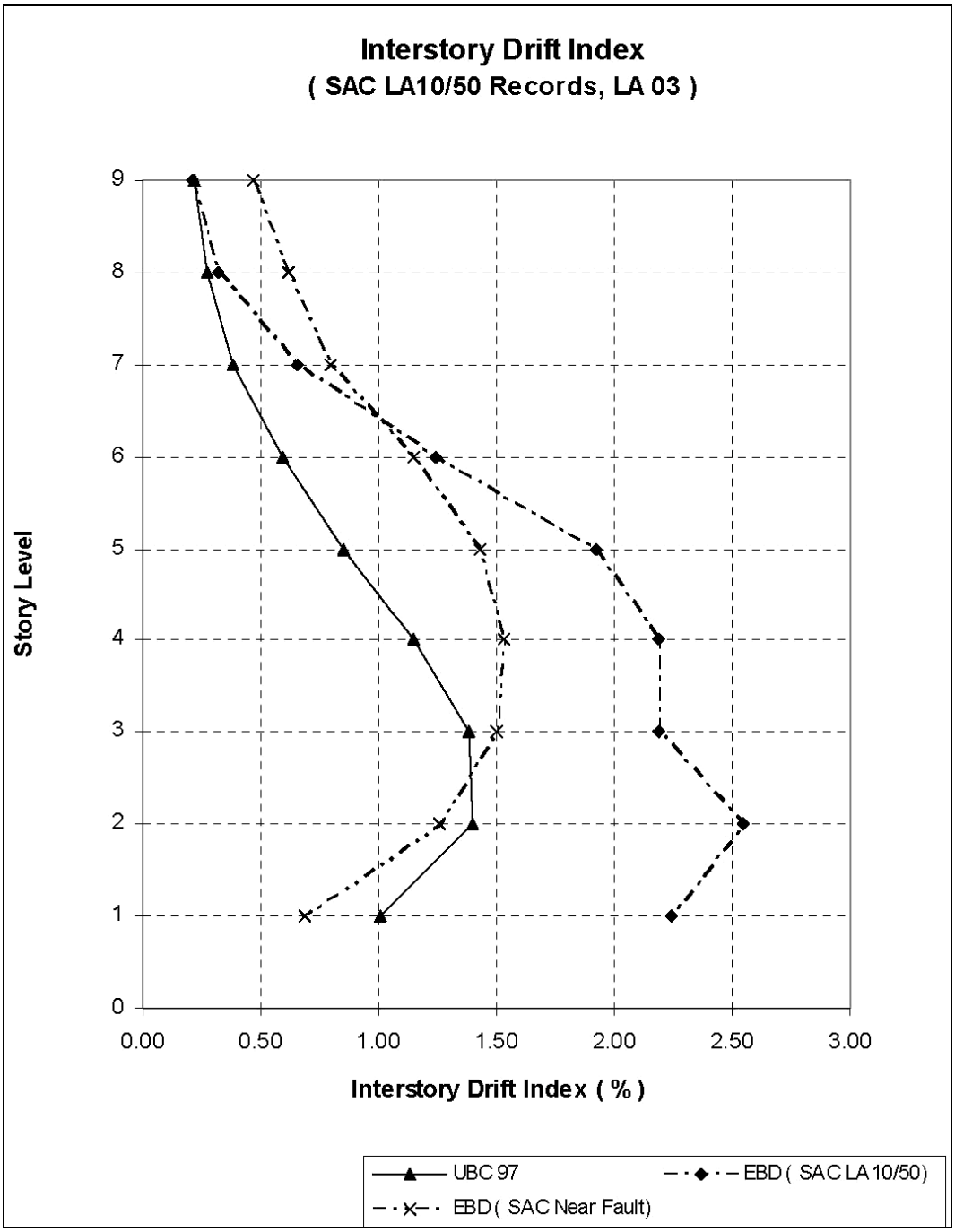

Fig. 6.34: Interstory drift index subjects to SAC LA 03

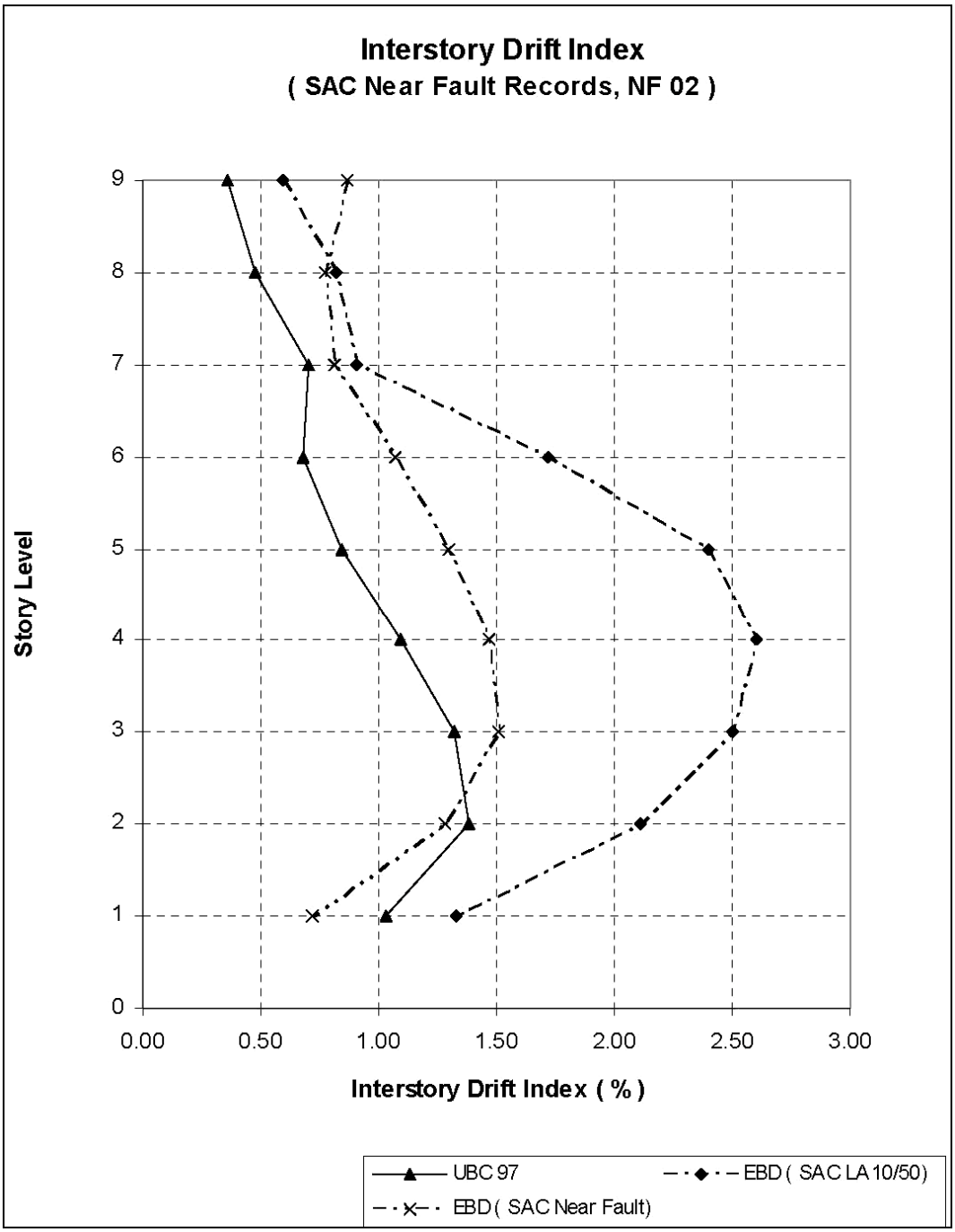

Fig. 6.35: Interstory drift index subjects to SAC NF 02

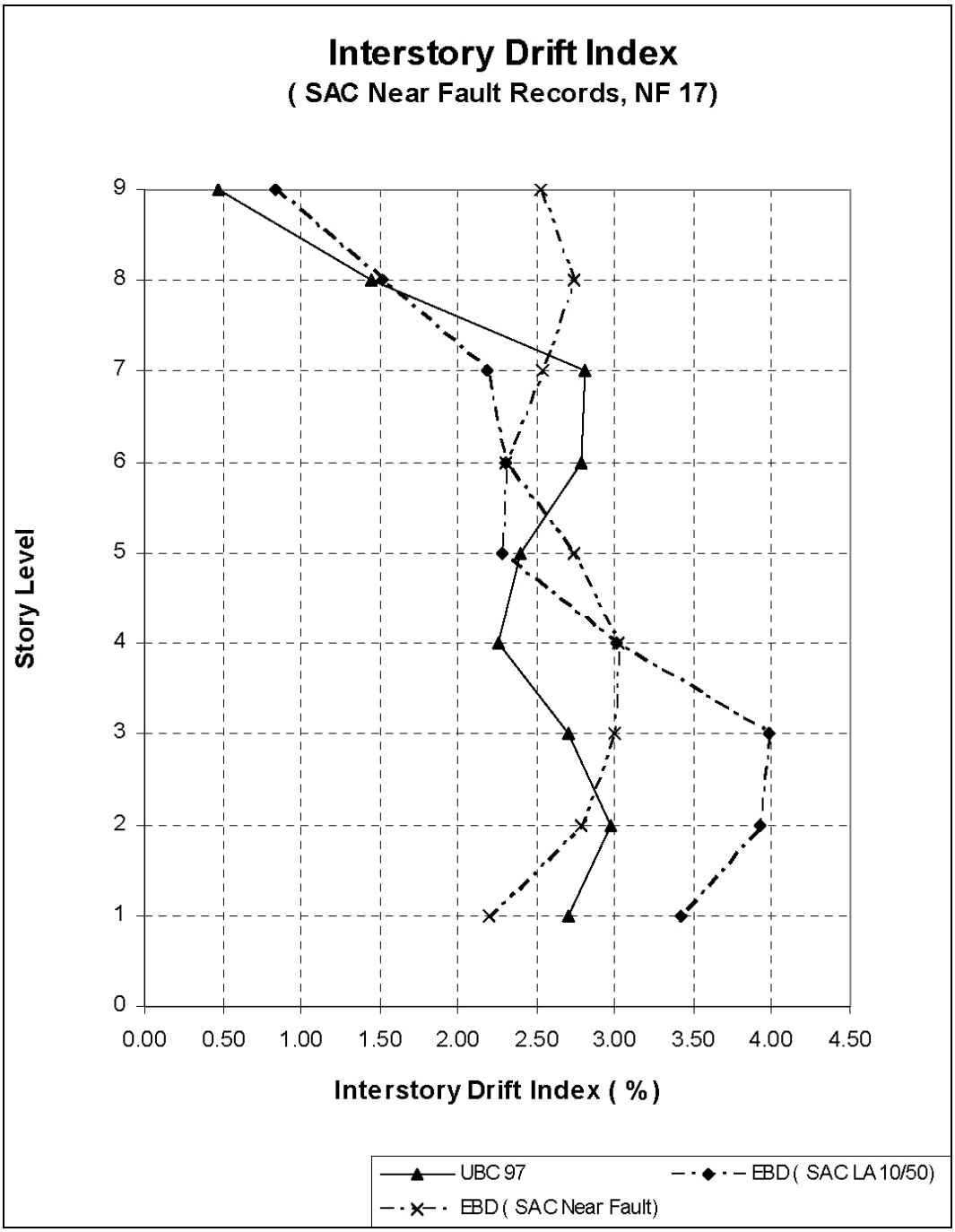

Fig. 6.36: Interstory drift index subjects to SAC NF 17

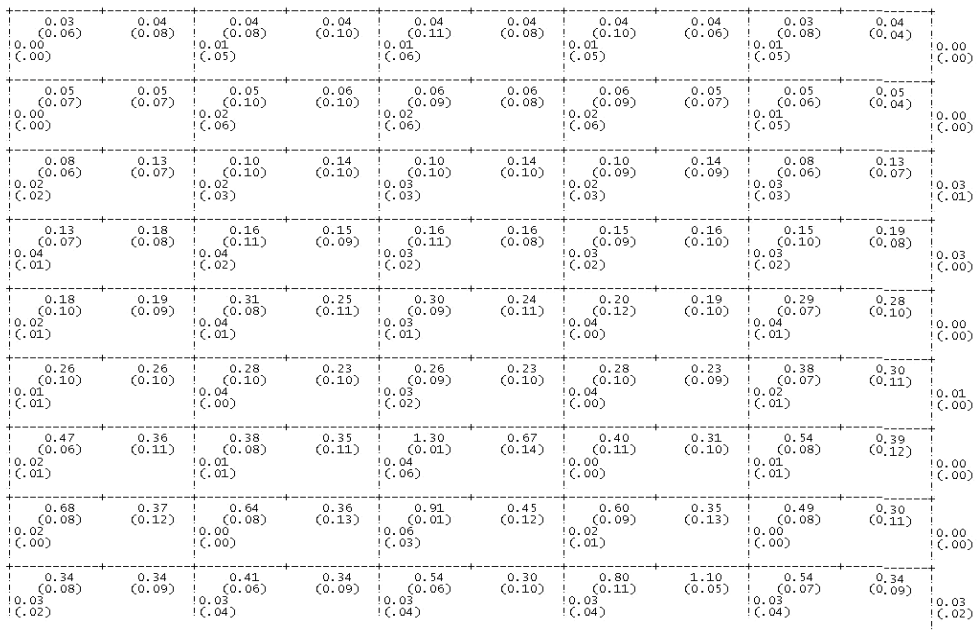

a) UBC 97

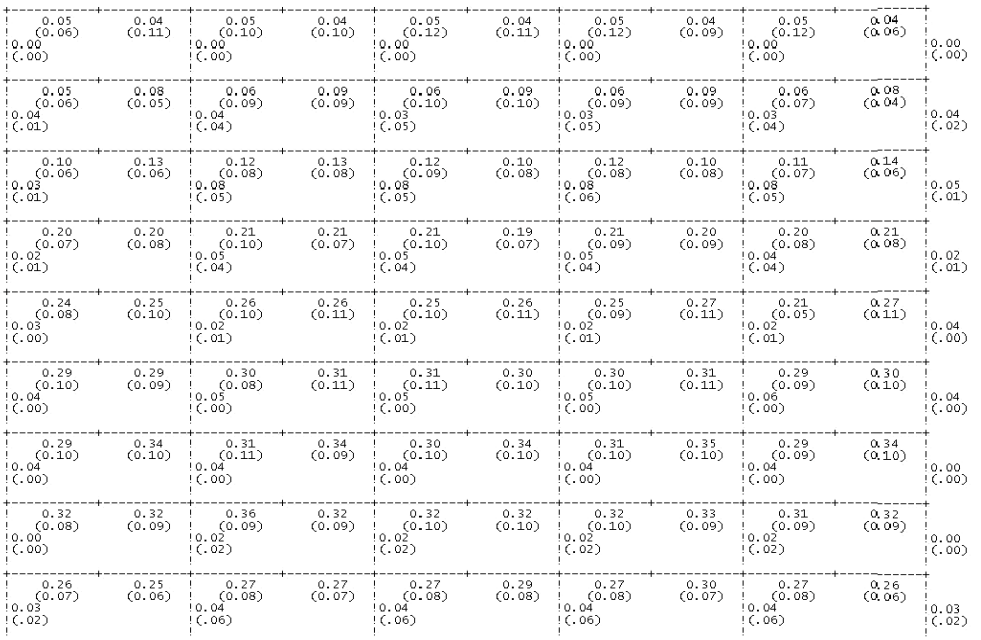

b) EBD (SAC LA10/50)

Fig. 6.37: Damage index for beams and columns subjects to SAC LA01

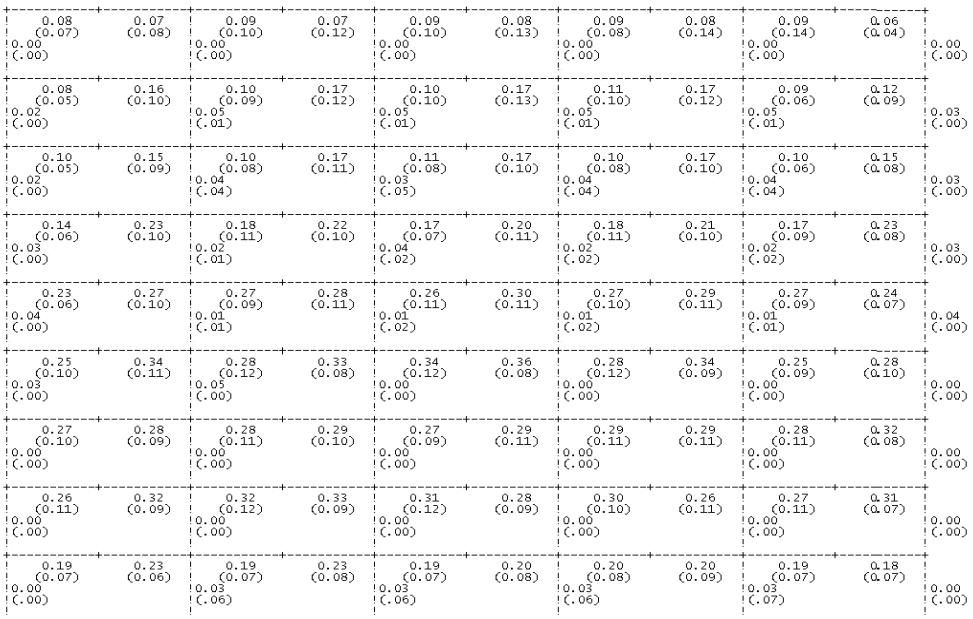

c) EBD (SAC NF)

(< 0.4 = Repairable; 0.4-1.0 = Beyond repair; > 1.0 = Loss of building)
*** Value in parenthesis is Energy ratio (see 2nd part of Eq. 5.1 of Chapter 5)

Fig. 6.37: Continued

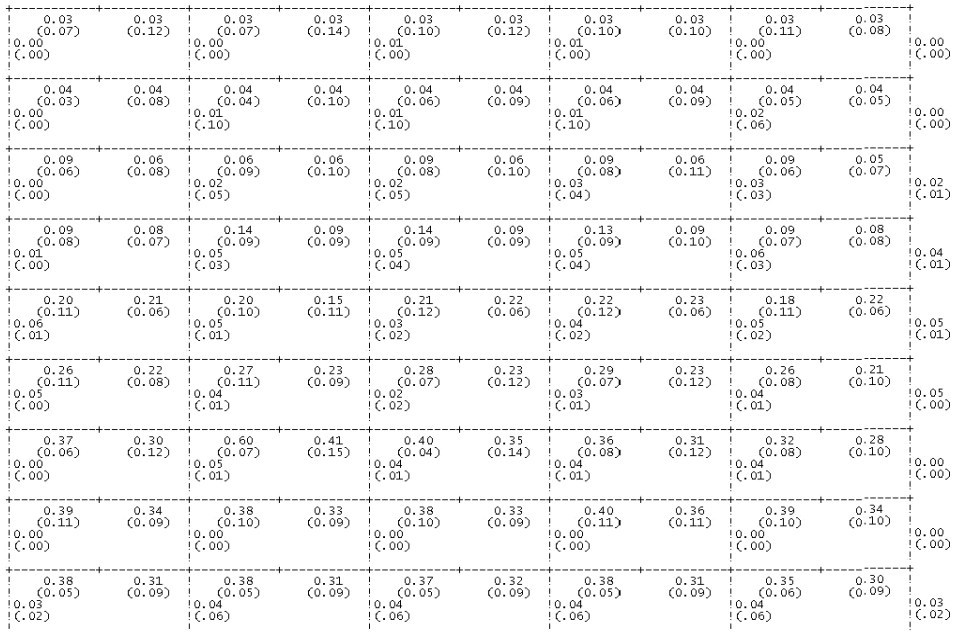

a) UBC 97

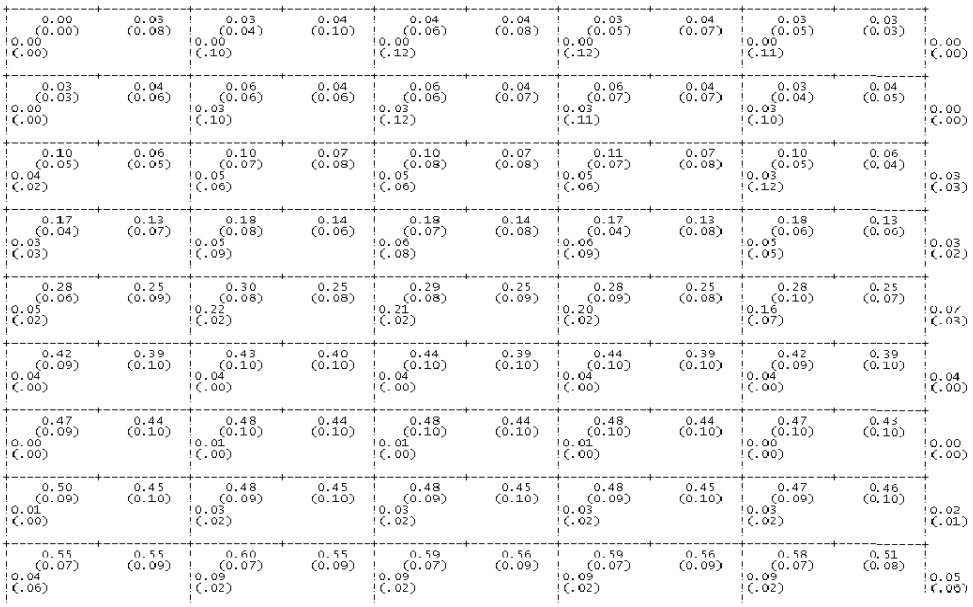

b) EBD (SAC LA10/50)

Fig. 6.38: Damage index for beams and columns subjects to SAC LA03

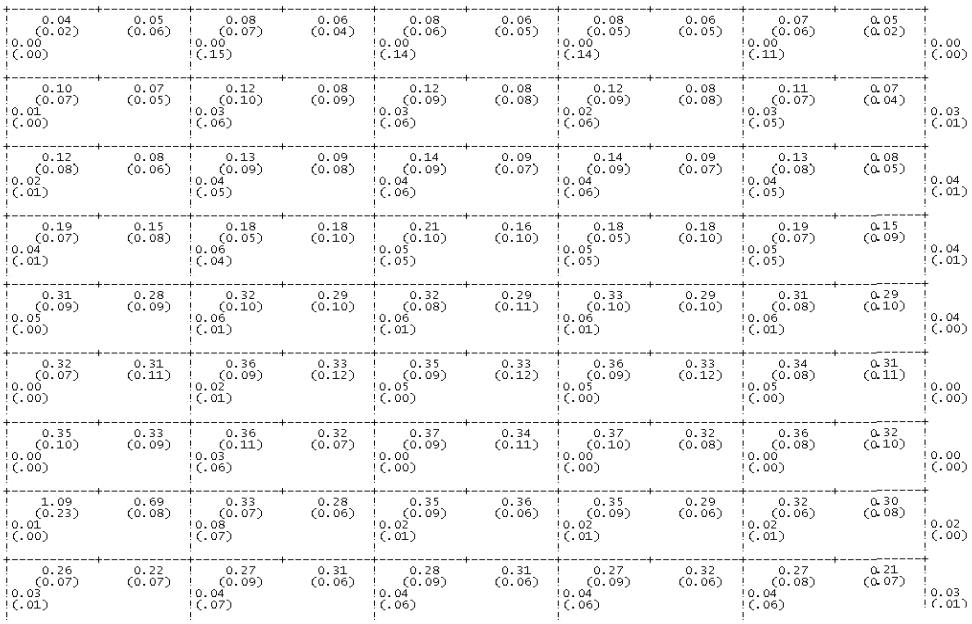

c) EBD (SAC NF)

(< 0.4 = Repairable; 0.4-1.0 = Beyond repair; > 1.0 = Loss of building)
*** Value in parenthesis is Energy ratio (see 2nd part of Eq. 5.1 of Chapter 5)

Fig. 6.38: Continued

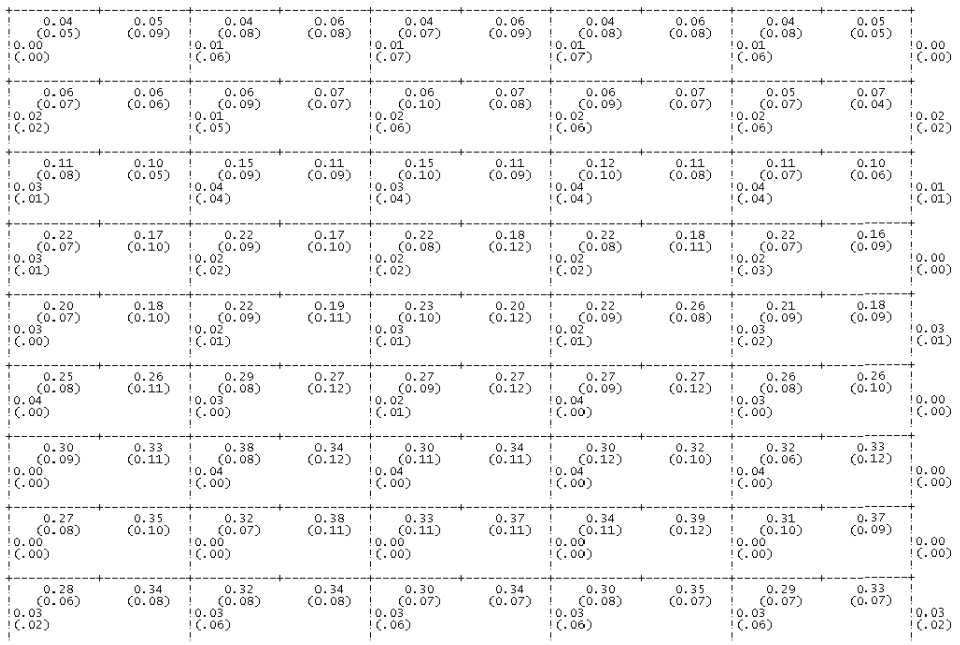

a) UBC 97

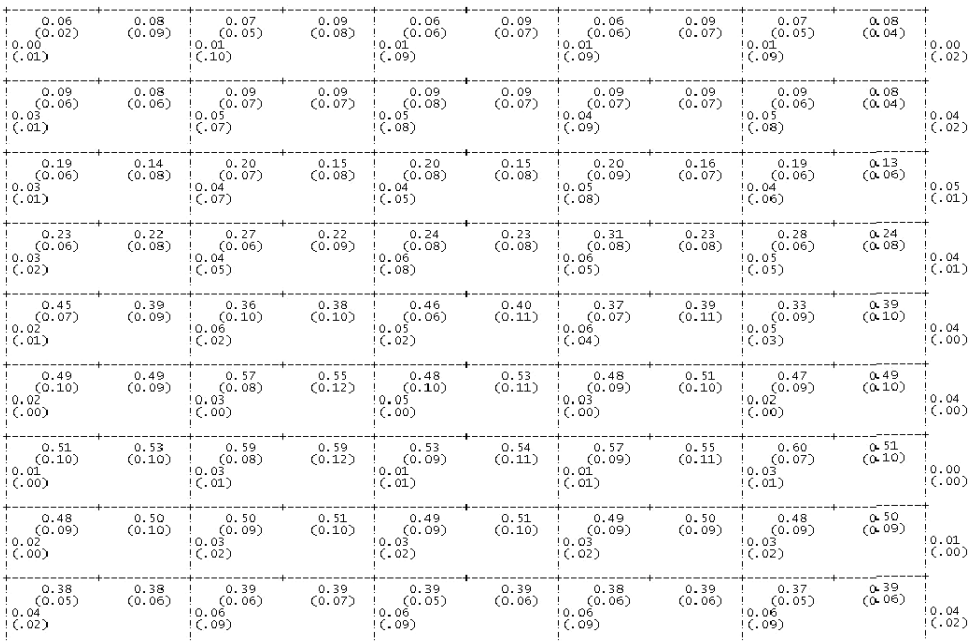

b) EBD (SAC LA10/50)

Fig. 6.39: Damage index for beams and columns subjects to SAC NF 02

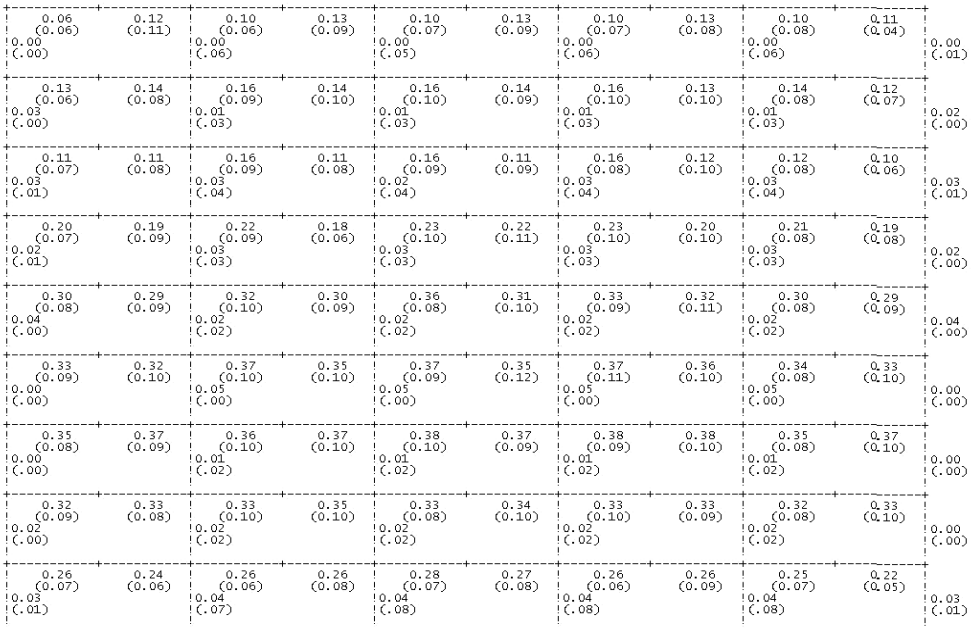

c) EBD (SAC NF)

(< 0.4 = Repairable; 0.4-1.0 = Beyond repair; > 1.0 = Loss of building)
*** Value in parenthesis is Energy ratio (see 2nd part of Eq. 5.1 of Chapter 5)

Fig. 6.39: Continued

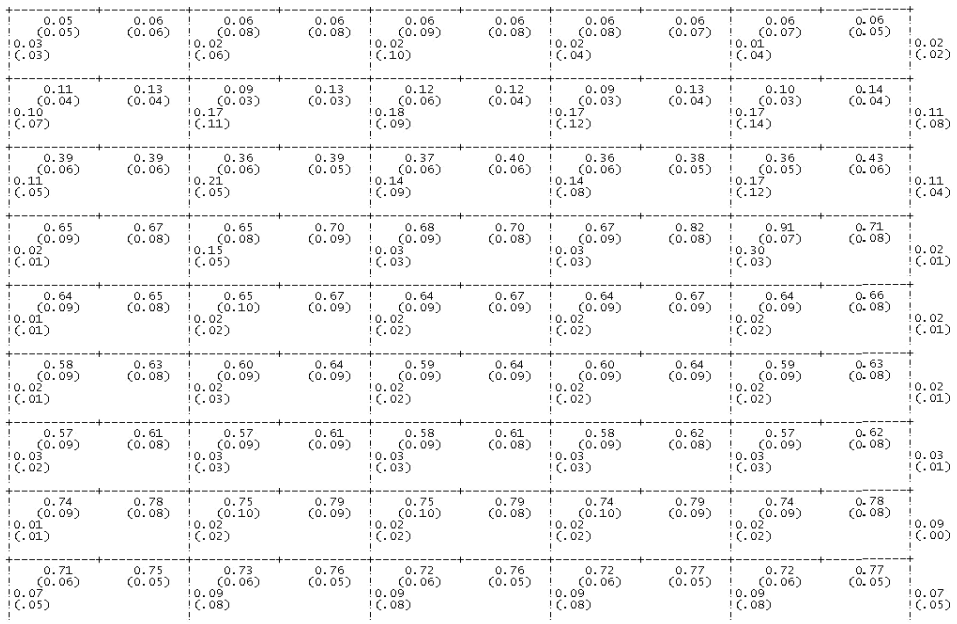

a) UBC 97

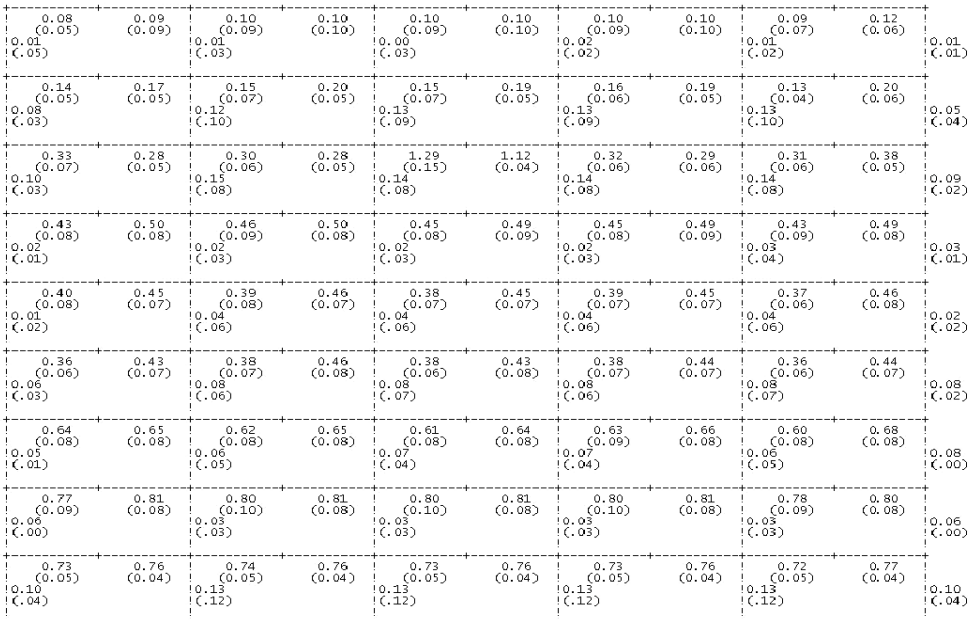

b) EBD (SAC LA10/50)

Fig. 6.40: Damage index for beams and columns subjects to SAC NF 17

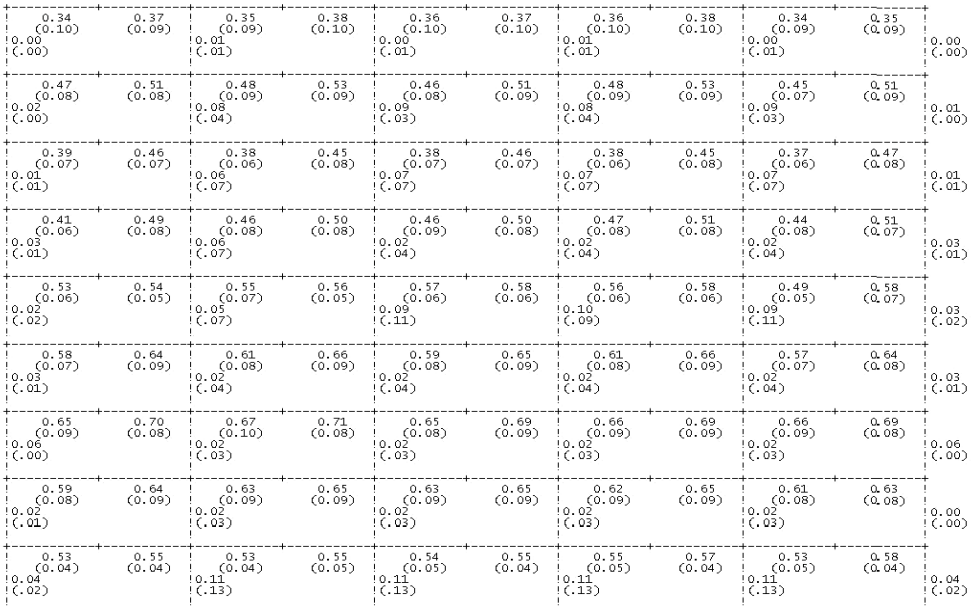

c) EBD (SAC NF)

(< 0.4 = Repairable; 0.4-1.0 = Beyond repair; > 1.0 = Loss of building)
*** Value in parenthesis is Energy ratio (see 2nd part of Eq. 5.1 of Chapter 5)

Fig. 6.40: Continued

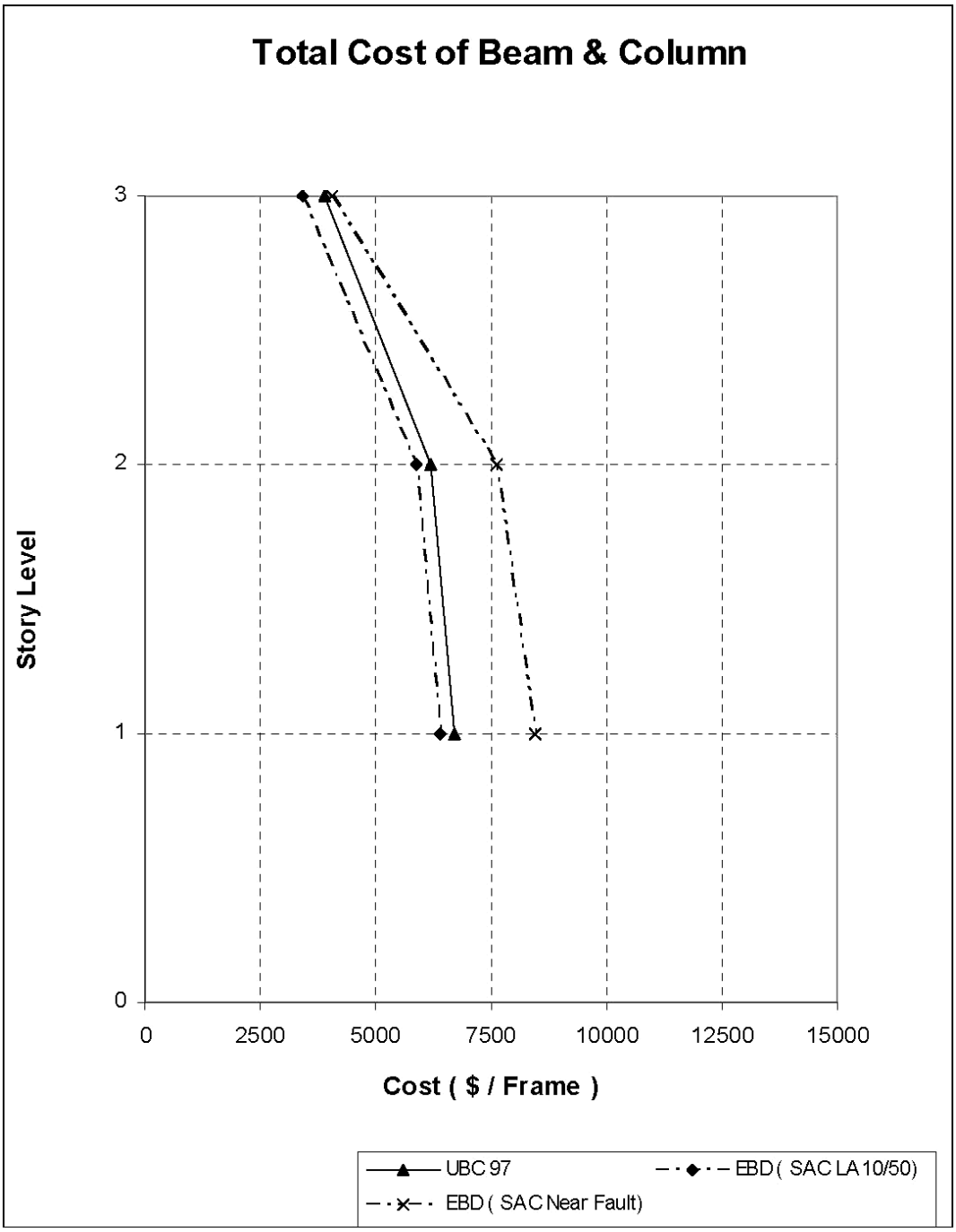

Fig. 6.41: Comparison of total cost for beams and columns subjects to three-story building

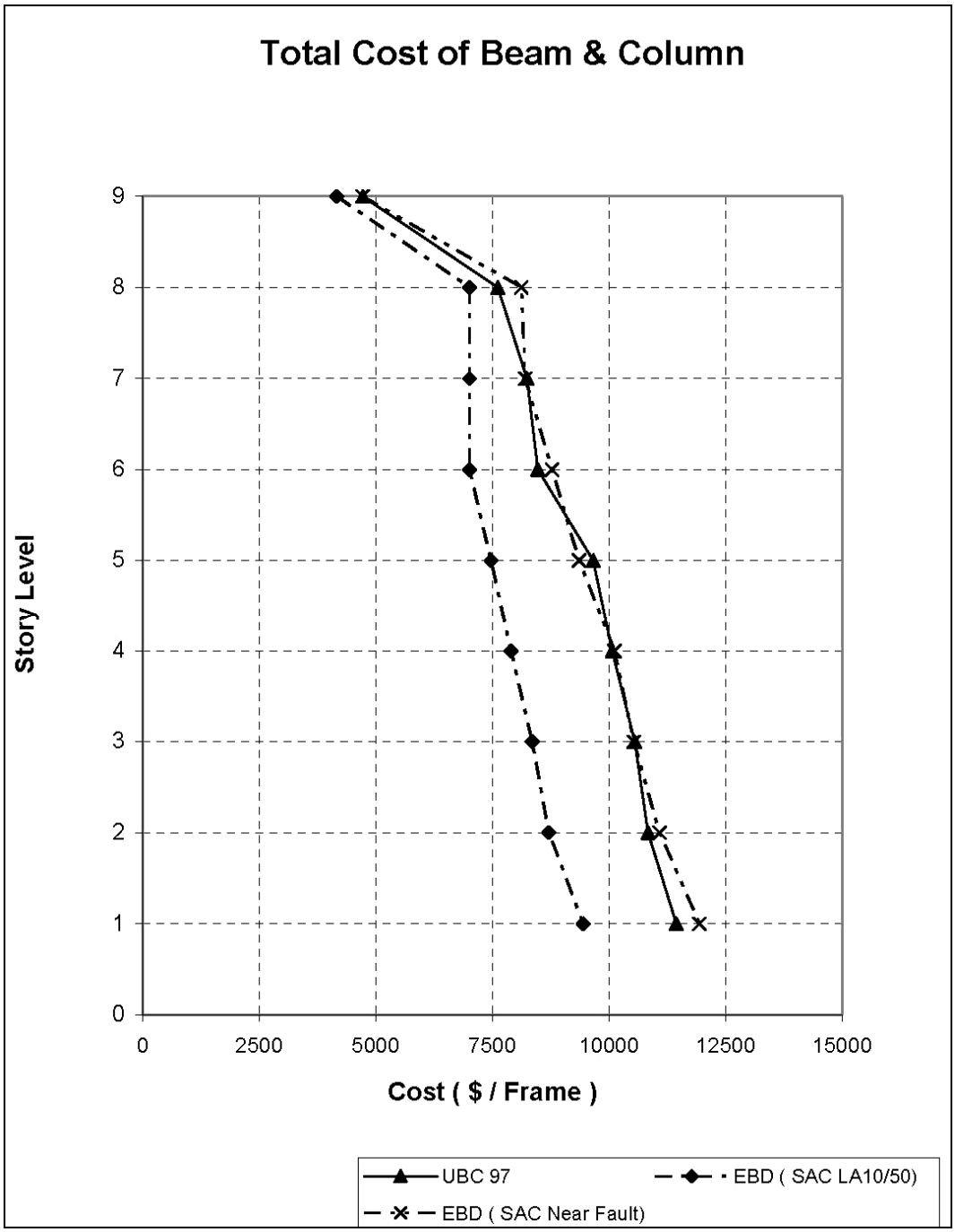

Fig. 6.42: Comparison of total cost for beams and columns subjects to nine-story building

References

ACI 318-95 (1995), " Building Code Requirements for Structural Concrete", American Concrete Institute, Farmington, Michigan.

Akiyama, H. (1985), "Earthquake Resistant Limit State Design for Buildings", University of Tokyo.

Berg, G. V. and Thomaides, S. S.(1960), "Energy Consumption by Structures in Strong Motion Earthquakes", Proceedings, Second World Conference on Earthquake Engineering, Tokyo, Japan, 1960.

Blume, J. A. (1960), "A Reserve Energy Technique for the Earthquake Design and Rating of Structures in the Inelastic Range", Proceedings, Second World Conference on Earthquake Engineering, Tokyo, Japan, 1960.

Estes, R. (2003), " An Energy Method for Seismic Design", Ph.D. Dissertation, Department of Civil Engineering, University of Southern California.

Fajfar P, Vidic T, and Fischinger M.(1989), " Seismic Demand in Medium and Long Period Structures", Earthquake Eng. Struct. Dyn., 18, 1133-1144.

Federal Emergency Management Agency (1997), FEMA-273, Guidelines for the Seismic Rehabilitation of Buildings and Commentary.

Federal Emergency Management Agency (2000), FEMA-356, National Guidelines for Prestandard and Commentary for Seismic Rehabilitation of Buildings.

Gerlein, M. A. and Beaufait F.W. (1980), " An Optimum Preliminary Strength Design of Reinforced Concrete Frames", Computers and Structures, Pergamon Press, Vol. 11, 515-524.

Goel, S. C. and Berg, G. V. (1968), " Inelastic Earthquake Response of Tall Steel Frames", Journal of the Structural Division (ASCE), 94(8).

Heyman, J. (1971), Plastic Design of Frames, Cambridge.

Housner, G. W. (1956), "Limit Design of Structures to Resist Earthquakes", Proceedings of the First World Conference on Earthquake Engineering.

International Conference of Building Officials (1997), The 1997 Uniform Building Code.

Jenning, P. C. (1965), " Earthquake Response of a Yielding Structure", Journal of the Structural Division (ASCE), 90(4).

Kanaan, A. E. and Powell, G. W. (1973), " DRAIN-2D-A General Purpose Computer Program for Dynamic Analysis of Inelastic Plane Structures", Reports No. UCB/EE-RC/73/06 and 73/22. University of California, Berkeley.

Kato, B. and Akiyama, H. (1982), " Seismic Design of Steel Buildings", Journal of the Structural Division (ASCE), 108(8), 1709-1721

Kent, D. C. and Park, R. (1971), " Flexural Members with Confined Concrete", Journal of the Structural Division (ASCE), 97(7), 1969-1990.

Kunnath, S. K. and Gross, J. L. (1995), " Inelastic Response of the Cypress Viaduct to the Loma Prieta Earthquake", Engineering Structure, 17, 485-493

Kunnath, S. K., Reinhorn, A. M. and Abel, J. F. (1992a), " A Computational Tool for Seismic Performance of Reinforced Concrete Buildings", Computers and Structures, Pergamon Press, Vol. 41, No. 1, 157-173.

Kunnath, S. K., Reinhorn, A. M. and Lobo, R. F. (1992b), " IDARC Version 3.0 – A Program for Inelastic Damage Analysis of RC Structures", Technical Report NCEER 92-0022, National Center for Earthquake Engineering Research, State University of New York, Buffalo.

Kunnath, S. K., Reinhorn, A. M. and Park, Y. J. (1990), " Analytical Modeling of Inelastic Seismic Response of R/C Structures", Journal of the Structural Division (ASCE), 116(4), 996-1017.

Leelataviwat, S., Goel, S., and Stojadinovic, B. (1999), " Towards Performance Based Seismic Design of Structures", Earthquake Spectra, 15, No.3

Leelataviwat, S., Goel, S., and Stojadinovic, B. (2002), " Energy-based Seismic Design of Structures using Yield Mechanism and Target Drift", Journal of the Structural Division (ASCE), 113, August.

Mander, J. B. (1984), " Seismic Design of Bridge Piers", Ph.D. Dissertation, Department of Civil Engineering, University of Canterbury, New Zealand

Manfredi, G. (2001), " Evaluation of Seismic Energy Demand", Earthquake Eng. Struct. Dyn., 30, 485-499

Mollaioli, F. and Decanini, L.(1998), " Formulation of Elastic Earthquake Input Energy Spectra", Earthquake Eng. Struct. Dyn., 27, 1503-1522

Nurtug, A. and Sucuoglu, H. (1995), " Earthquake Ground Motion Characteristics and Seismic Energy Dissipation", Earthquake Eng. Struct. Dyn., 24, 1195-1213

Park, Y. J., and Ang, A. H-S. (1985), " Mechanic Seismic Damage Model for Reinforced Concrete", Journal of the Structural Division (ASCE), 111(4), 722-739

Park, Y. j., Reinhorn, A. M., and Kunnath, S. K. (1987), " IDARC: Inelastic Damage Analysis of Reinforced Concrete Frame – Shear Wall Structures", Technical Report NCEER -87-0008, State University of New York, Buffalo

Reinhorn, A. M. and Valles, R. E. (1995), " Damage Evaluation in Inelastic Response of Structures: A Deterministic Approach", Report NCEER 95, National Center for Earthquake Engineering Research, State University of New York, Buffalo.

Tembulkar, J. M. and Nau, J .M. (1987), " Inelastic Modeling and Seismic Energy Dissipation", Journal of the Structural Division (ASCE), 113, 1373-1377

Uang, C. M. and Bertero, V. V.(1988), " Use of Energy as a Design Criterion in Earthquake-Resistant Design", EERC Report No. UCB/EERC-88/18.

Zagajeski, S. and Bertero, V. (1977), " Computer-Aided Optimum Seismic Design of Ductile Reinforced Concrete Moment-Resisting Frames", Reort No. UCB/EERC-77/16.

Zahrah, T. and Hall, J. (1984), "Earthquake Energy Absorption in SDOF Structures", Journal of the Structural Division (ASCE), 110, 1757-1772.

Appendix A: Figures and Tables

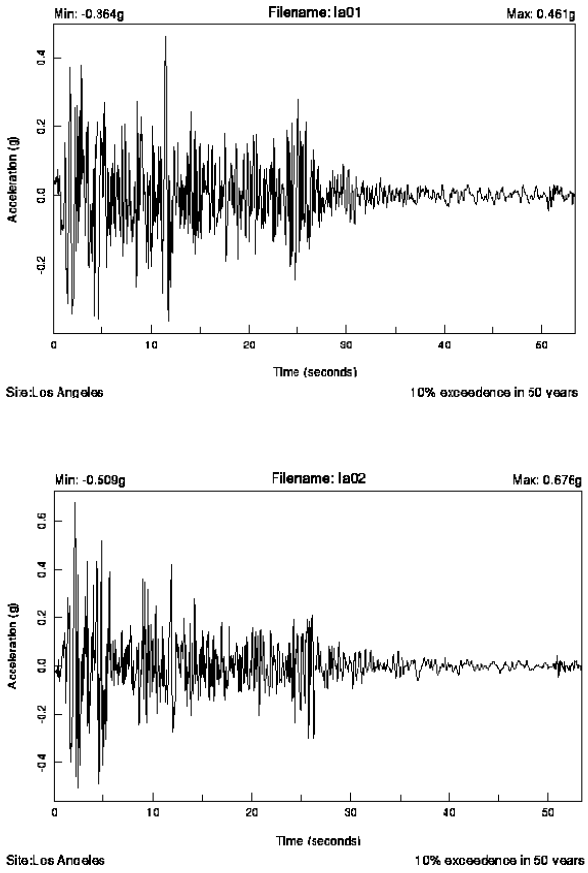

Fig. A.1: SAC LA10/50 records

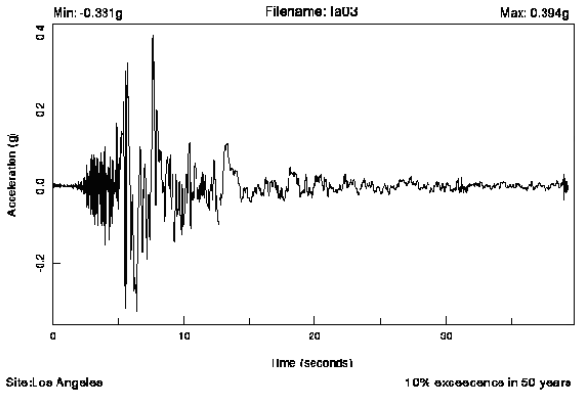

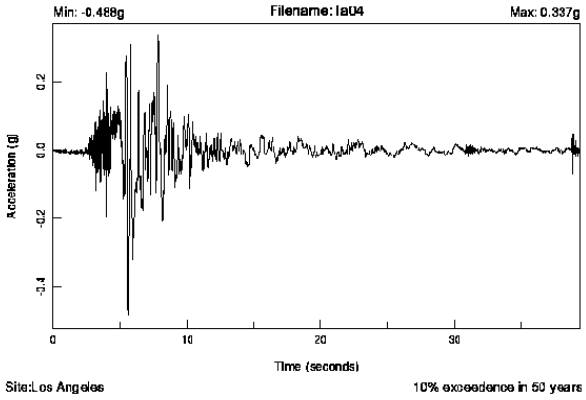

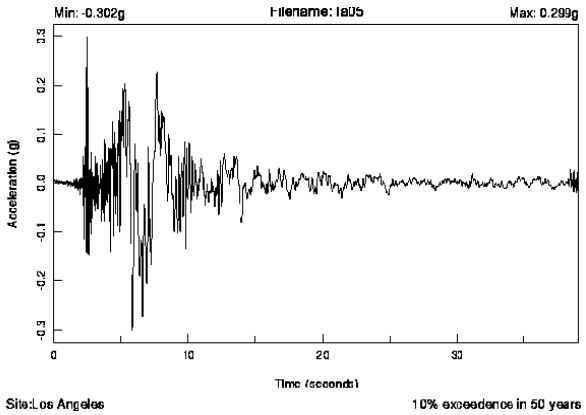

Fig. A.1: Continued

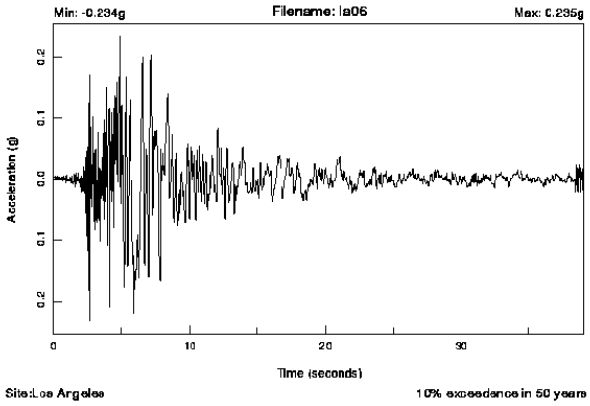

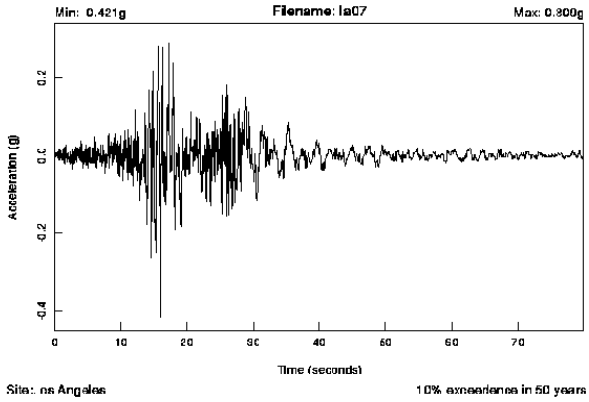

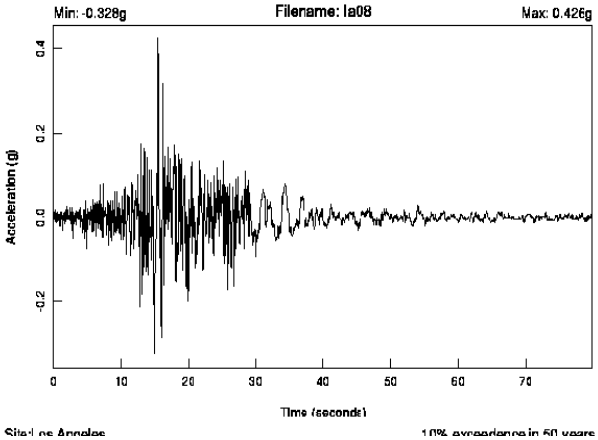

Fig. A.1: Continued

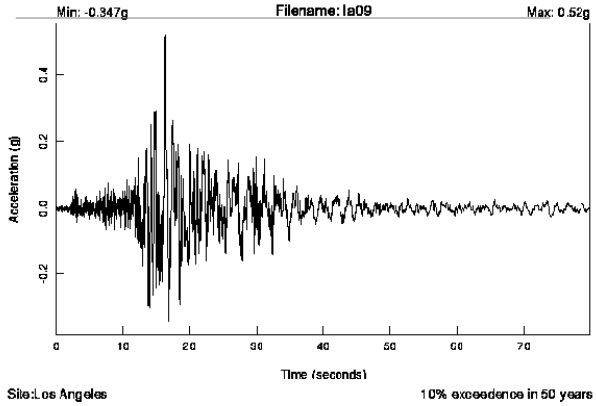

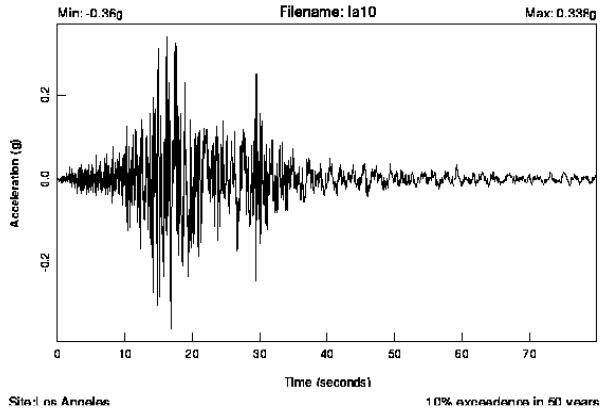

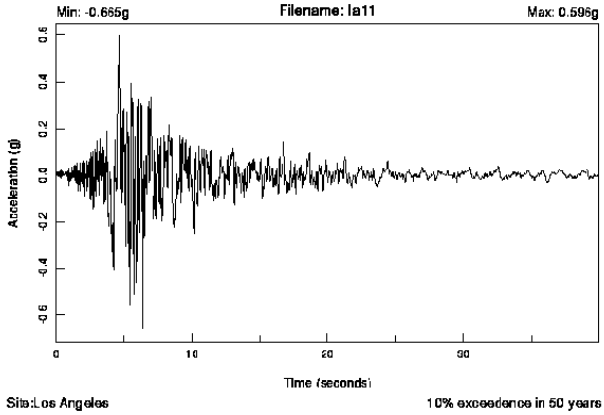

Fig. A.1: Continued

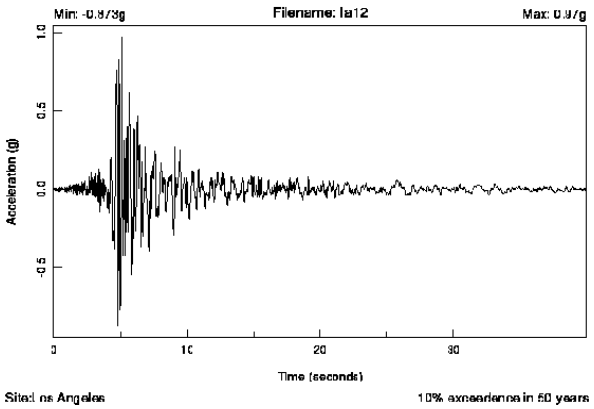

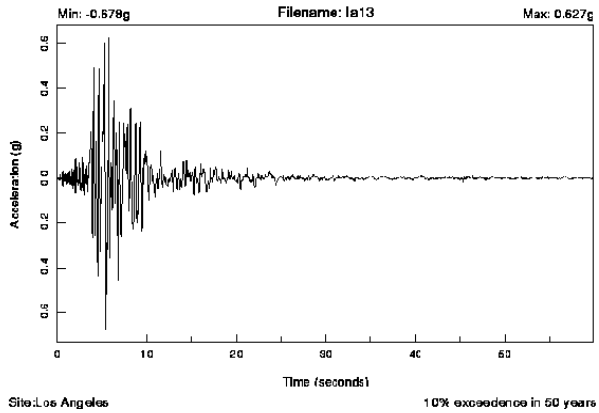

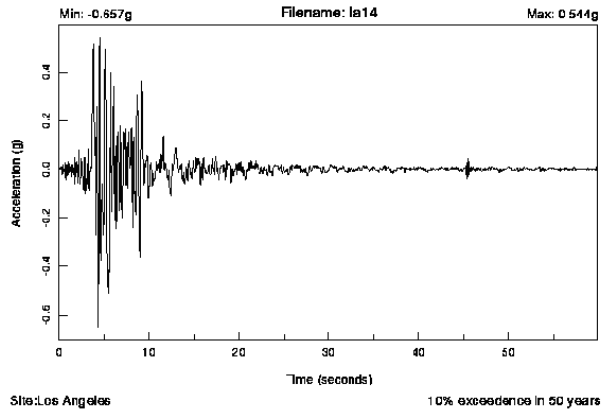

Fig. A.1: Continued

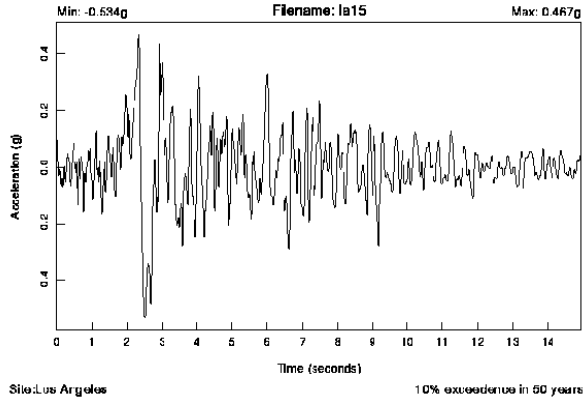

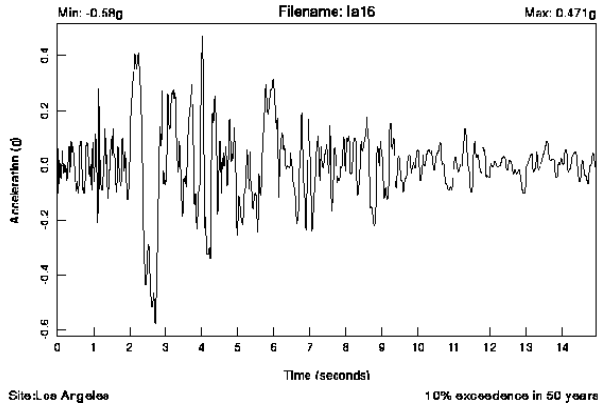

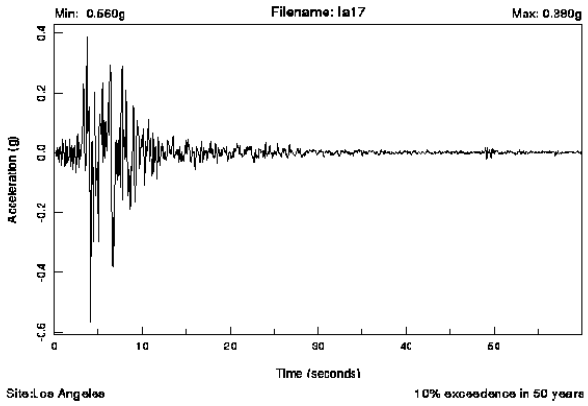

Fig. A.1: Continued

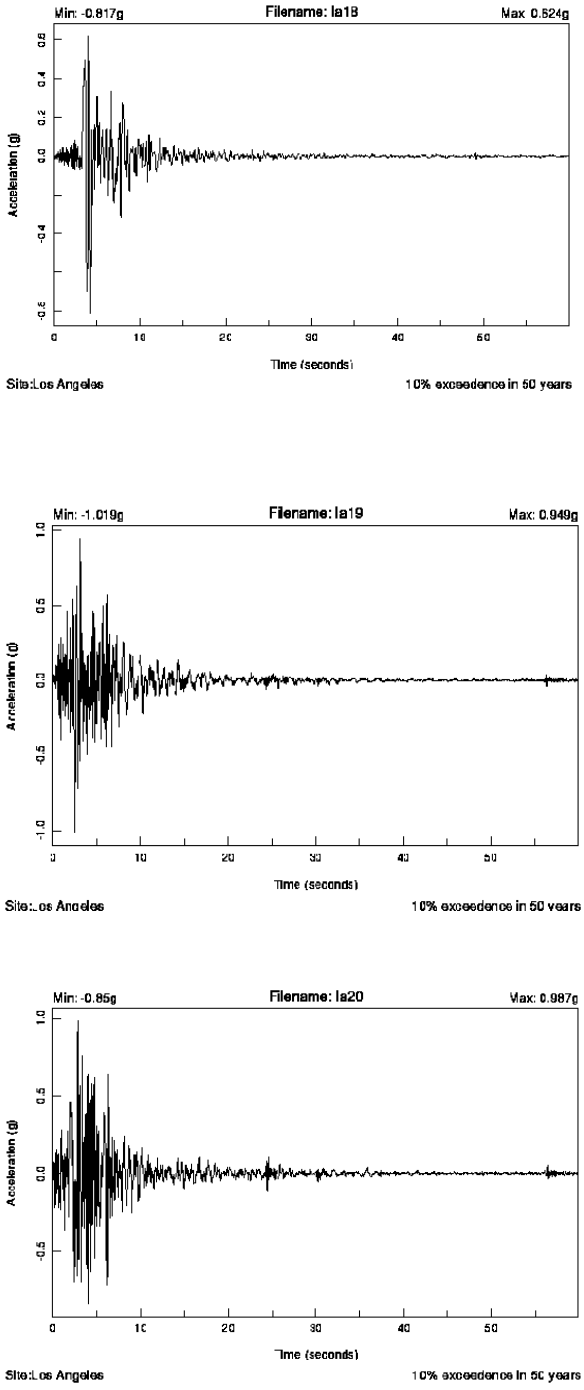

Fig. A.1: Continued

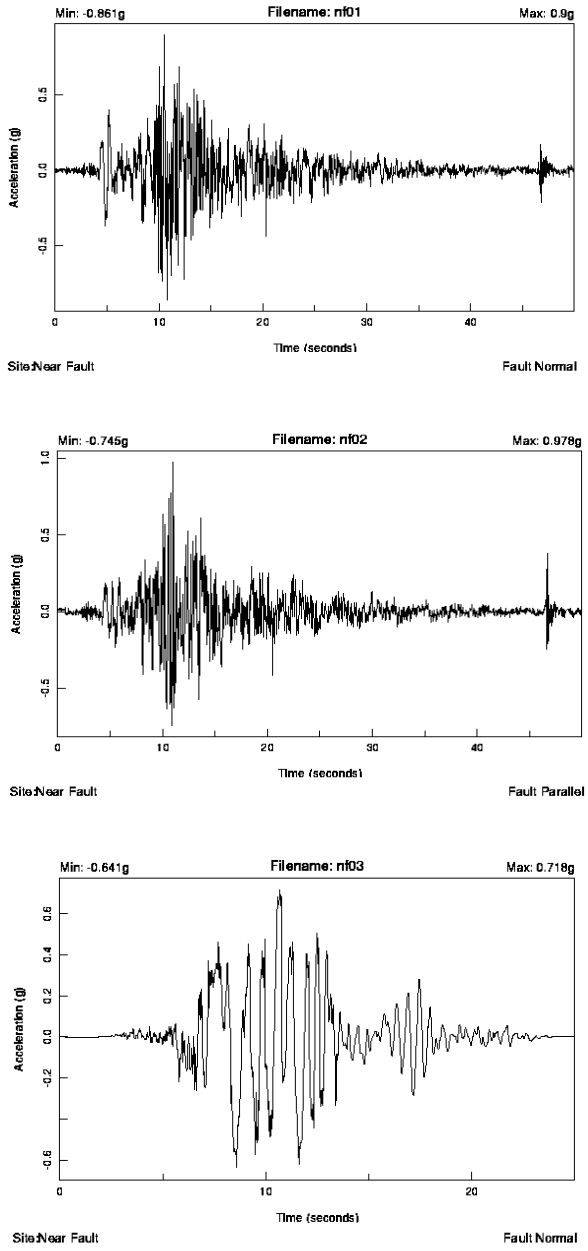

Fig. A.2: SAC Near Fault records

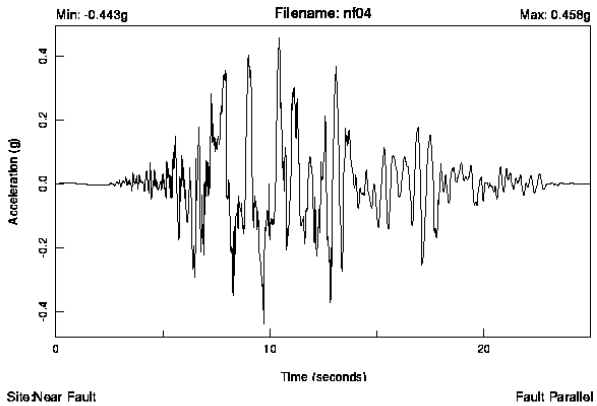

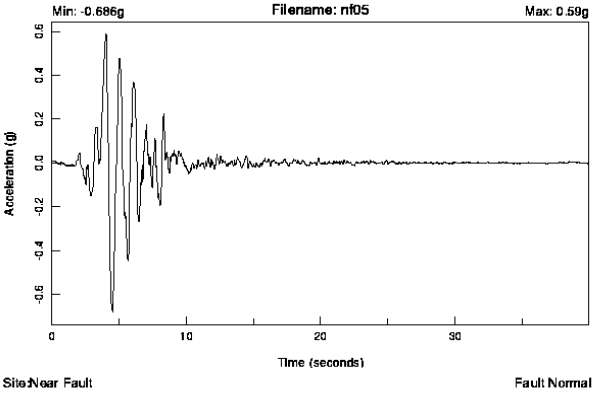

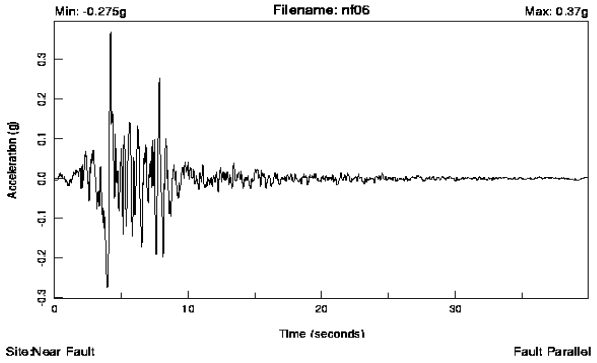

Fig. A.2: Continued

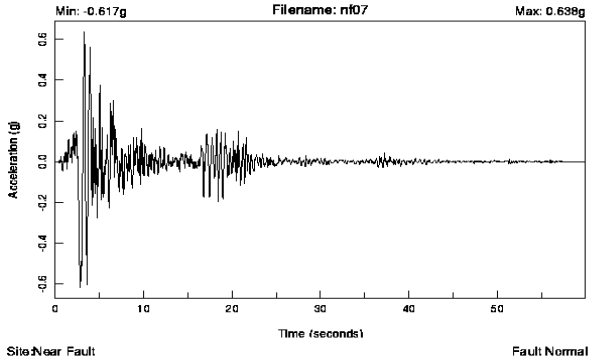

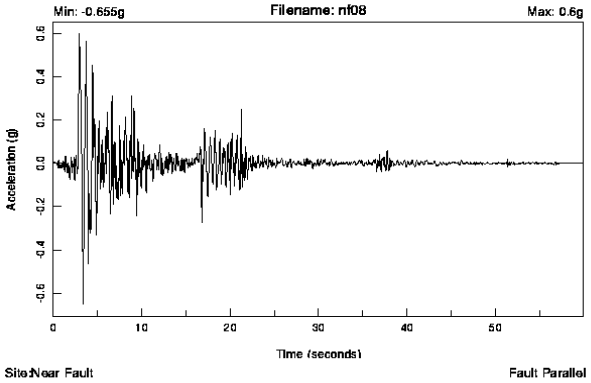

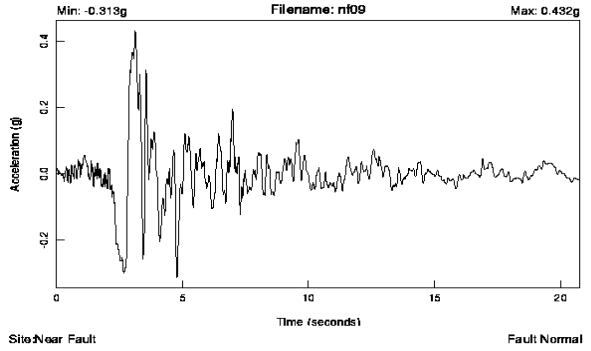

Fig. A.2: Continued

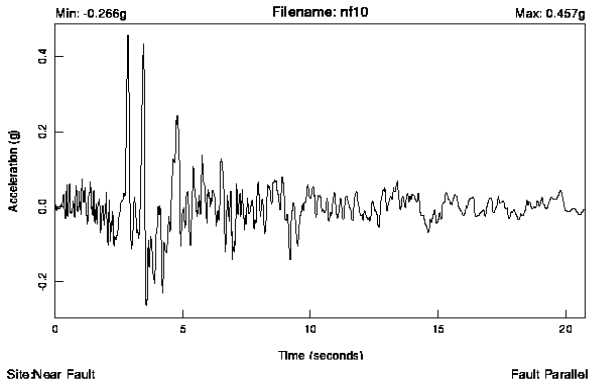

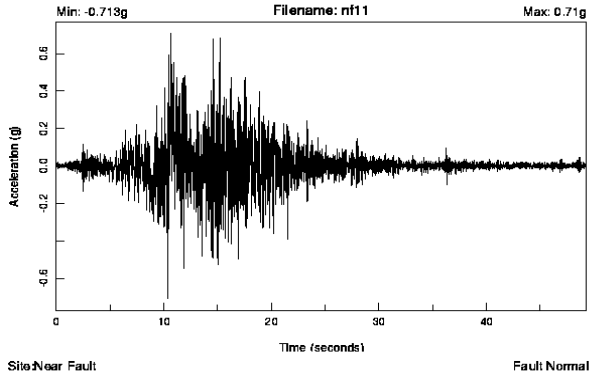

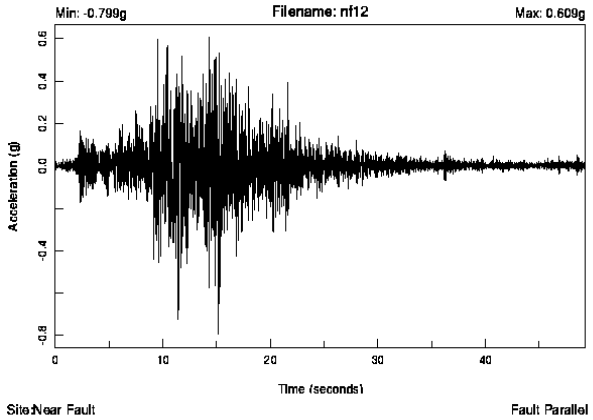

Fig. A.2: Continued

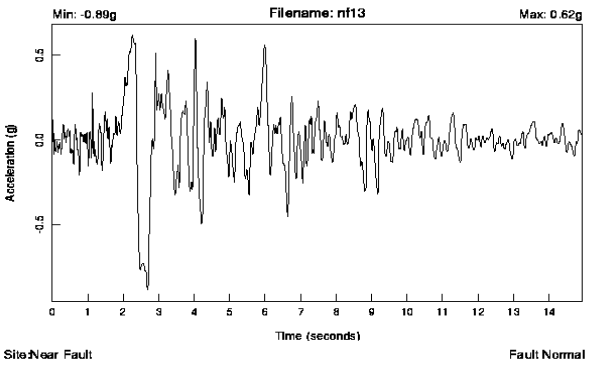

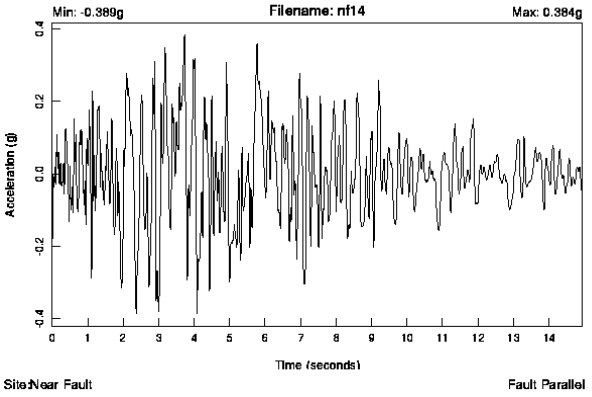

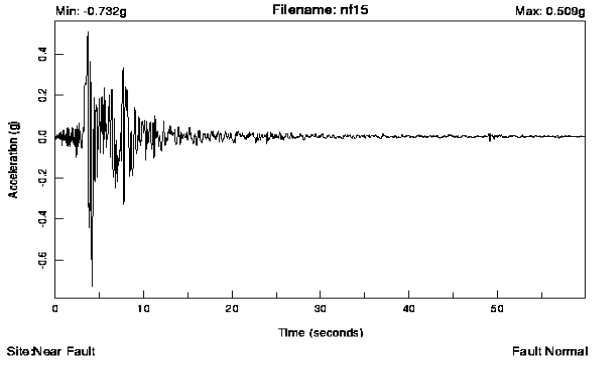

Fig. A.2: Continued

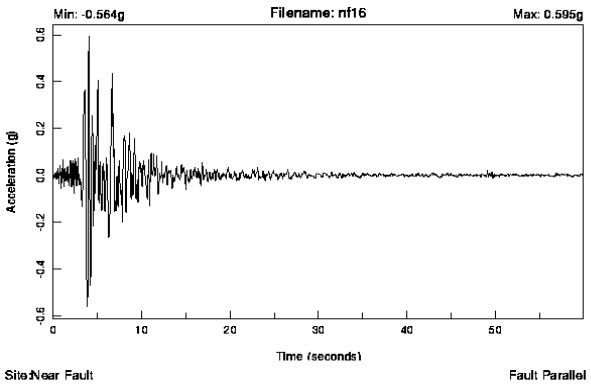

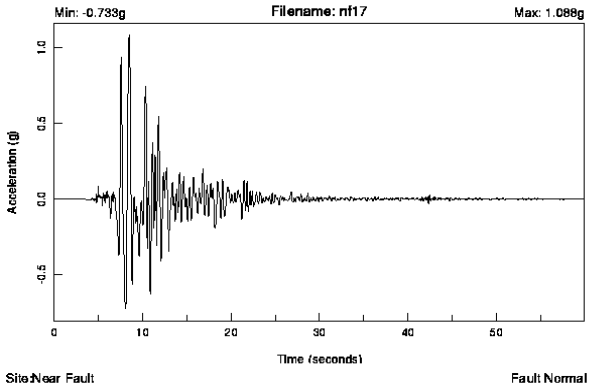

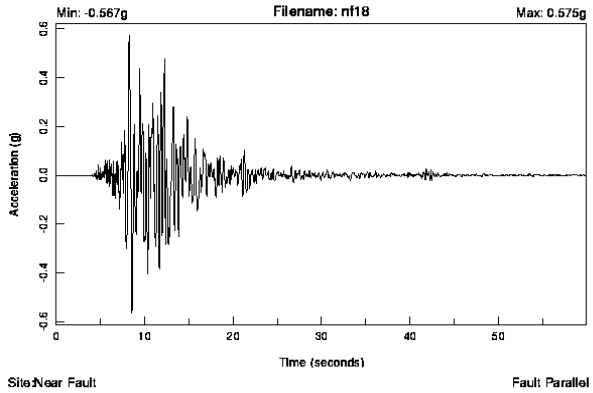

Fig. A.2: Continued

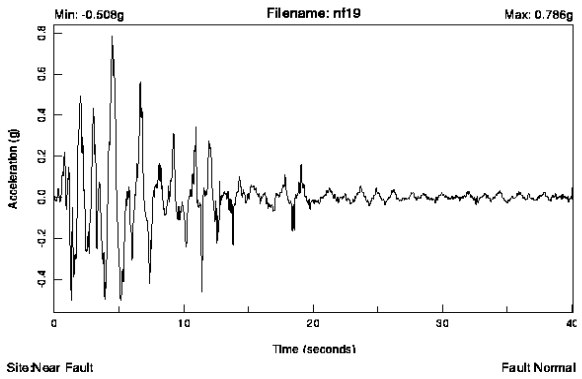

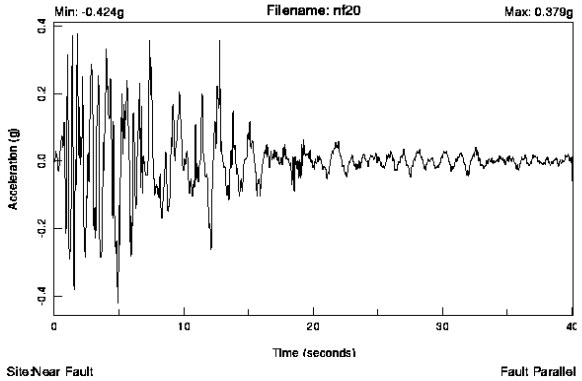

Fig. A.2: Continued

Conditions			Modeling Parameters[3]			Acceptance Criteria[3]				
			Plastic Rotation Angle, radians		Residual Strength Ratio	Plastic Rotation Angle, radians				
						Performance Level				
							Component Type			
							Primary		Secondary	
			a	b	c	IO	LS	CP	LS	CP
i. Beams controlled by flexure[1]										
$\frac{\rho - \rho'}{\rho_{bal}}$	Trans. Reinf.[2]	$\frac{V}{b_w d\sqrt{f'_c}}$								
≤ 0.0	C	≤ 3	0.025	0.05	0.2	0.010	0.02	0.025	0.02	0.05
≤ 0.0	C	≥ 6	0.02	0.04	0.2	0.005	0.01	0.02	0.02	0.04
≥ 0.5	C	≤ 3	0.02	0.03	0.2	0.005	0.01	0.02	0.02	0.03
≥ 0.5	C	≥ 6	0.015	0.02	0.2	0.005	0.005	0.015	0.015	0.02
≤ 0.0	NC	≤ 3	0.02	0.03	0.2	0.005	0.01	0.02	0.02	0.03
≤ 0.0	NC	≥ 6	0.01	0.015	0.2	0.0015	0.005	0.01	0.01	0.015
≥ 0.5	NC	≤ 3	0.01	0.015	0.2	0.005	0.01	0.01	0.01	0.015
≥ 0.5	NC	≥ 6	0.005	0.01	0.2	0.0015	0.005	0.005	0.005	0.01
ii. Beams controlled by shear[1]										
Stirrup spacing ≤ d/2			0.0030	0.02	0.2	0.0015	0.0020	0.0030	0.01	0.02
Stirrup spacing > d/2			0.0030	0.01	0.2	0.0015	0.0020	0.0030	0.005	0.01
iii. Beams controlled by inadequate development or splicing along the span[1]										
Stirrup spacing ≤ d/2			0.0030	0.02	0.0	0.0015	0.0020	0.0030	0.01	0.02
Stirrup spacing > d/2			0.0030	0.01	0.0	0.0015	0.0020	0.0030	0.005	0.01
iv. Beams controlled by inadequate embedment into beam-column joint[1]										
			0.015	0.03	0.2	0.01	0.01	0.015	0.02	0.03

1. When more than one of the conditions i, ii, iii, and iv occurs for a given component, use the minimum appropriate numerical value from the table.
2. "C" and "NC" are abbreviations for conforming and nonconforming transverse reinforcement. A component is conforming if, within the flexural plastic hinge region, hoops are spaced at ≤ d/3, and if, for components of moderate and high ductility demand, the strength provided by the hoops (V_s) is at least three-fourths of the design shear. Otherwise, the component is considered nonconforming.
3. Linear interpolation between values listed in the table shall be permitted.

Fig. A.3: Modeling parameters and numerical acceptance criteria for RC beam (FEMA 356)

Conditions			Modeling Parameters[4]			Acceptance Criteria[4]				
			Plastic Rotation Angle, radians		Residual Strength Ratio	Plastic Rotation Angle, radians				
						Performance Level				
							Component Type			
							Primary		Secondary	
			a	b	c	IO	LS	CP	LS	CP
i. Columns controlled by flexure[1]										
$\frac{P}{A_g f'_c}$	Trans. Reinf.[2]	$\frac{V}{b_w d \sqrt{f'_c}}$								
≤ 0.1	C	≤ 3	0.02	0.03	0.2	0.005	0.015	0.02	0.02	0.03
≤ 0.1	C	≥ 6	0.016	0.024	0.2	0.005	0.012	0.016	0.016	0.024
≥ 0.4	C	≤ 3	0.015	0.025	0.2	0.003	0.012	0.015	0.018	0.025
≥ 0.4	C	≥ 6	0.012	0.02	0.2	0.003	0.01	0.012	0.013	0.02
≤ 0.1	NC	≤ 3	0.006	0.015	0.2	0.005	0.005	0.006	0.01	0.015
≤ 0.1	NC	≥ 6	0.005	0.012	0.2	0.005	0.004	0.005	0.008	0.012
≥ 0.4	NC	≤ 3	0.003	0.01	0.2	0.002	0.002	0.003	0.006	0.01
≥ 0.4	NC	≥ 6	0.002	0.008	0.2	0.002	0.002	0.002	0.005	0.008
ii. Columns controlled by shear[1, 3]										
All cases[5]			—	—	—	—	—	—	.0030	.0040
iii. Columns controlled by inadequate development or splicing along the clear height[1,3]										
Hoop spacing ≤ d/2			0.01	0.02	0.4	0.005	0.005	0.01	0.01	0.02
Hoop spacing > d/2			0.0	0.01	0.2	0.0	0.0	0.0	0.005	0.01
iv. Columns with axial loads exceeding $0.70P_o$[1, 3]										
Conforming hoops over the entire length			0.015	0.025	0.02	0.0	0.005	0.01	0.01	0.02
All other cases			0.0	0.0	0.0	0.0	0.0	0.0	0.0	0.0

1. When more than one of the conditions i, ii, iii, and iv occurs for a given component, use the minimum appropriate numerical value from the table.
2. "C" and "NC" are abbreviations for conforming and nonconforming transverse reinforcement. A component is conforming if, within the flexural plastic hinge region, hoops are spaced at ≤ d/3, and if, for components of moderate and high ductility demand, the strength provided by the hoops (V_s) is at least three-fourths of the design shear. Otherwise, the component is considered nonconforming.
3. To qualify, columns must have transverse reinforcement consisting of hoops. Otherwise, actions shall be treated as force-controlled.
4. Linear interpolation between values listed in the table shall be permitted.
5. For columns controlled by shear, see Section 6.5.2.4.2 for acceptance criteria.

Fig. A.4: Modeling parameters and numerical acceptance criteria for RC column (FEMA 356)

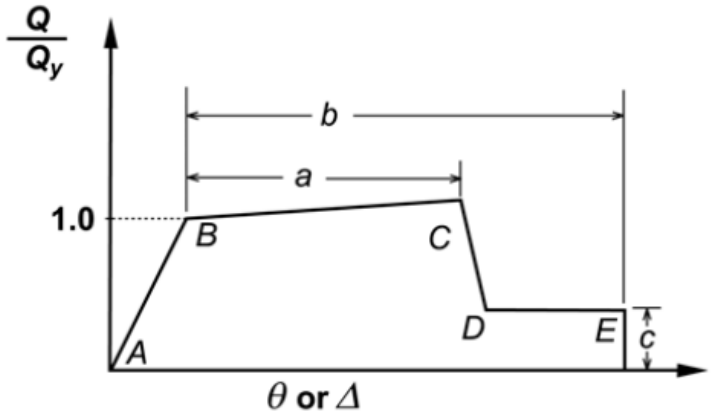

Fig. A.5: The relation between normalized force and deformation (FEMA 356)

Degree of Damage	Physical Appearance	DI	State of Building
Collapse	Partial or total collapse of building	> 1.0	Loss of building
Severe	Extensive crashing of concrete ; disclosure of buckled reinforcement	0.4 – 1.0	Beyond repair
Moderate	Extensive large cracks; spalling of concrete in weaker elements	< 0.4	Repairable
Minor	Minor cracks; partial crushing of concrete in columns		
Slight	Sporadic occurrence of cracking		

Fig. A.6: The overall damage index level

Appendix B: Simplex Method

As invented by George Dantzig in 1947, with advantages in less time consumer and operation with computer implementation, simplex method has gained more popular in use today as efficiently fundamental concept in solving linear program (LP) problems. It is a method of choice that started at arbitrary corner of the feasible solutions. At each iteration, the entering basic variable and leaving basic variable will be selected by the simplex methods. They will be swapped and move our concentration to the next related feasible solution corner closer to the final (optimum) solution. If the new entering basic variable cannot be drawn at upcoming iteration, it means the optimum point has been reached. It is potential method to solve LP problem since our interesting points are limited on corners of feasible solution, instead of every interior point concerning that produces uneconomical time consumer. In the case of large system like hundreds, thousands of variables which come with huge numbers of intersection point (solution corners), the simplex method is more effective due to its suitability in account of well known methods for finding the intersection of linear equations, such as Gaussian elimination. Therefore, the equation can systematically be solved in the matrix format. It is known as simplex tableau. The procedure to optimize the equation is summarized in details as illustrated in Fig B.2.

Note that starting with standard form of linear programs as shown in Fig. B.1 the first and second lines represent objective function and constraint functions, respectively. This format defines the origin (0,0,0,…) as initially feasible corner point and make

simplex method always begins here. It allows the simplex method produces more convenient for tracking the optimality. Moreover, another kind of optimal problem like minimization based on duality principle can transform into this standard form to avoid the sophisticated procedure in solving feasible solution. This will be described in detail on the later section.

$$
\begin{aligned}
&\textit{Maximize} \quad \sum c_j x_j \\
&\textit{Subject to} \quad \sum a_{ij} x_j \le b_i \\
&\textit{where} \qquad x_j \ge 0 \ \textit{and} \ b_i \ge 0 \\
&\textit{for} \ \ i = 1, 2, ..., m \ \ \& \ \ j = 1, 2, ..., n
\end{aligned}
$$

Fig B.1: Standard form of linear programming

To explain how simplex method work out, the optimization problem of simple two variables with three constraint equations are examined as shown below:

1. Set up the initial simplex tableau

The tableau is convenient way to solve optimal problem since containing all information that is required to decide on. To adjust into simplex tableau, additional requirement and slack variables are introduced to objective function and constraint equations above as the following page:

$$z - 20x_1 - 10x_2 = 0$$
$$x_1 + s_1 = 3$$
$$x_2 + s_2 = 4$$
$$x_1 + x_2 + s_3 = 5$$

Where s_1, s_2 and s_3 are slack variables. Now unequal equations have been shifted to equal equations. Arrange into tableau, it will show as below. Note RHS means the values in right hand side of equations.

Basic Variable	x_1	x_2	s_1	s_2	s_3	RHS
s_1	1	0	1	0	0	3
s_2	0	1	0	1	0	4
s_3	1	1	0	0	1	5
Z	-20	-10	0	0	0	0

Obviously, if value of slack variable goes to zero, the related variable will reach the limiting value subjected to constrain function. This plays important role in guarantee in movement of solution within feasible region since slack variable cannot be negative value.

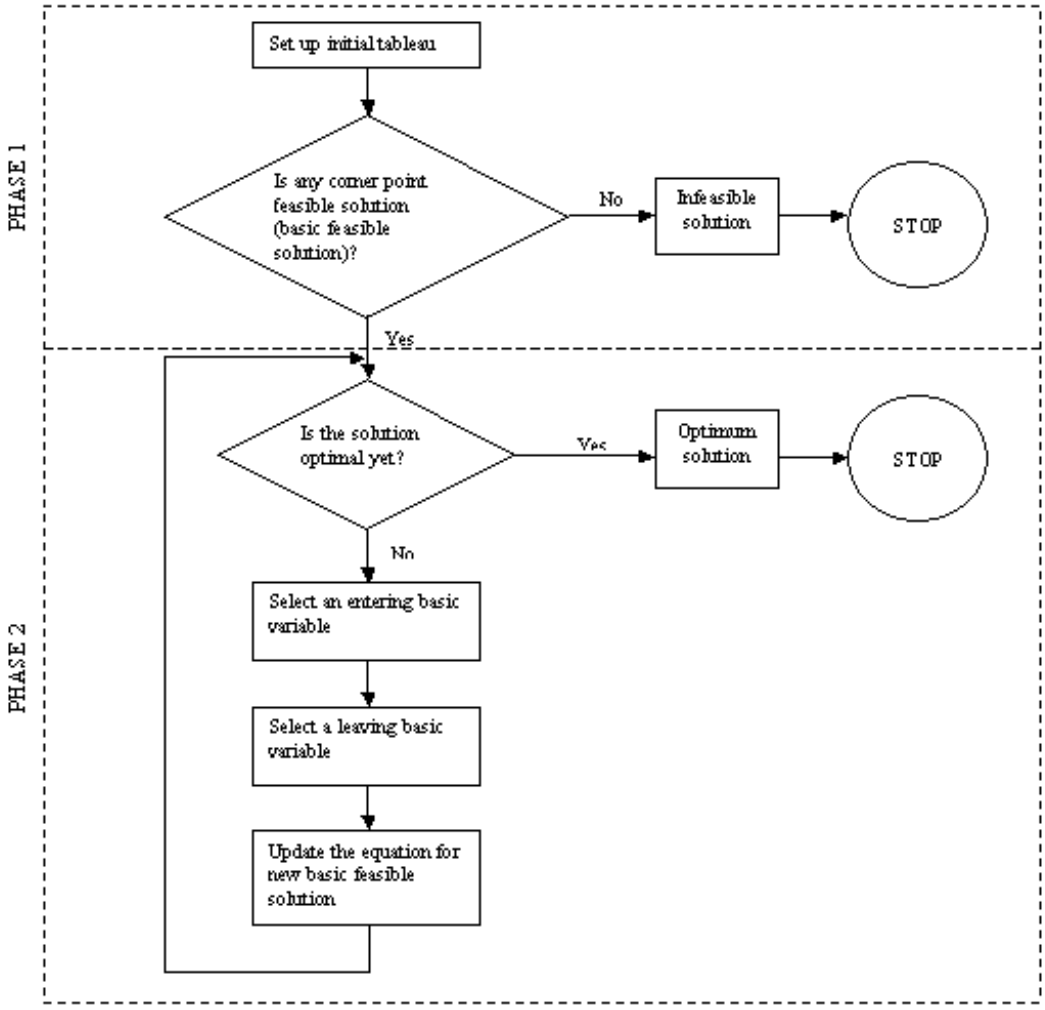

Figure B.2: Flowchart of simplex method

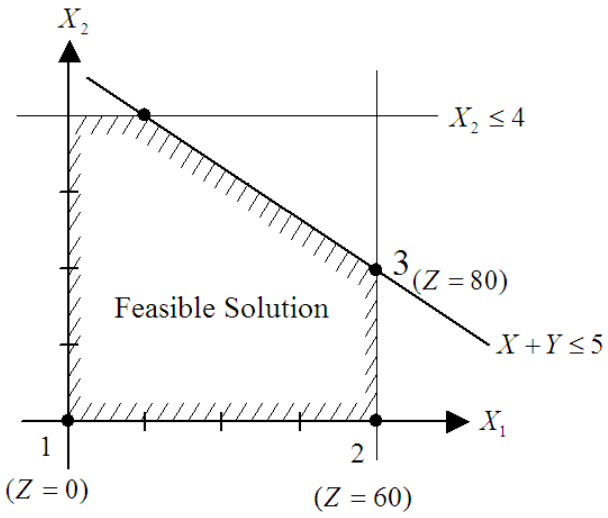

Fig. B.3: Maximization problem

2. Are any corner point feasible solution ?

Feasible solution is points in feasible region. These points with including border lines are satisfied all of constraints. Shaded area of Fig B.3 is simple demonstration for this sample problem. Since this optimization problem enables to exist as the standard form LP, it confirms the original (x_1=0, x_2=0) is always a basic feasible solution. Then it satisfies the 2nd requirement in flowchart. However, replace zero values for x_1 and x_2 into the objective function, outcome is zero and represents the point #1 in Fig. B.3.

3. Is the solution optimal yet ?

Simplex method terms that the solution is optimal if no entering basic variable appeared. The entering basic variable is the variable that provides the faster rate of increasing in objective function. As seen in above equations, it indicates not being optimal solution, yet due to existing of entering basic variable. Variable x_1, which allows a higher rate than x_2 (20 versus 10), is considered as entering variable subjected to this problem. Alternatively, within a tableau format, the entering variable is simply withdrawn as the one holds the most negative value in objective function.

- Select the entering basic variable

As above mention, variable x_1 is current entering variable. The column where this variable is located may known as pivot column. It shows as shaded area in the table below:

Basic variable	x_1	x_2	s_1	s_2	s_3	RHS
s_1	1	0	1	0	0	3
s_2	0	1	0	1	0	4
s_3	1	1	0	0	1	5
Z	-20	-10	0	0	0	0

- Select the leaving basic variable

Simplex method introduces a minimum ratio test to determine which the current basic variable will be changed to a new leaving basic variable. With illustrated in the procedure #4, variable x_1 have been considered as the entering variable. If dividing value in RHS in the same row with shaded value, the outcome ratio enable to represent how each constraint speed toward zero is. The constraint holds the minimum ratio will be taken care as leaving basic variable because of providing the most limiting in switch between the new entering basic variable and new leaving basic variable. However, there are some special rules need to consider beyond this calculation as the following:

1) If the coefficient of the entering basic is zero, then no limit is declared for minimum ratio test.
2) If the coefficient of the entering basic is negative, then no limit is declared for minimum ratio test.

Refer to tableau in procedure #4, s_1, s_2, and s_3 are now basic variables. After ratios of 3, no limit, and 5 evaluated for row #1, 2, and 3, respectively, s_1 will be considered as leaving variable. Note that a row that this variable is located may pronounce as pivot row. It shows as shade area in table of the following page:

Basic Variable	x_1	x_2	s_1	s_2	s_3	RHS
s_1	1	0	1	0	0	3
s_2	0	1	0	1	0	4
s_3	1	1	0	0	1	5
Z	-20	-10	0	0	0	0

- Update the equation for new basic feasible solution

Now, the entering and leaving basic variables are defined. We can move to the better and new basic feasible solution by switching variables x_1 with s_1 and setting coefficient of entering basic variable equal to 1. Gaussian operations are used to eliminate the rest of coefficient in pivot column to zero for satisfying simplex method procedure. The new tableau is updated and shown as below. Result in x_1 move to new solution corner.

Basic Variable	x_1	x_2	s_1	s_2	s_3	RHS
x_1	1	0	1	0	0	3
s_2	0	1	0	1	0	4
s_3	0	1	-1	0	1	2
Z	0	-10	20	0	0	60

The point#2 of Fig. B.3, the solution has been moved to new feasible solution corner to and its solution value of 60. Repeat procedure from # 2 to #6 until the solution

is reached the optimum point. For this problem, point # 3 in Fig B.3 is final answer with values of 3, 2, and 80 for variables x_1, x_2 and Z, respectively.

However, we may suspect in previous section that all of reinforced concrete design beyond the scope of this paper is dealing with minimum problem instead of maximizing as demonstrated in chapter 4. The below is a process used to transform the minimize problem to maximize problem is discussed. Start with the standard form for minimization problem as Fig. B.4. The negative sign applies to all of them. Then, the minimization problem will turn to maximization problem as shown in Fig. B.5. Set up the tableau.

$$\begin{aligned} &\textit{Minimize} && \sum c_j x_j \\ &\textit{Subject to} && \sum a_{ij} x_j \geq b_i \\ &\textit{where} && x_j \geq 0 \ \textit{and} \ b_i \geq 0 \\ &\textit{for} && i = 1, 2, ..., m \ \ \& \ \ j = 1, 2, ..., n \end{aligned}$$

Fig. B.4: the minimization problem.

$$\begin{aligned} &\textit{Maximize} && -\sum c_j x_j \\ &\textit{Subject to} && -\sum a_{ij} x_j \leq -b_i \\ &\textit{where} && x_j \geq 0 \ \textit{and} \ b_i \geq 0 \\ &\textit{for} && i = 1, 2, ..., m \ \ \& \ \ j = 1, 2, ..., n \end{aligned}$$

Fig. B.5: the maximization problem.

However, before the maximization process will perform, no negative value of right side of each constraint equation should occur. Use Gaussian operation to eliminate that negative sign.

Appendix C: MATLAB Source Codes

a) Simplex Method

```
clear
% Simplex Method
%=============================================
% Input Data
%=============================================
M=load('data.txt')
Msize=size(M);
Mrow=Msize(1,1);
Mcol=Msize(1,2);
z1r=4;
z2r=13;
z3r=14;
%
%=================================================
% Part 1: Convert Minimization to Maximization
%=================================================
%==============================
need =1;
More=1;
for k=1:10
   k
   M;
     if More==1
% I) Eliminate negative entry in last column ===================
%
   ICy=100000000;
      for i=1:Mrow-1
         if M(i,z3r)<ICy
            IDy(1,1)=i;
            IDy(1,2)=z3r;
            ICy=M(i,z3r);
         end
      end
      ICx=0;
       for j=1:z2r
          if M(IDy(1,1),j)<ICx
            IDx(1,1)=IDy(1,1);
            IDx(1,2)=j;
            ICx=M(IDy(1,1),j);
         end
         TICx=ICx;
      end
 % II) Unit that pivot ===================================
 %
     for k=1:Mcol
        M(IDx(1,1),k)=M(IDx(1,1),k)/ICx;
     end
```

```
      for m=1:Mrow
         if m~=IDx(1,1)
            Div=M(m,IDx(1,2))/M(IDx(1,1),IDx(1,2));
            for n=1:Mcol
               M(m,n)=M(m,n)-Div*(M(IDx(1,1),n));
            end
         end
      end
 % III)  Check more negative entry ==========================
      More=0;
       for i=1:Mrow-1
          if M(i,z3r)<0
            More=1;
          end
       end

end
end
% IV)Check more negative entry==============================
cont=0;
for p=1:Mcol-1
    if M(Mrow,p)<0
       cont=1
      end
 end
 cont
%
%================================================
% Part II: Apply Maximization Procedure
%================================================
%
% I) Locate the most negative entry ======================
  if cont==1
     Neg=1;
       for kk=1:5
          if Neg==1
               IZ=0;
          for p=1:Mcol-1
               if M(Mrow,p)<IZ
                   IZ=M(Mrow,p);
                   IZx=M(Mrow,p);
                   IZxc=p;
               end
            end
          for q=1:Mrow-1
             if M(q,IZxc) ==0
                 Divv(q)=900;
                 DivvI(q)=0;
            else
                 Divv(q)=M(q,Mcol)/M(q,IZxc);
                 DivvI(q)=M(q,IZxc);
             end
          end
```

```
      IZZ=100000;
       for s=1:Mrow-1
          if (Yes~=1)&(Divv(s)>0)
              if Divv(s)<IZZ
                  IZZ=Divv(s);
                  IZyc=s;
              end
          end
       end
        for r=1:Mrow-1
           if (Divv(r)==0)&(DivvI(r)>0)
               IZyc=r;
               Yes=1;
           end
       end
% II)  Unit that entry ===================================
       MX=M(IZyc,IZxc);
        for k=1:Mcol
            M(IZyc,k)=M(IZyc,k)/MX;
        end
       for m=1:Mrow
           if m~=IZyc
              Div=M(m,IZxc)/M(IZyc,IZxc);
               for n=1:Mcol
                   M(m,n)=M(m,n)-Div*(M(IZyc,n));
               end
           end
       end
% III)  Check more negative entry ========================
       Neg=0;
        for t=1:Mcol-1
            if M(Mrow,t)<0
                Neg=1;
            end
        end
  end
 end
end
 M;
```

b) Optimized Beam Design

```
clear
% BeamOpV3.m
%======INPUT ========================
fc= 4000; % psi
fy=60000; % psi
CC= 90;   % Cost of concrete per ton
CS= 750;  % Cost of steel per ton
Mu =660% k-ft of bending moment
col=20   %width of column (in)
%=====================================
rho=0.003;
k=0;
m=1;
MinC=1000000;
for i=1:11
  rho=rho+0.002;
  b=8;
    for j=1:11
       k=k+1;
       b=b+2;
       w=rho*fy/fc;
       kn=fc*w*(1-(w/1.7));
       d=(Mu*12000/(b*kn))^0.5;
       cost=(CC*b*(d+2.5)*150/(144*2000))+(CS*rho*b*(d)*490/(144*2000));
       rat=d/b;
      % Optimize the size
          if k==1 %
           if rat>=1.0 %%
                if rat<=2.5
                  if b<= col
                        %=========================
                        Table(m,1)=m;
                        Table(m,2)=b;
                        Table(m,3)=d;
                        Table(m,4)=rho;
                        Table(m,5)=cost;
                         m=m+1;
                      %=========================
                      % Find the minimum cost
                      %-----------------------------
                             if MinC>cost
                             MinB=b;
                              MinD=d;
                              MinC=cost;
                               Xrho=rho;
                                Xrat=rat;
                                  end
                    %-----------------------------
                   end
```

```
            end
        end   %%
       else  %
         if rat>=1.0
          if rat<=2.5
                 if b<= col
                    %=========================
                      Table(m,1)=m;
                      Table(m,2)=b;
                      Table(m,3)=d+2.5;
                      Table(m,4)=rho;
                      Table(m,5)=cost;
                      m=m+1;
                   %=========================
                   % Find the minimum cost
                   %----------------------------
                          if MinC>cost
                            MinB=b;
                            MinD=d;
                            MinC=cost;
                             Xrho=rho;
                             Xrat=rat;
                          end
                           %------------------------------
             end
           end
         end
     end %
  end
end
Table
%================================================
% Check fitting of steel bars to beam depth
%================================================
j=1;
for i=1:m-1
  As=(Table(i,2))*(Table(i,3)-2.5)*(Table(i,4));
  nb=ceil(As/(1.0));
  bmin=4+1*(nb-1)+nb*1.128;
  if bmin<=Table(i,2)
    Ans(j,1)=j;
    Ans(j,2)=Table(i,2);
    Ans(j,3)=Table(i,3);
    Ans(j,4)=Table(i,4);
    Ans(j,5)=Table(i,5);
    j=j+1;
  end
end
Ans
MinCost=10000000;
for k=1:j-1
  if Ans(k,5)<MinCost
    MinCost=Ans(k,5);
```

```
    kk=k;
  end
end
FinalB=Ans(kk,2)
FinalD=Ans(kk,3)
FinalRho=Ans(kk,4
```